VNIVERSITAT DE VALÈNCIA Facultat de Química

Departamento de Química Analítica

Estrategias verdes para el análisis de muestras alimentarias y medioambientales

MEMORIA PRESENTADA PARA OPTAR AL

TITULO DE DOCTOR POR

LIDIA HERREROS CHAVEZ

Programa de doctorado

"Técnicas Experimentales en Química"

Directores:

Dr. M. L. Cervera Sanz

Dr. Á. Morales Rubio

Valencia, enero 2021

El Prof. Dr. M. Luisa Cervera Sanz, Catedrático de Universidad, y el Prof. Dr. Ángel Morales Rubio, Catedrático de Universidad del Departamento de Química Analítica de la Universidad de Valencia (Estudi General)

CERTIFICAN

Que D. Lidia Herreros Chavez ha realizado la presente Tesis Doctoral titulada "**Estrategias verdes para el análisis de muestras alimentarias y medioambientales**" bajo su dirección en el Departamento de Química Analítica de la Universidad de Valencia, y autorizan su presentación para optar al Grado de Doctor en Técnicas Experimentales en Química.

Y para que así conste, firman la presente en Burjassot a 13 de enero de 2021.

Prof. Dr. M. Luisa Cervera Sanz

Prof. Dr. Ángel Morales Rubio

A mi familia

AGRADECIMIENTOS

En primer lugar, me gustaría agradecer a todas las personas que han hecho posible que llegase a este punto.

A mis directores de tesis, Marisa y Ángel, por la confianza depositada en mí, todo lo que me han enseñado y el apoyo que me han dado en estos tres años. Por el tiempo y el esfuerzo invertido en que este proyecto llegase a buen puerto.

Me gustaría agradecer en segundo lugar, a mi familia, en especial a mi padre y a mi hermano por todo lo que me han ayudado, ya que junto con mi yaya han sido los pilares de esta tesis.

A Soraya, Aitor y Rocío, por todos esos momentos vividos que no se van a olvidar con el tiempo y por ser con quien compartir las penas y alegrías. Sin ellos esta tesis no hubiese sido lo mismo.

A Sofía por escucharme siempre y por todos los consejos que me has dado en el camino. A todos los TFGs y TFMs que me llevo como amigos en especial a Adri, Mario, Álvaro, Pili, David, a Andrea por su implacable apoyo y a Javi por compartir y entender este duro camino.

A mis compañeros de laboratorio, Roberto, Mirco, Sonia, Kevin, Paco y Sergio por enseñarme cada día una cosa nueva y por sus ánimos y consejos, sobretodo en la última etapa del doctorado. A Gianni, por guiarme en el mundo de la quimiometría y por ver siempre el lado bueno de las cosas.

Gracias a todos vosotros.

ÍNDICE

ÍNDICE DE ACRÓNIMOS

AESAN	Agencia Española de Seguridad Alimentaria y Nutrición
ANNs	Artificial neuronal networks / Redes neuronales artificiales
CA	Cluster analysis / Análisis clúster
CCA	Canonical correlation analysis / Análisis de correlación canónica
CCM	Chlorophyll content meter / Medidor del contenido de clorofila
CIE	Comission Internationale de l'Éclairage / Comisión Internacional de la Iluminación
CMYK	Cyan, magenta, yellow and key / Cian, magenta, amarillo y negro
TPC	Total polar compounds / Compuestos polares totales
CV	Cross validation / Validación cruzada
CVA	Canonical variate analysis / Análisis de variables canónicas
DRI	Daily reference intake / Ingesta diaria recomendada
DMF	*N,N*-Dimethylformamide / *N,N*-Dimetil formamida
DMSO	Dimethyl sulfoxide / Dimetil sulfóxido
ED-XRF	Energy dispersive X-ray fluorescence / Fluorescencia de rayos X de energía dispersiva
EFSA	European Food Safety Authority / Autoridad Europea de Seguridad Alimentaria
EPMA	Electron probe micro-analyzer / Microanálisis de sonda electrónica

FAO	Food and Agriculture Organization / Organización de las Naciones Unidas para la Agricultura y la Alimentación
FD	First derivate / Primera derivada
HSV	Hue, saturation and value / Tono, saturación y brillo
ICP-MS	Inductively coupled plasma mass spectrometry / Espectrometría de masas con plasma de acoplamiento inductivo
ICP-OES	Inductively coupled plasma optical emission spectrometry / Espectrometría de emisión óptica con plasma de acoplamiento inductivo
L*a*b*	Luminosidad, gradiente de rojo a verde y gradiente de azul a amarillo
LDA	Linear discriminant analysis / Análisis discriminante lineal
LOD	Limit of detection / Límite de detección
LV	Latent variable / Variable latente
MC	Mean center / Centrado en la media
NEMI	National Environmental Methods Index / Índice Nacional de Métodos Ambientales
NIES	National Institute of Environmental Studies / Instituto Nacional de Estudios Medioambientales
NIST	National Institute of Standards and Technology / Instituto Nacional de Estándares y Tecnología
OSC	Orthogonal signal correction / Corrección de la señal ortogonal
PC	Principal component / Componente principal
PCA	Principal component analysis / Análisis de componentes principales

PIXE	Particle-induced X-ray emission / Rayos X inducidos por partículas de emisión
PLS	Partial least squares / Regresión por mínimos cuadrados parciales
RGB	Red, green and blue / Rojo, verde y azul
RMSEC	Root mean square error of calibration / Error cuadrático medio de calibración
RMSECV	Root mean square error of cross valiation / Error cuadrático medio de validación cruzada
RMSEP	Root mean square error of prediction / Error cuadrático medio de predicción
RRMSECV	Relative root mean square error of cross validation / Error relativo cuadrático medio de validación cruzada
RRMSEP	Relative root mean square error of prediction / Error relativo cuadrático medio de predicción
RSD	Relative standard deviation / Desviación estándar relativa
SD	Second derivate / Segunda derivada
SMO	Smoothing / Suavizado
SNV	Standard normal variation / Variación normal estándar
SPAD	Soil plant analysis development / Desarrollo de análisis de plantas de suelo
WD-XRF	Wavelength dispersive X-ray fluorescence / Fluorescencia de rayos X de longitud de onda dispersiva
WHO	World Health Organization / Organización Mundial de la Salud
XRF	X-ray fluorescence / Fluorescencia de rayos X

RESUMEN

Los retos actuales de la Química Analítica Verde son el desarrollo, y su implementación en el análisis de rutina, de nuevas metodologías "verdes", que sean más sostenibles con el medio ambiente.

Por ello, el objetivo de esta tesis es desarrollar métodos de análisis directos mediante el empleo de la fluorescencia de rayos X en la determinación del perfil mineral y fomentar el uso del Smartphone como una herramienta de análisis complementaria a las técnicas convencionales en la determinación de compuestos de interés en muestras de alimentos y medioambientales. La presente tesis se estructura en 7 capítulos que de acuerdo con su temática pueden clasificarse en dos apartados:

1. Análisis de alimentos mediante fluorescencia de rayos X, técnica aplicada al análisis de la composición mineral en cacaos solubles, leches infantiles, frutas y legumbres.

2. Análisis mediante Smartphone, técnica desarrollada para la determinación del contenido de clorofila en hojas de cítricos y la determinación de compuestos polares totales (TPC) en aceite de girasol usado.

Esta Tesis Doctoral se basa en la idea del desarrollo y optimización de métodos directos aplicando el concepto de la Química Analítica Verde, reduciendo el coste y el tiempo del análisis, así como el volumen de los reactivos empleados y de los residuos generados.

En los primeros cinco capítulos de la tesis se analiza el perfil mineral en alimentos empleando la espectrometría de emisión óptica con plasma de acoplamiento inductivo (ICP-OES) como técnica de referencia.

En el caso del análisis de clorofila (capítulo 6) se ha empleado como técnica de referencia la espectroscopia UV-Vis, se han realizado calibraciones con los datos de los dispositivos portátiles Chlorophyll Content Meter (CCM) y Soil Plant Analysis Development (SPAD) y las fotografías realizadas con el fin de predecir la concentración de clorofila en las hojas analizadas. En el trabajo del análisis de TPC en aceite (capítulo 7) se ha empleado el dispositivo portátil TESTO-270 como técnica de referencia.

1. Química Analítica Verde

La Química Analítica Verde se basa en el empleo de metodologías analíticas más sostenibles con el medio ambiente y surge como respuesta a la demanda de métodos más rápidos, con un menor consumo de reactivos, una menor generación de residuos o sustitución de reactivos peligrosos por otros menos tóxicos, manteniendo a su vez las propiedades analíticas.[1] En 1998, Anastas y Warner[1] propusieron los doce principios de la Química Verde que son un criterio para evaluar lo "verde" que es un procedimiento analítico y que se resumen en el acrónimo *PRODUCTIVELY* (ver **Figura 1**).[2]

P - Prevent wastes
R - Renewable materials
O - Omit derivatization steps
D - Degradable chemical products
U - Use safe synthetic methods
C - Catalytic reagents
T - Temperature, Pressure ambient
I - In-Process Monitoring
V - Very few auxiliary substances
E - E-factor, maximize feed in products
L - Low toxicity of chemical products
Y - Yes, it is safe

Figura 1. 12 principios abreviados de la Química Verde

La Química Analítica Verde surge en el año 2000 a partir de la Química Verde[3] y en 2013, Galuszka, Migaszewski y Namiesnik[4] introdujeron los 12 principios de la Química Analítica Verde creados a partir de los principios de la Química Verde pero adaptados a las necesidades analíticas. La **Figura** 2 muestra los 12 principios de la Química Analítica Verde.

Figura 2. 12 principios de la Química Analítica Verde.

Al igual que en los principios de la Química Verde, los 12 principios de la Química Analítica Verde se pueden abreviar mediante el acrónimo *SIGNIFICANCE (*ver **Figura 3***)*.[4]

S - Select direct analytical technique
I - Integrate analytical process and operations
G - Generate as little waste as possible and treat it properly
N - Never waste energy
I - Implement automation and miniaturization of methods
F - Favor reagents obtained from renewable source
I - Increase safety for operator
C - Carry out *in-situ* measurements
A - Avoid derivatization
N - Note that the sample number and size should be minimal
C - Choose multi-analyte or multi-parameter method
E - Eliminate or replace toxic reagents

Figura 3. 12 principios de la Química Analítica Verde abreviados

En los últimos años han aparecido diferentes propuestas de clasificación de las metodologías "verdes", en función del grado de sostenibilidad. En 2007, Keith, Gron y Young[5] plantearon la evaluación de los métodos analíticos mediante los pictogramas propuestos por el *National Enviormental Methods Index* (NEMI).[6] Al mismo tiempo, de la Guardia y Armenta[7] propusieron la evaluación de los métodos analíticos en función del riesgo operacional, el consumo de energía y de reactivos, y el volumen de residuos. Más tarde, Galuszka *et al*.[8] introdujeron la Eco-Escala, concepto empleado para la evaluación semicuantitativa de los procedimientos analíticos en función de su sostenibilidad. Esta escala asigna una serie de puntos de penalización en función de la cantidad de reactivos empleados y de residuos generados, además de tener en cuenta su peligrosidad, el riesgo para el operador, la seguridad y el medio ambiente, siendo 100 el método analítico "verde" ideal. Esta evaluación de los métodos analíticos fue revisada y modificada posteriormente por Armenta, de la Guardia y Namiesnik en 2017[9] y clasifica los métodos mediante el "Green Certificate". Esta escala se basa en la aplicación de letras (de la A a la G) y colores (del verde al rojo) siendo la clasificación A verde la más "verde" (ver **Figura 4**). Cada puntuación de los métodos evaluados se asocia con el número de puntos de penalización asignados según el uso de reactivos, la cantidad utilizada de los mismos, su peligrosidad, la energía consumida, los posibles riesgos laborales y los residuos generados.

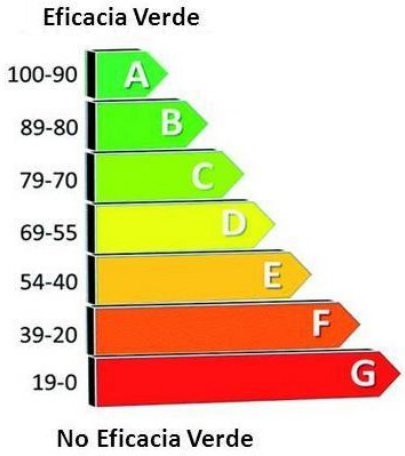

Figura 4. Pictograma del Green Certificate y clasificación de los métodos analíticos propuestos[9]

Actualmente, los métodos analíticos han conseguido elevar el grado de autonomía y de automatización, e implementar el análisis multielemental, la miniaturización y la reducción de los residuos que se generan. Sin embargo, estas técnicas tradicionales no consiguen llegar a la puntuación más alta en esta Eco-Escala. En este sentido, la fluorescencia de rayos X portátil se erige como una alternativa sostenible a los métodos tradicionales de análisis de metales debido a:

- Mínimo tratamiento de la muestra que minimiza el uso de reactivos
- Bajo coste y reducción del tiempo de análisis
- Capacidad de análisis multielemental
- Posibilidad de realizar la determinación *in situ* en el caso de los equipos portátiles

A su vez, los dispositivos portátiles de análisis como el Smartphone han sido un gran avance en el análisis y puede llegar a ser una herramienta complementaria a las técnicas habituales debido a:

- Miniaturización de los sistemas debido a su pequeño tamaño
- Mínimo consumo de reactivos y de energía
- Lleva a cabo determinaciones *in situ*
- Simplificación del proceso de análisis

2. Perfil mineral de los alimentos

Hay 25 elementos esenciales para el ser humano, 13 metales y 12 no metales que participan de forma activa en una gran variedad de procesos biológicos.[10] Estos elementos son esenciales para la vida ya que un suministro insuficiente al organismo produce efectos patológicos que se evitan o mitigan con el aporte adecuado. La esencialidad y toxicidad de un elemento son cualidades contrapuestas, pero un mismo elemento puede ser esencial y tóxico dependiendo de la dosis en la que se ingiera. La forma más habitual de que estas sustancias se introduzcan en el cuerpo es a través de

la dieta. Por tanto, es necesario controlar la cantidad de elementos tanto esenciales como no esenciales que se introducen en el organismo con cada ingesta de comida.

Por esta razón, en los últimos años el análisis de alimentos ha evolucionado proporcionando límites de detección y cuantificación inimaginables hace unas décadas. Las técnicas de análisis han mejorado los parámetros analíticos, pero no han conseguido reducir el coste del análisis, ni el volumen de residuos que se genera. A su vez, estas técnicas requieren a menudo del empleo de reactivos tóxicos para la salud y poco respetuosos con el medio ambiente. Por tanto, es necesario desarrollar nuevos equipos y técnicas que mantengan estas mejoras en los parámetros analíticos y que a su vez sean más sostenibles.

2.1. Seguridad alimentaria

La seguridad alimentaria vela que todos los alimentos sean aptos para el consumo humano y cumplan con las condiciones de salubridad establecidas por las diferentes organizaciones, como son la AESAN (Agencia Española de Seguridad Alimentaria y Nutrición) en España, la EFSA (Autoridad Europea de Seguridad Alimentaria) en Europa, la OMS (Organización Mundial de la Salud) o la FAO (Organización de las Naciones Unidas para la Agricultura y la Alimentación). Estos organismos se encargan de garantizar que los alimentos que se consuman no sean peligrosos para nuestra salud, ya que, si no se procesan bien y no se cumplen unas condiciones mínimas de higiene, los alimentos pueden transmitir patógenos que pueden provocar enfermedades en personas y, a su vez, controlan que los contaminantes no superen los valores límites establecidos. La Comisión de las Comunidades Europeas creó el "Libro blanco sobre seguridad alimentaria"[11] donde se pone de manifiesto la necesidad de garantizar un alto grado de seguridad alimentaria. Este documento se realizó como consecuencia de los avances que se estaban desarrollando tanto en los métodos de producción y de transformación de alimentos como en los controles necesarios para garantizar el respeto de normas de seguridad aceptables. En este documento no se recoge la cantidad máxima permitida de contaminantes en alimentos sino las buenas prácticas que se deben realizar para poder garantizar la higiene de los alimentos en todo el proceso que conlleva su puesta en el mercado.

A su vez en España se aprobó la Ley 17/2011, de 5 de julio, de seguridad alimentaria y nutrición,[12] que complementa al Libro blanco sobre seguridad alimentaria. Esta ley viene a completar y ordenar las regulaciones existentes a nivel nacional y que tienen incidencia en los aspectos referidos a la seguridad alimentaria y la nutrición.

En referencia a los metales hay una serie de ellos que son tóxicos para la salud humana y que su nivel está controlado por diferentes organismos reguladores. Estos elementos de interés son As inorgánico, Cd, Hg y sus diferentes formas, Pb y Sn inorgánico.[13] Con el paso de los años este reglamento ha sufrido numerosas modificaciones con el objetivo de adecuar la concentración máxima de los contaminantes en los productos alimenticios. En 2008 se redujeron los límites establecidos para el Pb, Cd y Hg (Reglamento CE Nº 629/2008)[14], en 2011 se especificaron los contenidos para determinados alimentos como crustáceos, legumbres y hortalizas (Reglamento CE Nº 420/2011)[15], en 2014 se modificó el contenido máximo en Cd en productos alimenticios (Reglamento CE Nº488/2014)[16] y en 2015 se incluyó el contenido máximo en As inorgánico en alimentos (Reglamento CE Nº 2015/1006).[17] En la **Tabla 1** se muestra el contenido máximo de estos metales en productos alimenticios recogidos en el Reglamento (CE) Nº 1881/2006 de la Comisión de 19 de diciembre de 2006 y sus modificaciones.

En la **Tabla 1** se muestra el contenido máximo permitido de los elementos en los diferentes alimentos. Los intervalos para cada elemento dependen del tipo concreto de alimento, es decir, por ejemplo, para el contenido en Cd en alimentos infantiles dependiendo del tipo de preparado (en polvo o liquido) y a partir del cual están elaborados (proteína de leche de vaca, proteína de soja solo o mezclado con las proteínas de leche de vaca) tiene un valor desde 0.005 hasta 0.020 mg/Kg.

Con estos reglamentos lo que se pretende es que todos los alimentos que se consumen cumplan con los principios de la seguridad alimentaria y si, por consiguiente, uno de estos alimentos analizados superase el valor límite permitido, dicho alimento no se comercializara. Cabe destacar que cuando se refiere en estos reglamentos a los contenidos máximos permitidos de cada alimento se aplican solo a la parte comestible, a excepción de que se indique lo contrario en el documento.

Hoy en día, con la implementación de la seguridad alimentaria y aplicando sus principios en toda la cadena de producción de alimentos, se evitan miles de enfermedades que vienen derivadas de contaminantes presentes en los mismos, y no solo los metales, sino también bacterias, pesticidas y toxinas, entre otros.

Tabla 1. Contenidos máximos de metales en los productos alimenticios (en mg/Kg en peso fresco).

Alimento	As	Cd	Hg	Pb	Sn
Leche y derivados	---	---	---	0.02	---
Alimentos infantiles	---	0.005/0.010/0.020	---	0.05	---
Carnes	---	0.05/0.20	---	0.10	---
Carne de pescado	---	0.05/0.10/0.25	0.5/1.0	0.30	---
Despojos de carne	---	1.0	---	0.50	---
Cereales y legumbres	0.10/0.30	0.10/0.20	---	0.20	---
Hortalizas	---	0.05/0.10/0.20	---	0.10/0.3	---
Frutas	---	---	---	0.10/0.2	---
Complementos alimenticios	---	1.0/3.0	0.10	3.0	---
Cacao y sus productos	---	0.10/0.30/0.60/0.80	---	---	---
Enlatados	---	---	---	---	50/100/200
Grasas, aceites y miel	---	---	---	0.10	---
Vinos	---	---	---	0.15/0.2	---

2.2. Toxicidad y esencialidad de los elementos

Debido a que la esencialidad y toxicidad son cualidades contrapuestas, se han establecido unos valores de ingesta diaria recomendada para los elementos esenciales y, para los contaminantes, unos valores máximos permitidos recogidos en el "Codex Alimentarius" de la FAO y OMS.[18] Estos valores se han ido actualizando y cada vez son más bajos para los contaminantes, de forma que el riesgo sea mínimo por la ingesta de estos elementos tóxicos.

Hay que tener en cuenta también que para no sufrir una deficiencia de un elemento esencial debemos ingerir un mínimo de dicho elemento, ya que una ingesta insuficiente puede provocar patologías. Existen dos tipos de deficiencia: la primaria, que tiene su origen en una dieta insuficiente y la secundaria, que es debida a otras causas, como la pobre absorción de un elemento, aunque se ingiera en las cantidades adecuadas o por interferencia con otro elemento, entre otras. Por lo general, la deficiencia secundaria tiene su origen en un mal funcionamiento de los mecanismos homeostáticos.[10] En la **Figura 5** se muestra la curva de dosis-respuesta de un elemento esencial.

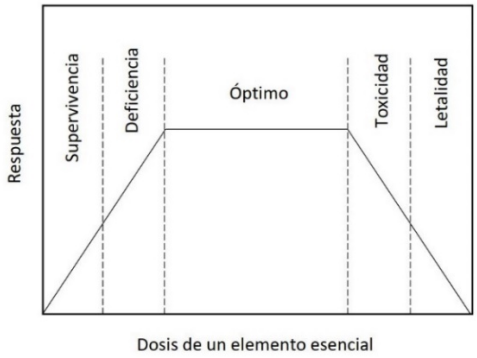

Figura 5. Curva dosis-respuesta para un elemento esencial[10]

La ingesta diaria recomendada (DRI, en inglés) es la cantidad mínima que se debe consumir de un nutriente para que se encuentre en los niveles óptimos en el cuerpo humano. En Europa, la EFSA marca la ingesta diaria recomendada de cada nutriente además de que cada país también tiene su propia ingesta diaria recomendada.

Diferentes organismos como el *Institute of Medicine* en Estados Unidos y el Parlamento Europeo en Europa publican los valores de DRI para los nutrientes esenciales y estas recomendaciones varían en función del sexo y la edad, y de las situaciones de embarazo y lactancia en el caso de la mujer. El reglamento (UE) Nº 1169/2011 del Parlamento Europeo y del Consejo de 25 de octubre de 2011[19] establece la información alimentaria y el etiquetado de los alimentos. En este etiquetado se indica la información nutricional, además de otras menciones obligatorias en dicha etiqueta, donde se muestra el contenido del alimento, así como la porción que representa en la ingesta recomendada diaria.

En la **Tabla 2** se muestra la ingesta diaria recomendada publicada por la FAO en su documento "Vitamin and mineral requirements in human nutrition"[20] teniendo en cuenta los diferentes grupos de consumidores.

En el caso de la ingesta de sal común se expresa en mg/g de Na al día.

El K y el Na tienen documentos específicos donde se indican las directrices a seguir con la ingesta de potasio y sodio en niños y adultos.[21,22] Esto es debido a que el potasio reduce la presión arterial y el riesgo de enfermedades cardiovasculares y mejora la densidad ósea. Además, se puede emplear como sustitutivo del sodio, reduciendo así las consecuencias negativas del consumo en grandes cantidades de sodio.[23-25] Sin embargo, la baja ingesta de potasio está asociada a la hipertensión, enfermedades cardiovasculares, nefrolitiasis crónica y la osteopenia.

En el caso del Na, y debido al consumo elevado, está asociado a hipertensión, enfermedades cardiovasculares y accidentes cerebrovasculares[26,27]. El objetivo principal es concienciar a la población de las elevadas cantidades de Na que se consumen diariamente y reducirlas.

Lo que se pretende con estos 2 documentos es reducir el riesgo de enfermedades no transmisibles que constituyen la primera causa de morbimortalidad en todo el mundo.[27,28]

Tabla 2. Ingesta diaria recomendada para los elementos en función del grupo al que pertenezcan.

Grupo	Ca (mg/día)	Se (µg/día)	Mg (mg/día)	Zn (mg/día)	Fe (mg/día)	I (µg/día)
0-6 meses	300	6	26	2.8	a	90
7-12 meses	400	10	54	4.1	9.3	90
Niños (1-9 años)	600	21	80	5.0	7.0	90
Adolescentes mujeres (10-18 años)	1300	26	220	7.2	32.0	150
Adolescentes hombres (10-18 años)	1300	32	230	8.6	15.0	150
Mujeres	1000	26	220	4.9	29.4	150
Hombres	1000	26	260	7.0	13.7	150
Embarazadas	1200	30	220	7.0	b	200
Mujeres lactantes	1000	35	270	8.5	15.0	200

Notas: en el caso del Zn y Fe hay tres tipos de biodisponibilidad en el organismo: elevada, moderada y baja. En ambos casos se han cogido los valores de biodisponibilidad moderada.

a: Las reservas neonatales de hierro son suficientes para cumplir con los requisitos de hierro durante los primeros 6 meses en recién nacidos a término. Los bebés prematuros y los bebés de bajo peso al nacer requieren hierro adicional.

b: Se recomienda administrar suplementos de hierro en forma de tabletas a todas las mujeres embarazadas debido a las dificultades para evaluar correctamente el estado del hierro en el embarazo. En mujeres embarazadas no anémicas, los suplementos diarios de 100 mg de hierro (por ejemplo, como sulfato ferroso) administrados durante la segunda mitad del embarazo son adecuados. En mujeres anémicas, generalmente se requieren dosis más altas.

3. Determinación del perfil mineral en alimentos

Los alimentos presentan concentración de elementos, ya sean esenciales o no esenciales, en diferentes cantidades. Debido a esto, es necesario conocer en todo momento los elementos presentes en los alimentos, así como las concentraciones y para ello, una de las características más demandadas en la actualidad es el análisis multielemental. Este análisis permite cuantificar simultáneamente gran variedad de elementos y para ello algunas de las técnicas que poseen esta cualidad son la espectrometría de emisión óptica con plasma de acoplamiento inductivo (ICP-OES), la espectrometría de masas con plasma de acoplamiento inductivo (ICP-MS) y la fluorescencia de rayos X (XRF), entre otras. En esta tesis se ha empleado la fluorescencia de rayos X de energía dispersiva como alternativa a las técnicas ICP.

3.1. Determinación del perfil mineral en alimentos mediante fluorescencia de rayos X (XRF)

El proceso de la generación del espectro de rayos X consta de 2 partes: la excitación, en la que la radiación primaria de rayos X incide sobre un electrón de las capas internas del átomo y se produce su expulsión, quedando así el átomo en estado excitado; y la emisión, en la que este átomo excitado tiende a volver a su estado más estable (estado fundamental), por lo que se producen saltos de los electrones que ocupan niveles más externos para cubrir los huecos en las capas internas. La excitación que se produce por el bombardeo de electrones se denomina excitación primaria, característica de los tubos de rayos X, y la emisión de otra radiación X, que se conoce como radiación secundaria, es la que se emplea para el análisis químico en los equipos de fluorescencia de rayos X. En la **Figura 6** se muestra representado el proceso de fluorescencia de rayos X. La energía involucrada en esta técnica tiene un intervalo entre 0.1 y 25 keV, con longitudes de onda desde 100 hasta 0.5 Å. La interacción entre la radiación de rayos X primaria y la matriz implica la dispersión de fotones y su posterior absorción a longitudes de onda características debido a cambios en el estado de excitación.[29]

Figura 6. Esquema del proceso de fluorescencia de rayos X.[30]

Dependiendo del detector que posean hay 2 tipos de equipos:

- Fluorescencia de rayos X de longitud de onda dispersiva (en inglés, **WD-XRF**): En este equipo el espectro de fluorescencia obtenido viene de la descomposición de la radicación en componentes monocromáticas en función de las longitudes de onda.

- Fluorescencia de rayos X de energía dispersiva (en inglés, **ED-XRF**): En este caso, el espectro de fluorescencia obtenido viene de la descomposición de sus componentes monocromáticas en función de la diferencia entre sus energías.

En la presente tesis se ha empleado un equipo portátil de fluorescencia de rayos X con dispersión de energía.

La fluorescencia de rayos X puede ser una alternativa no destructiva, de bajo coste y rápida en la determinación de elementos en cualquier tipo de matriz. El campo de aplicación de esta técnica no conoce límites, debido a que es aplicable a la determinación de cualquier elemento a partir de Z = 11, dependiendo de las indicaciones del fabricante. Las únicas desventajas que posee esta técnica son la problemática para determinar los elementos más ligeros de la tabla periódica y el efecto matriz, debido a la elevada dependencia de la señal con la matriz y el bajo poder de penetración de los rayos X, pues si la superficie no es regular ni homogénea ni tiene una cierta densidad puede dar lugar a errores en la medición.

3.1.1. Fluorescencia de rayos X de energía dispersiva

La espectrometría de fluorescencia de rayos X de energía dispersiva mide la energía de los rayos X secundarios, principalmente, en las líneas K y L de rayos X, que son las más intensas que se generan al excitar una muestra.[31] Debido a que la radiación de fluorescencia es característica de cada elemento, es posible identificar un elemento si se conoce la energía entre los orbitales atómicos implicados.

Hoy en día la espectroscopia portátil supone un gran avance entre las técnicas analíticas.[32] Debido al carácter no invasivo y a la posibilidad de realizar medidas *in situ*, este equipo es tremendamente útil en las aplicaciones forenses,[33] así como en el análisis de alimentos[34] y en el de suelos.[35]

La espectroscopia de fluorescencia de rayos X de energía dispersiva se ha convertido en una alternativa verde a los métodos atómicos tradicionales para la determinación de metales en cualquier tipo de muestra debido a la mínima o nula manipulación de la muestra, a su bajo coste y a su no generación de residuos. La determinación del perfil mineral mediante el empleo de ED-XRF ha ido aumentando en los últimos años como método analítico y permite analizar todo tipo de muestras. Debido a la posibilidad de que el equipo sea portátil las primeras aplicaciones que se realizaron fueron en el campo de la arqueología y en este sentido, la ED-XRF supone una gran ventaja frente a las técnicas convencionales. Además, en los últimos años no solo se ha empleado este equipo en este campo de la ciencia, sino que también se ha empleado en el análisis de alimentos[36], análisis medioambiental[37] y análisis clínico.[38-40] Comparada con otras técnicas portátiles también verdes como son los rayos X inducidos por partículas de emisión (PIXE) o el microanálisis de sonda electrónica (EPMA), se puede afirmar que la técnica más simple y menos costosa es la ED-XRF.[41]

Cabe destacar que, en el caso de la presente tesis, para la validación y comprobación de los resultados obtenidos mediante la ED-XRF, se hizo uso de un equipo ICP-OES, y sus resultados se emplearon como referencia.

Uno de los grandes inconvenientes de la ED-XRF es su baja sensibilidad, comparada con las técnicas tradicionales, y la gran dependencia de la matriz analizada. Además, la calibración interna que poseen estos equipos

portátiles suele ser para realizar el análisis en muestras medioambientales como son rocas y suelos, no para el análisis de muestras alimenticias. Como consecuencia, y como se ha comprobado en la presente tesis, en el caso de las muestras de alimentos, es necesario realizar una calibración monovariante externa o multivariante para los analitos a cuantificar. En este sentido la mejor herramienta para el tratamiento de los datos es el análisis quimiométrico.

En los cinco trabajos realizados en la presente tesis empleando un equipo portátil ED-XRF se llevó a cabo la determinación de 5 elementos en cacaos solubles y en leches infantiles; 9 elementos en frutas y legumbres, y 10 elementos en cacaos y chocolates a la taza. En las determinaciones de los cacaos y las leches infantiles se optó por realizar calibrados externos monovariantes con cada uno de los elementos a determinar. Para ello, los calibrados se realizaron con matriz alimentaria, concretamente con una muestra de cacao soluble, que se diluyó para abarcar todo el rango de concentración que presentaban el resto de las muestras. Los calibrados externos que se realizaron para el análisis de cacaos se emplearon también para predecir las concentraciones de las leches infantiles con la obtención de resultados satisfactorios en ambos tipos de matrices. Sin embargo, en el resto de las determinaciones se empleó la calibración multivariante, en concreto se hizo uso de la herramienta quimiométrica PLS (del inglés, partial least squares).

En todas las determinaciones de alimentos mediante ED-XRF es fundamental el control del efecto matriz. En el primer artículo realizado en esta tesis, se comprobó que no es factible la determinación directa en muestras alimenticias mediante ED-XRF utilizando los calibrados internos del equipo debido al fuerte efecto matriz que poseen estas muestras. Los resultados del análisis mediante ED-XRF se compararon con los datos obtenidos mediante ICP-OES y se vio que no eran coincidentes. La realización de calibrados mono y multivariantes para cada tipo de matriz permitió obtener a partir de las medidas de ED-XRF correctamente la concentración de los analitos en muestras alimenticias.

Se seleccionaron las energías más intensas de cada elemento y en todos los casos se eligieron las kα entre el intervalo de energía de 0 a 15 keV. Se escogieron las siguientes condiciones de medida: 50 kV de voltaje y 7 µA de amperaje.

3.1.2. Tratamiento de la muestra para la determinación del perfil mineral en alimentos

La ED-XRF es capaz de medir directamente sobre la superficie de la muestra, es por lo que en las 5 determinaciones se optó por triturar las muestras hasta polvo, y posteriormente se prensaron para obtener pastillas y poder medirlas mejor debido a que para que la ED-XRF pueda medir correctamente la superficie de la muestra debe tener un mínimo de espesor.

En el método de referencia empleado en estas determinaciones mediante ICP-OES, es necesario que las muestras estén en disolución. Para ellos, se requiere una etapa de tratamiento de la muestra mediante digestión acida con ácidos oxidantes concentrados.

Los reactivos que se emplearon fueron ácido nítrico y peróxido de hidrógeno. El ácido nítrico a alta temperatura incrementa su poder oxidante y el peróxido de hidrogeno facilita la descomposición de toda la materia orgánica presente en la muestra. Con esta combinación de reactivos las muestras se digerían en su totalidad.

En todas las muestras analizadas, para tener una porción homogénea y representativa de la muestra, se digerían 0.5 g. Esta cantidad de muestra podría suponer un riesgo en la digestión por microondas y por ello se realizó siempre una pre-digestión en baño de ultrasonidos durante 40 minutos para eliminar la mayor parte de los gases de la reacción entre la muestra y los ácidos. De esta forma, se evita la posibilidad de fugas en los reactores debido a la elevada presión que se genera en ellos.

3.1.3. Tratamiento quimiométrico

La quimiometría es la disciplina química que, con el uso de métodos matemáticos y estadísticos, empleando la lógica formal para diseñar o seleccionar los parámetros y procedimientos óptimos, proporciona la máxima información química relevante con el análisis de datos químicos.[42]

La quimiometría emplea técnicas multivariantes, es decir, que consideran todas las variables al mismo tiempo y de esta manera el modelo creado se ajusta a todos los datos. En una calibración monovariante, se consideran las mínimas variables. La ventaja que posee las técnicas multivariantes es que las correlaciones obtenidas entre variables se pueden utilizar y la desventaja es que las constantes en los modelos generados no necesariamente tienen relevancia física. Sin embargo, el enfoque clásico y el quimiométrico son complementarios, uno no puede sustituir al otro y viceversa.

En quimiometría es conveniente clasificar las variables en función de tres escalas:

- Nominal: estas variables son solo de naturaleza cualitativa. A su vez se diferencian 2 tipos: binarias (solo pueden tener 2 valores como si/no) y escalas de agrupamiento (pueden tener varias categorías como la edad).
- Ordinal: también son variables cualitativas, pero pueden clasificar los elementos medidos en términos de cantidad de la variable (como la toxicidad de un compuesto).
- Numérico: estas variables son de naturaleza cuantitativa. Esta escala permite clasificar, cuantificar y comparar los elementos de una escala.

Los datos en las técnicas multivariantes se organizan en forma de vectores y matrices. Los valores escalares se organizan en columnas o filas, generando así los vectores. Estos vectores a su vez se denominan descriptores o variables que nos indican las características de los analitos a analizar en los modelos quimiométricos. Cuando los vectores columna se disponen uno tras otro se forma lo que se denomina matriz.

Usualmente hay 2 tipos de matrices llamadas X e Y. En la matriz X se colocan las variables independientes y en la matriz Y se disponen las variables dependientes y sus valores en esta matriz son predichos mediante los modelos.

En el mercado actual hay diversos programas que permiten el uso de las técnicas quimiométricas como son el Matlab o el Opus, entre ellos. En la presente tesis se ha empleado el programa Matlab (Natick, MA, EEUU) junto con la herramienta complementaria PLS Toolbox (Wenatchee, WA, EEUU) para el tratamiento y predicción de datos.

3.1.3.1. Técnicas multivariantes

Las técnicas multivariantes son modelos estadísticos que tienen como finalidad analizar simultáneamente conjuntos de datos multivariantes, permitiendo así un entendimiento completo del objeto a estudiar. En la **Figura 7** se muestra la clasificación de las técnicas multivariantes.

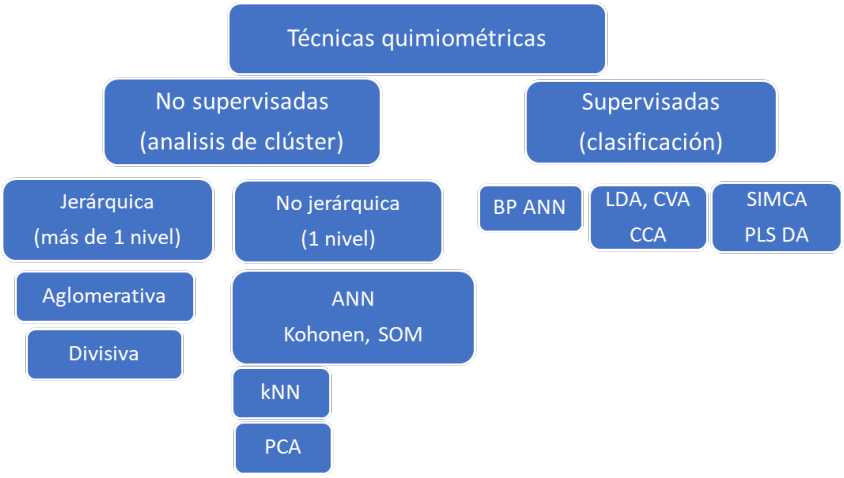

Figura 7. Clasificación de las técnicas quimiométricas[42]

ANN, redes neuronales artificiales; BP ANN, retropropagación ANN; CCA, análisis de correlación canónica; CVA, análisis de variación canónica; kNN, métodos de vecino k-cercano; LDA, análisis de discriminantes lineal; PCA, análisis de componentes principales; PLS DA, análisis de discriminantes por regresión de mínimos cuadrados parciales; SIMCA, modelación independiente suave de analogía de clase; SOM, mapas auto organizados.

Dependiendo de si los datos se pueden organizar en una matriz (X) sin información previa para explorar y conocer el conjunto de datos o si intentan relacionar las variables con alguna propiedad de la muestra, se clasifican en técnicas no supervisadas o técnicas supervisadas.

- Técnicas no supervisadas: i) análisis de componentes principales (en inglés, principal component analysis, PCA) y ii) análisis clúster (en inglés, cluster analysis, CA).

- Técnicas supervisadas: i) análisis de discriminantes lineales (en inglés, linear discriminant analysis, LDA), ii) análisis de correlación canónica (en inglés, canonical correlation analysis, CCA), iii) redes neuronales artificiales (en inglés, artificial neuronal networks, ANNs), iv) mínimos cuadrados parciales (en inglés, partial least squares, PLS) y v) análisis de variables canónicas (en inglés, canonical variate analysis, CVA).

En esta tesis se ha empleado la técnica PLS, por ello, se explicará más en profundidad en los siguientes apartados.

3.1.3.2. Regresión por mínimos cuadrados parciales (PLS)

La regresión por mínimos cuadrados parciales (en inglés, PLS) es una técnica supervisada de calibración multivariante que permite calibrar uno o varios componentes sin necesidad de conocer el resto de las fuentes de variación. Para ello se intenta modelar la relación entre 2 o más variables explicativas con una variable de respuesta, ajustándolas a una ecuación lineal. Es una de las técnicas más populares de modelización para predecir concentraciones a partir de datos espectrales cuando se combinan con métodos de selección de variables.[43]

En el PLS se construyen 2 conjuntos o *sets*; el *set* de calibración y el de validación. Los *sets* pueden crearse mediante el empleo de patrones externos (bastante infrecuente en el análisis de datos) o mediante el empleo de muestras del mismo tipo de las que se desean analizar.

- *Set* de calibración: conjunto de muestras que se emplea para construir el calibrado a partir de los datos de las muestras de una composición conocida. Este *set* debe ser representativo de todo el

sistema de estudio. Para realizar la calibración, primero se debe realizar una validación cruzada (CV, en inglés) que es un proceso en el cual se obtiene un modelo con todas las señales del conjunto de calibración excepto una la cual se sustituye posteriormente en el modelo para obtener el error de predicción de dicha señal. Este proceso se realiza con todos los datos obteniéndose así el *set* de calibración.

- *Set* de validación: conjunto de muestras de las que se conoce la propiedad a determinar y no han sido incluidas en el *set* de calibración. Este conjunto sirve para verificar la efectividad del modelo creado en el sistema de estudio.

Antes de llevar a cabo la construcción del set de calibración se deben realizar una serie de tratamientos a los datos con el fin de evitar errores en la creación de los modelos. Esto es debido a que esta técnica se emplea sobre todo con datos espectrales y con estos tratamientos se corrige la línea base o la relación señal/ruido. Existe numerosos tratamientos para llevar a cabo este fin, pero los que se han empleado en la presente tesis son:

- Derivadas (primera y segunda derivada): eliminan la señal de referencia no importante de las muestras con la derivada de las repuestas medidas con respecto al número de variable u otra escala como es el número de onda, longitud de onda, etc. Este filtro solo se debe emplear cuando las variables están fuertemente correlacionadas entre sí y las variables adyacentes tienen una señal similar conocida.

- Variable normal estándar (en inglés, SNV): es una normalización ponderada (no todos los puntos contribuyen a la normalización por igual). En ella se calcula la desviación estándar de todas las variables agrupadas para una muestra en concreto. Luego toda la muestra se normaliza por este valor, generando así en la muestra una desviación estándar de la unidad.

- Centrado en la media (en inglés, mean center, MC): calcula la media de cada columna y la resta de la columna, es decir, cada fila de los datos centrados en la media incluye únicamente como esa fila difiere de la muestra promedio en la matriz de datos original.

- Autoescalado: se emplea en el centrado en la media y a continuación se divide cada variable por la desviación estándar de la columna.

- Suavizado (en inglés, smoothing, SMO): filtro empleado para eliminar el ruido de alta frecuencia de las muestras. Se emplea en espectros, el suavizado supone que las variables que están cerca de otras en la matriz de datos y que contienen información similar que se puede promediar para reducir el ruido sin pérdida de señal de interés.

- Normalización: este método se basa en calcular una de varias métricas diferentes utilizando todas las variables de cada muestra. Consiste en dividir cada variable por la suma del valor absoluto de todas las variables.

- Corrección de la señal ortogonal (en inglés, orthogonal signal correction, OSC): filtro que elimina la varianza en el bloque X que es ortogonal al bloque Y. Esta varianza se identifica como un numero de factores del bloque X que se han hecho ortogonales al bloque Y. Al aplicar este preprocesado a los nuevos datos, se eliminan las mismas direcciones de estos datos antes de aplicar el modelo.

Las técnicas quimiométricas de reducción de variables como el PLS, permiten obtener la información contenida en todas las variables, en un menor número de éstas, siendo estas variables denominadas como variables latentes (en inglés, LV). Para que el modelo creado sea bueno, el número de variables debe ser siempre menor que el número de muestras que se emplean en la calibración. Si se genera un modelo con muchas variables latentes, se está sobredimensionando dicho modelo y predecirá las muestras erróneamente. Para saber qué modelo se debe seleccionar como el mejor hay unos parámetros que indican el error de la validación cruzada, el que más debe tener en cuenta es el error cuadrático medio de validación cruzada (*root mean square error of cross validation*, RMSECV). Cuanto menor sea el valor de este error mejor será el modelo teniendo siempre en cuenta de seleccionar el menor número de variables latentes.

Para saber si los datos predichos mediante el modelo creado con el *set* de calibración son correctos o no hay una serie de parámetros a analizar, como son:

- Error cuadrático medio de calibración (RMSEC): error asociado a la calibración del modelo.
- Error cuadrático medio de validación cruzada (RMSECV): error asociado a la calibración cuando se realiza la validación cruzada.
- Error cuadrático medio de predicción (RMSEP): error asociado a la predicción de los valores mediante el modelo creado. Cuanto más bajo sea este valor mejor será el modelo creado para predecir. Es el parámetro más importante a tener en cuenta en un modelo PLS ya que valora la capacidad predictiva del modelo.
- Coeficiente de determinación (r^2): asociado al ajuste de la ecuación de la recta que se obtiene en el modelo.

En resumen, el PLS se basa en la creación de una calibración a partir del *set* de calibración mediante la modelización de los datos obtenidos con la ED-XRF, de los cuales se sabe la concentración exacta de las muestras medida con la técnica de referencia ICP-OES, y posteriormente con este "calibrado" predecir la variable independiente a partir de un conjunto de datos en el set de predicción.

3.1.4. Perfil mineral en cacaos solubles y chocolates

En la actualidad el cacao es un alimento básico para la gran mayoría de los humanos en todo el mundo. Se puede ingerir en multitud de formas diferentes ya sea en polvo o líquido, y puro o con más ingredientes. Es una excelente fuente de nutrientes y de aporte calórico. Sin embargo, en la mayoría de estos productos no se indica el contenido de minerales. Así pues, la falta de datos sobre el contenido mineral en estos alimentos motivó la determinación de elementos esenciales en cacaos y chocolates a la taza.

En este artículo se realizó, con resultados satisfactorios, la cuantificación de 5 elementos esenciales (Ca, Cu, Fe, K y Zn). Las concentraciones obtenidas en las muestras fueron del orden de $\mu g\ g^{-1}$ en todos los casos.

Se comprobó que mediante la realización de calibrados externos empleando una muestra de cacao de concentración conocida diluida con glucosa se podía cuantificar el contenido mineral en las muestras mediante la ED-XRF sin errores significativos.

En primer lugar, se comprobó que los resultados obtenidos mediante la medida directa de la ED-XRF empleando el calibrado interno del equipo no eran coherentes con las concentraciones obtenidas mediante el método de referencia ICP-OES. Por tanto, se optó por realizar 2 calibrados externos empleando dos muestras de concentración conocida diluidas con glucosa. Se emplearon 2 muestras debido a que una abarcaba el intervalo alto de la concentración de Ca y la otra muestra el intervalo bajo del Ca. Los resultados obtenidos mediante el uso de calibrados externos son coincidentes con los resultados obtenidos mediante el método de referencia en todos los analitos.

Los límites de detección del método, teniendo en cuenta la sensibilidad de la ED-XRF para los 5 elementos estudiados fueron de 114, 1.9, 14.4, 178 y 1.7 µg g^{-1}, respectivamente para Ca, Cu, Fe, K y Zn. La desviación estándar relativa del método fue de 1.4-26 % para Ca, 3-8 % para Cu, 0.7-3 % para Fe, 0.9-3 % para K y 0.5-6 % para Zn. La exactitud del método se garantizó mediante el análisis de la muestra certificada de referencia Rice Flour-Unplolished del NIES (National Institute of Environmental Studies). Se comprobó el efecto matriz al interpolar muestras diluidas y no diluidas en los calibrados externos, y a la vista de los resultados se pudo concluir que no existe efecto matriz, evitando el error sistemático.

Los datos obtenidos se compararon con los resultados publicados de otros estudios en muestras de cacao y derivados. Las concentraciones obtenidas para los 5 elementos son similares a los reportados en la bibliografía.

3.1.5. Perfil mineral en leches infantiles

La leche es un alimento básico en la vida de los humanos, pero es en los primeros meses de vida cuando este alimento es indispensable para una buena alimentación del recién nacido. Son muchas las madres hoy en día que, por diferentes motivos, optan por alimentar al bebé desde el primer día con leche infantil en polvo. Es un alimento muy completo y que contiene

todos los minerales y nutrientes necesarios para su correcto desarrollo. Las técnicas más empleadas para la determinación del contenido mineral en leches infantiles son el ICP-OES/ICP-MS, aunque en los últimos años ha ido aumentando el número de artículos que emplean la técnica de fluorescencia de rayos X para la cuantificación. Este estudio se ha enfocado en la determinación directa de 5 elementos esenciales (Ca, Cu, Fe, K y Zn) mediante la ED-XRF portátil para evitar la preparación de muestra, el consumo de reactivos y la generación de residuos.

Debido a los estudios anteriores y a la no posibilidad de cuantificar directamente el contenido mineral en muestras alimenticias, se optó por medir e interpolar las cuentas por segundo obtenidas mediante ED-XRF de las muestras analizadas en los calibrados realizados para la determinación del contenido mineral en cacaos solubles. Se tomaron muestras aptas para todas las edades y con fórmulas diferentes, para una mayor representatividad del mercado actual.

Los rangos de concentración obtenidos son de 0-2600, 0-12, 0-160, 0-4400 y 0-15 $\mu g\ g^{-1}$, respetivamente para Ca, Cu, Fe, K y Zn.

Los resultados obtenidos mediante los calibrados externos se compararon con las concentraciones obtenidas mediante el método de referencia obteniéndose resultados coincidentes. Para saber si el resultado que proporciona la etiqueta es el correcto se compararon estos valores con la concentración cuantificada mediante ICP-OES obteniéndose prácticamente los mismos valores. Finalmente, se compararon los resultados obtenidos mediante los calibrados externos y la concentración indicada en la etiqueta del producto, obteniéndose también una buena correlación entre ambos.

El efecto matriz fue comprobado mediante la interpolación del calibrado externo de muestras diluidas con lactosa y muestras no diluidas. Se obtuvo como conclusión que no existe efecto matriz tanto a bajas concentraciones como a altas concentraciones en las muestras, por lo que no hay error sistemático.

La exactitud del método fue confirmada mediante el análisis de la muestra de referencia certificada Non-Fat Milk Powder del NIST (National Institute of Standards and Technology). Los resultados obtenidos muestran una exactitud de 86-102 % en los 5 analitos, confirmando de esta forma los

buenos resultados obtenidos mediante el uso del calibrado externo. Los límites de detección obtenidos fueron en μg g^{-1} 114, 0.09, 0.2, 258 y 2, respectivamente para Ca, Cu, Fe, K y Zn y la desviación estándar relativa fue para cada analito de 0.7-7 % para Ca, 2-14 % para Cu, 0.4-3 % para Fe, 0.8-5 % para K y 1.1-10 % para Zn.

3.1.6. Perfil mineral kakis (*Diospyros kaki.* L)

El kaki es una de las frutas más consumidas a nivel mundial. Se han realizado muchos estudios en los que se cuantifica el contenido mineral en la pulpa de este fruto, pero no en la piel. Muchos consumidores de kakis lo ingieren con piel, por tanto, es importante conocer el contenido mineral de la pulpa y la piel. Además, la piel protege al fruto de las inclemencias del tiempo y de los posibles ataques de los insectos, y depende que ésta sea más gruesa o más delgada de la concentración de Ca y K de allí el interés del análisis del perfil mineral. En este trabajo, se puso a punto una metodología para la determinación de 9 elementos (Al, Ca, Cr, Fe, K, Mg, Ni, P y Sr) en kakis con denominación de origen "Kaki Ribera del Xúquer".

Debido a la rápida degradación de estas muestras, se optó por medirlas inmediatamente y para obtener la concentración mediante el método de referencia se peló la fruta con un escalpelo y se secaron las pieles en estufa durante 8 horas a 60°C, antes de su digestión ácida asistida por microondas y su cuantificación mediante ICP-OES.

Para poder cuantificar correctamente la concentración de estos 9 elementos en los kakis se hizo uso de una calibración multivariante empleando el PLS. De esta forma, con los espectros obtenidos de la ED-XRF y la concentración obtenida mediante ICP-OES se realizó un set de calibración con el 30 % de las muestras y el restante 70 % se empleó como set de validación.

Se realizó un estudio para comprobar cuál era la mejor región espectral para construir el set de calibración. Se seleccionó la región espectral de 0 a 15 keV, donde están las energías de los analitos. Así mismo, se estudió el pre-procesamiento más adecuado teniendo en cuenta el RMSECV, siendo seleccionado en cada analito el que menor error proporcionaba.

De los 9 elementos estudiados fue posible la cuantificación de 5 analitos (Ca, Fe, K, Mg y P) con RRMSECV < 20 %. Las concentraciones obtenidas en todos ellos fueron del orden de $\mu g\ g^{-1}$.

Por último, se realizó una comparación de las concentraciones obtenidas mediante la predicción del modelo PLS creado y las obtenidas directamente con la ED-XRF para los analitos Ca y K. Se obtuvo como resultado que las concentraciones entre ambas técnicas no son coincidentes y por tanto la medida directa nos proporciona información errónea de la concentración de estos 2 analitos.

En vista de los resultados se puede concluir que el modelo PLS creado a partir de los espectros ED-XRF y de las concentraciones obtenidas mediante ICP-OES cuantifica de forma correcta la concentración en el resto de muestras de kakis.

3.1.7. Perfil mineral en legumbres y frutos

Las frutas y las legumbres constituyen dos de los pilares fundamentales de la dieta mediterránea. Estos alimentos son fuente de proteínas, hidratos de carbono, vitaminas y minerales. Presentan un elevado contenido de elementos esenciales para nuestro correcto funcionamiento. La mayoría de las determinaciones del perfil mineral en frutas y legumbres emplean métodos destructivos de preparación de las muestras para su determinación por ICP-OES e ICP-MS. En este caso, se planteó la determinación del perfil mineral en legumbres y cerezas basada en la medida directa empleando la ED-XRF y el uso de técnicas quimiométricas para el tratamiento de los datos.

Se cuantificó el contenido mineral en 8 analitos con resultados satisfactorios siendo estos Ca, Cu, Fe, K, Mg, P, Sr y Zn. Como técnica de referencia se usó ICP-OES y con las concentraciones obtenidas en las muestras mediante este equipo se pudieron realizar los sets de calibración. Para corroborar la exactitud del método de referencia mediante ICP-OES se analizó el material certificado de referencia ZC73013 Spinage del National Analysis Center, que junto a los datos obtenidos en estudios previos muestran la buena exactitud de la técnica ICP-OES.

El intervalo de concentración encontrado es de 0.4-15 para Al, de 623-1554 para Ca, de 3.7-9.0 para Cu, de 9.7-77 para Fe, de 1218-14156 para K, de 498-1655 para Mg, de 711-4267 para P, de 1.6-10 para Sr y de 3.2-32 μg g^{-1} para Zn.

Se utilizó la técnica PLS para la creación de modelos predictivos de las concentraciones. Se realizaron 3 modelos, uno solo con las muestras de legumbres, otro solo con las muestras de cerezas y el último que contenía ambos tipos de muestras. Para la cuantificación del contenido mineral se emplearon el 40 % de las muestras en el set de calibración y el 60 % restante en el set de validación. La región espectral seleccionada fue de 0 a 15 keV, región donde se encontraban las intensidades de los elementos a determinar. En todos los analitos se empleó 2 o 3 preprocesados, dependiendo del analito, con el fin de obtener el mejor modelo para cada elemento.

El mejor modelo se seleccionó teniendo en cuenta el menor número de variables latentes, el menor RRMSEP y el mayor coeficiente de determinación. Por ello, el mejor modelo predictivo de todos los creados fue el conjunto con muestras de cerezas y de legumbres. Se cuantificó de forma correcta mediante este modelo el Ca, Cu, Fe, K, Mg, P, Sr y Zn, con errores de predicción menores del 16 %, a excepción del Al con un RRMSEP del 33 % y del Sr que era del 23 %.

3.1.8. Determinación de elementos esenciales y no esenciales en cacaos solubles

El consumo de cacao y sus productos derivados ha ido en aumento con el paso de las décadas hasta convertirse en un alimento esencial para muchas personas. En una gran cantidad de estos productos, no se indica el aporte de elementos esenciales con la ingesta, por lo que es interesante saber qué cantidad de estos elementos son ingeridos en cada porción. También es de gran interés conocer la presencia de elementos no esenciales en estos productos, ya que en algunos de ellos está legislado la cantidad máxima permitida al día.

Es por esto que se llevó a cabo la determinación de 20 elementos, 14 esenciales (B, Ca, Co, Cr, Cu, Fe, K, Mg, Mn, Mo, Na, Ni, P and Zn) y 6 no esenciales (Al, Ba, Cd, Pb, Sr and Ti) mediante ICP-OES. A su vez, se determinó el perfil mineral en 10 analitos mediante la combinación de las técnicas de ED-XRF y PLS.

Para la correcta medida de las muestras mediante ICP-OES se tuvieron que digerir previamente las muestras con una mezcla de HNO_3 y H_2O_2. Las muestras analizadas eran de diferente formulación para abarcar así el mercado de cacaos y chocolates a la taza.

El intervalo de concentración analizado, expresado en $\mu g\ g^{-1}$, fue de 4160-9600 para K, de 1270-2660 para P, de 310-2680 para Ca, de 875-2550 para Mg, de 41-1340 para Na y de 64-350 para Fe, para los elementos mayoritarios. El intervalo de concentración para los elementos minoritarios fue de 31-78 para Al, de 6.9-15.7 para Cu, de 8.8-16.7 para Mn y de 11-52 para Zn. Finalmente, el intervalo de concentración para los elementos en cantidades traza fue de 3.5-6.4 para B, de 2.6-4.9 para Ba, de 0.0008- 0.252 para Cd, de 0.18-1.19 para Co, de 0.09-2.54 para Cr, de 0.04-0.26 para Mo, de 1.8-3.2 para Ni, de 0.013- 0.090 para Pb, de 3.4-8.1 para Sr y de 0.8-51.8 para Ti.

Mediante el análisis de la muestra certificada Rice Flour-Unpolished del NIES, se corroboró la exactitud del método de referencia ICP-OES. Los datos obtenidos confirmaron la exactitud de dicho método siendo en todos los analitos entre 87 y 120 %.

Se crearon modelos para cuantificar la concentración de manera directa en las muestras a partir de los espectros de ED-XRF y las concentraciones obtenidas del método de referencia. Se cuantificó de manera satisfactoria 10 elementos esenciales (Ca, Fe, K, Mg, Mn, Mo, Ni, P, Sr y Zn) mediante el modelo PLS-ED-XRF. En este caso se empleó el 30 % de las muestras en el set de calibración y el restante 70 % en el set de validación. Los resultados muestran para todos los analitos una elevada correlación entre la concentración predicha mediante el modelo PLS y la concentración cuantificada mediante ICP-OES obteniéndose valores de coeficiente de determinación de 0.71 a 0.99.

Además, se calculó la ingesta diaria teniendo en cuenta la cantidad diaria recomendada en cada producto y la concentración obtenida mediante ICP-OES. La ingesta recomendada al día para los distintos analitos va desde un 2 hasta un 51 %.

Se realizó un dendrograma para clasificar las muestras según su composición mineral y su formulación, sabiendo que se habían seleccionado 3 tipos de productos: cacaos del tipo original, cacaos solubles y chocolates a la taza. El dendrograma reveló la existencia de 3 grupos claramente diferenciados entre ellos con la excepción de una muestra anómala, siendo estos resultados coherentes con las formulaciones de cada muestra.

Finalmente, los resultados obtenidos se compararon con los datos de la bibliografía de otros estudios similares en cacaos y productos derivados. Cabe destacar que los niveles encontrados en los cacaos en el presente estudio son similares a los obtenidos en los otros estudios del perfil mineral de cacaos solubles. La concentración cuantificada para los elementos no esenciales fue baja no presentando ningún riesgo para el consumidor en estos productos.

4. Análisis mediante Smartphone

Hoy en día existen más de 3500 millones de usuarios de Smartphone en todo el mundo[44] y este dispositivo se ha convertido en una herramienta indispensable en nuestras vidas. En la **Figura 8** se muestra el aumento en el número de usuarios en los últimos años. Actualmente si se tiene en cuenta el número de usuarios en función del sistema operativo solo hay 2 grandes competidores: Android e iOS (de Apple), siendo Android el líder en dicho mercado. Aproximadamente el 80 % de los usuarios de todo el mundo poseen un Smartphone con sistema operativo Android y el restante 20 %, iPhone. Estos 2 sistemas operativos abarcan el 99.9 % de todo el mercado mundial quedando como minoría los sistemas Windows Phone, Blackberry OS y Symbian OS, entre otros.

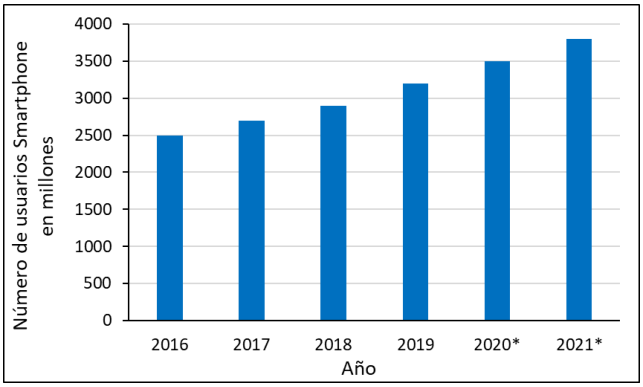

Figura 8. Número de usuarios Smartphone en todo el mundo (años 2020-2021 son previsiones. Fuente: Statista.[44]

Sin embargo, este dispositivo móvil no solo sirve para la comunicación, fin con el que se diseñó en un principio, sino que nos permiten realizar cualquier tipo de acción y, si nos centramos en el campo de la ciencia con este pequeño dispositivo se pueden determinar y cuantificar analitos sin perder las propiedades analíticas a día de hoy.

Los Smartphones se han convertido en una herramienta complementaria y verde de las técnicas convencionales en el análisis de sustancias y en los últimos años el empleo del Smartphone como herramienta analítica ha crecido de forma exponencial debido a su capacidad de realizar análisis *in situ* y a la no destrucción de las muestras. En el caso de determinaciones colorimétricas es necesario el uso de reactivos y de una preparación específica de la muestra, por lo que en estos casos no sería una herramienta tan "verde". En la **Figura 9** se muestra el aumento en el número de publicaciones en el campo de la química analítica que emplean un Smartphone como herramienta analítica.

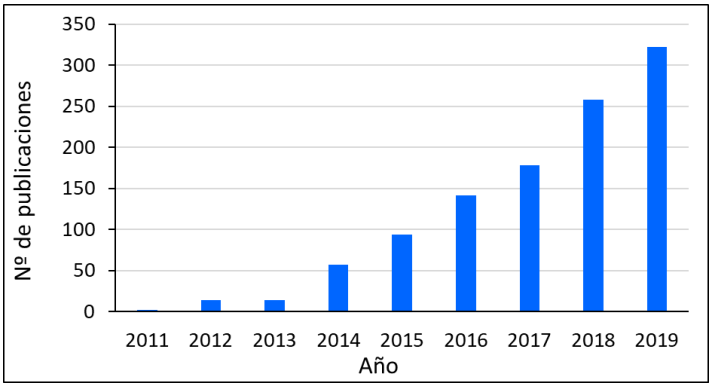

Figura 9. Número de publicaciones en la última década sobre Smartphone en aplicaciones analíticas. Fuente: Web of Science.

Las aplicaciones de los Smartphone son muy variadas, desde aplicaciones en el campo de la salud humana[45], epidemiologia medioambiental[46], seguridad alimentaria[47], control de calidad[48] y monitoreo de la contaminación.[49]

La propiedad analítica más empleada para correlacionarla, ya sea de forma cualitativa como cuantitativa, es el color en todos los casos. Esto es debido a que el fundamento para que una determinación empleando el Smartphone como técnica analítica sea exitosa se basa en correlacionar el color de la muestra o de un compuesto en el cual esté el analito a determinar con la presencia o la cantidad de dicho analito. De esta forma, mediante una sencilla fotografía con un Smartphone se puede saber si está presente o no en la muestra a analizar.

Este fundamento es sencillo teóricamente, pero hay que tener en cuenta una serie de condiciones para que sea fructífera la determinación. Uno de los parámetros más importantes en esta técnica es la correcta selección del espacio de color en cada caso. También cabe destacar que las determinaciones más habituales empleando el Smartphone son reacciones colorimétricas y menos habituales son las determinaciones directas, sin tratamiento de muestra.

4.1. Espacio de color

En un espacio de color se define un sistema de coordenadas, generalmente tridimensional, de sus componentes, y cada punto corresponde con un color específico. Existen diversos espacios de color actualmente, pero los más conocidos y los que se van a detallar en los siguientes puntos son el espacio RGB (rojo, verde y azul), HSV (tono, saturación y brillo), CMYK (cian, magenta, amarillo y negro) y CIE L*a*b* (luminosidad, gradiente de rojo a verde y gradiente de amarillo a azul).

4.1.1. RGB

El espacio de color más expandido y aceptado es RGB (Red, Green and Blue)[50] y es el preferido para la cuantificación colorimétrica debido a su simplicidad ya que descompone y cuantifica el color en 3 colores.[51] En este modelo rojo, verde y azul, los colores primarios, transmiten la luz para mostrar el color y son almacenados en 256 niveles, en una escala del 0 a las 255 unidades para cada parámetro (R, G o B), donde el valor 0 en las 3 coordenadas es negro puro y el valor 255 en las 3 coordenadas es blanco puro.[52] Los valores RGB obtenidos en una fotografía dependen de varios factores como la luz de la fuente de iluminación, la reflectancia del objeto y los efectos de interpretación y corrección en la cámara que dependen del Smartphone empleado.[50] Al ser un sistema no estandarizado y los valores depender del Smartphone empleado es necesario realizar un calibrado y la transformación de las coordenadas de color si se desea modelizar el procedimiento.

Es el espacio de color más empleado en las aplicaciones en el campo de la Química Analítica para cuantificar analitos.[53-57] En la **Figura 10** se muestra el modelo de color RGB.

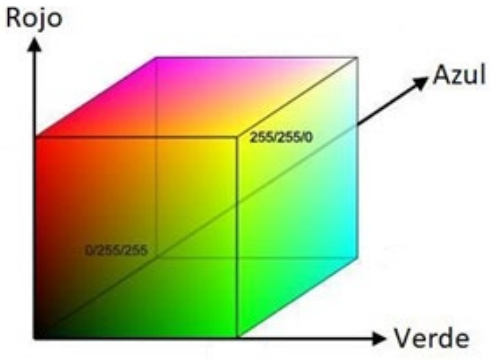

Figura 10. Modelo del espacio de color RGB.[58]

4.1.2. HSV

El espacio de color HSV describe el color en tres coordenadas: tono (H), la saturación (S) y el brillo (V). Es una transformación no lineal del modelo RGB. Este espacio de color es empleado debido a que su componente V esta desacoplada de la información cromática que posee la fotografía y las componentes H y S están correlacionadas con la forma en que los humanos percibimos el color. En este modelo H toma valores desde 0 hasta 360 (debido al círculo cromático) y S y V tienen valores desde 0 hasta 100. Es poco empleado en las aplicaciones con Smartphone en la Química Analítica.[59-61] En la **Figura 11** se muestra el modelo del espacio de color HSV.

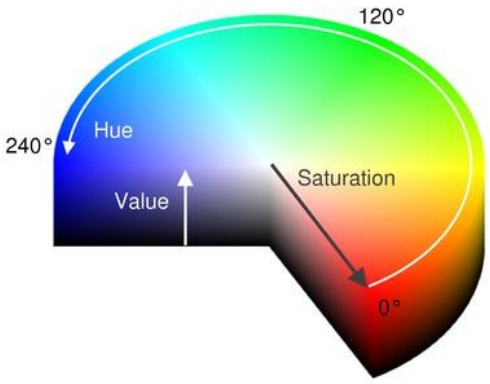

Figura 11. Modelo del espacio de color HSV.[62]

4.1.3. CMYK

Este espacio de color está basado en los colores secundarios de la luz, o bien los colores primarios de los pigmentos. Se denominan sustractivos ya que se utilizan como filtros para sustraer los colores de la luz blanca. Este espacio de color se emplea sobretodo en la mayoría de los dispositivos de impresión, como son impresoras y fotocopiadoras en color, aunque existen algunas aplicaciones en el campo de la química analítica que emplean este espacio de color para cuantificar el analito en la muestra.[63,64] En la **Figura 12** se muestra de forma esquemática el espacio de color CMYK.

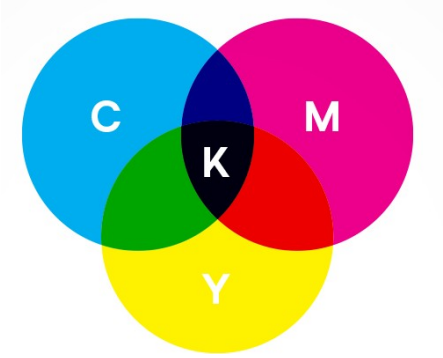

Figura 12. Modelo del espacio de color CMYK.[65]

4.1.4. CIE L*a*b*

En 1976 la Comisión Internacional de la Iluminación (CIE) propuso el espacio de color CIELAB, también llamada CIE 1976 como una aproximación a un espacio de color uniforme para todos y es el empleado para describir todos los colores que puede percibir el ojo humano. Junto con el espacio de color RGB, es uno de los espacios de color más populares y uniformes empleado para evaluar el color de un objeto.

En CIE 1976 L*a*b*, el color depende de la luminosidad (L*), el gradiente de color rojo a verde (a*) y del gradiente de amarillo a azul (b*). CIELAB permite obtener una percepción uniforme del color, lo que significa que un cambio mínimo en las coordenadas cromáticas produce un cambio igual en la percepción visual del color.[63] En este modelo, L* toma valores desde 0 a 100,

a* de negativo (verde) a positivo (rojo) y b* de negativo (azul) a positivo (amarillo).

A diferencia del modelo RGB, en CIE L*a*b*, las coordenadas de color no dependen de las condiciones de iluminancia, por lo que es, junto con RGB, el espacio más empleado en las aplicaciones analíticas.[66] En la **Figura 13** se muestra un esquema del modelo de espacio de color CIE L*a*b*.

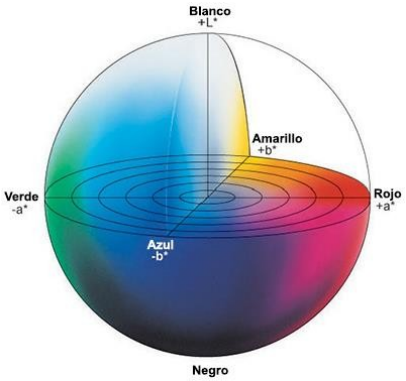

*Figura 13. Modelo del espacio de color CIE L*a*b*.*[67]

Para poder obtener las coordenadas propias de cada espacio de color lo más común es usar un software que permita el procesado de las imágenes, sin embargo, también hay equipos colorimétricos que permiten obtener estos datos midiendo directamente en la superficie a analizar. Estos softwares permiten la adquisición de cada coordenada solo con introducir las fotografías deseadas. En los programas más fáciles, como es el caso de ImageJ o GIMP solo permite obtener las coordenadas en el espacio de color RGB. Sin embargo, hay otros programas más complejos como es Matlab, que mediante la creación de comandos *script* permite obtener todos los valores que se quieran mediante la conversión de los valores RGB de la fotografía a otras coordenadas en otros espacios de color. En otras ocasiones no solo se han introducido las imágenes en los programas de procesado, sino que se ha desarrollado una aplicación Smartphone específica para dicha determinación.[68,69]

Como se ha comentado en los párrafos anteriores uno de los factores que más afectan a la toma de fotografías es la iluminación. Si se selecciona un espacio de color dependiente del Smartphone empleado se debe tener en

cuenta la cámara de éste, pues cuanto mayor sea la resolución de la cámara más precisa será la fotografía del objeto a analizar. Tanto si se selecciona un espacio de color dependiente como independiente se debe tener en cuenta la iluminación exterior ambiental.

En este sentido, para que la exactitud y precisión sea la misma siempre se tienen que tomar las fotografías con las mismas condiciones de iluminación, y es por ello por lo que muchos autores optan por iluminar artificialmente la muestra, ya sea simplemente con el flash del Smartphone o con tiras LED alrededor del objeto a estudiar.[70-73] Otros autores optan por fabricar un acople para modificar y adaptar el Smartphone a las condiciones de iluminación que desean.[47,56]

4.2. Determinación de clorofila en hojas

La clorofila es un pigmento verde que se encuentra en todas las plantas y algunas algas.[74] La clorofila se sintetiza en los cloroplastos de las células eucariotas y juega un papel fundamental en la salud de la planta. Es el pigmento fotosintético principal de las plantas y es una molécula capaz de absorber la radiación visible debido a los dobles enlaces conjugados presentes en su estructura. Participa en el proceso de la fotosíntesis y es un indicador del contenido de nitrógeno, del estrés y de las deficiencias nutricionales que pueda presentar la planta.[75,76] Los métodos tradicionales para la extracción de clorofila son destructivos, empleando a su vez reactivos tóxicos para la salud como es la acetona, dimetil formamida (DMF) o dimetil sulfóxido (DMSO).[77-79] Las técnicas más empleadas en la determinación de clorofila son mediante HPLC con detector de UV o la espectroscopia UV-Vis o de fluorescencia.[76,80]

Sin embargo, en los últimos años se han desarrollado métodos alternativos a los métodos tradicionales que evitan el uso de reactivos. En este sentido, los equipos no destructivos están siendo de gran versatilidad debido a la no necesidad de arrancar hojas a la planta y no requerir ni el uso de disolventes ni la presencia de personal especializado, tal y como ocurre con los métodos tradicionales[77,79,81]. A su vez, son dispositivos pequeños, fáciles de usar y que indican *in situ* de forma instantánea un valor numérico relacionado con el contenido de clorofila de la hoja.

En el presente estudio se ha desarrollado una nueva metodología para la cuantificación de clorofila en hojas de cítricos mediante el empleo del Smartphone con los parámetros RGB de las hojas fotografiadas. Se emplearon dos variedades diferentes de hojas de cítricos en este estudio (*Citrus limon* y *Citrus sinensis*).

Como métodos de referencia, la clorofila de las hojas se midió mediante 2 equipos portátiles de medida, el CCM-200 y el SPAD-502; equipos que se emplean usualmente en los trabajos que determinan clorofila en plantas, y mediante la espectroscopia UV-Vis. Estos dispositivos portátiles proporcionan un valor numérico que se correlaciona con la concentración de clorofila en la hoja dependiente del color. Las señales proporcionadas por ambos equipos no son coincidentes, pero se ha encontrado una correlación exponencial entre ambos con una regresión de 0.96.

Se estudió la degradación que sufre la clorofila con el tiempo. Se concluyó que la clorofila extraída no se degrada hasta el tercer día, pero es recomendable realizar los análisis en el mismo día que se extrae para evitar pérdidas.

De las fotografías realizadas en secciones circulares de las hojas, se crearon modelos con los valores de R, G, B, L*, a*, b*, h y C, con los valores numéricos obtenidos mediante CCM, SPAD y con la concentración obtenida mediante la extracción y determinación UV-Vis. Los modelos creados muestran un elevado coeficiente de determinación en todos ellos desde 0.87 hasta 0.97 y un error cuadrático medio < 20 %. En base a estos parámetros, se eligió el modelo RGB como el mejor y con el que se interpolaron el resto de muestras para predecir la concentración de la clorofila.

Las concentraciones predichas mediante el modelo RGB muestran elevados coeficientes de determinación comparando estos datos con las concentraciones obtenidas mediante la extracción con acetona y determinación UV-Vis ($\mu g\ g^{-1}$, $\mu g\ cm^{-2}$), CCM y SPAD de 0.95, 0.94, 0.94 y 0.97, respectivamente para cada uno de ellos. A la vista de los resultados se puede concluir que mediante las fotografías y con los valores RGB de éstas se puede cuantificar de forma exacta la concentración de clorofila en hojas de cítricos.

4.3. Determinación de compuestos polares totales en aceite de girasol

Los compuestos polares totales (en inglés TPC) son compuestos tóxicos, que poseen carácter polar, que se producen en el proceso de cocción del aceite. Debido al alto contenido en ácidos grasos poliinsaturados presente en el aceite, aproximadamente entre un 85-95 %,[82] éstos son susceptibles a procesos de degradación oxidativa, hidrolisis y polimerización de las cadenas de ácidos grasos, generando así estos compuestos polares.

El método oficial para determinar el contenido de compuestos polares en aceites y grasas usados se basa en la cromatografía en columna.[83] Este método requiere del uso de reactivos tóxicos y de un largo tiempo de análisis. Como alternativa a los métodos tradicionales existe un equipo portátil de medición directa de estos compuestos que se emplea a menudo en las industrias alimenticias, el TESTO-270.

En este trabajo se ha desarrollado un modelo mediante la imagen tomada con el Smartphone del color del aceite de fritura para predecir el contenido en TPC y se ha estudiado las veces que puede llegar a reusarse dicho aceite para cocinar sin presentar riesgo para la salud. Para ello en una freidora se calentaba solo aceite y en otra freidora igual se freían patatas fritas.

El rango de concentración de los polares en aceite de girasol frito fue desde 9 hasta 25.8 %. Mediante un estudio se comprobó el número de veces que podía ser reusado el aceite sin llegar a sobrepasar el valor máximo permitido en España de un 25 % de compuestos polares.[83] Así mismo, se realizó el mismo estudio solo calentando aceite sin añadir ningún alimento. De esta forma se comprobó que el aceite puede ser reusado durante aproximadamente 40 ciclos en el caso de la fritura sin llegar a superar el nivel máximo.

Con las fotografías que se tomaron del aceite tras cada ciclo de fritura o calentamiento y los valores de TPC obtenidos mediante el método de referencia TESTO, se realizaron modelos para predecir la concentración utilizando los valores L*a*b* de las imágenes.

Se emplearon tres Smartphone distintos (2 iPhone 6 Plus y un Samsung S7) para llevar a cabo esta modelización. Uno de los iPhone (iPhone-1) y el Samsung habían sido calibrados previamente mediante el atlas de color Munsell.

Los 3 modelos generados, empleando un Smartphone en cada uno de ellos, presentan bajos errores cuadráticos medios de calibración siendo 1.87, 2.19, y 1.59 %, respectivamente para el iPhone-1, iPhone-2 y Samsung.

Con los modelos generados se predijeron las concentraciones de compuestos polares a partir de los valores L*a*b* de las fotografías y se obtuvieron resultados satisfactorios. En todos los modelos a bajas concentraciones, las muestras que se predicen con más error son las del aceite solo calentado, y a medias y altas concentraciones se predice correctamente las muestras de aceite de girasol usado para freír.

5. Conclusiones

Los trabajos que componen esta tesis desarrollados mediante el empleo de la fluorescencia de rayos X y el Smartphone en el campo del análisis de alimentos han permitido la puesta a punto de metodologías directas siguiendo con los principios de la Química Analítica Verde. Por consiguiente, en estas metodologías no se ha empleado ningún tipo de disolvente ni de reactivo toxico ya que no era necesario. Una de las grandes ventajas que poseen tanto la fluorescencia de rayos X como el uso del Smartphone como técnica analítica es su capacidad de análisis *in situ* y directo, a la vez que su versatilidad debido al hecho de que se pueden analizar una amplia variedad de alimentos. Debido a esto, se evita la etapa en la que se producen más contaminaciones en todo el proceso analítico, que es el tratamiento de la muestra.

En el bloque de análisis de muestras mediante ED-XRF se ha conseguido mediante el mínimo tratamiento de la muestra y con la realización siempre de calibrados externos al propio equipo la cuantificación del perfil mineral en diferentes matrices alimentarias. Hay que tener en cuenta que para poder mejorar esta técnica se ha hecho uso de una técnica menos verde como es el ICP-OES. La gran mayoría de los analitos estudiados se han cuantificado correctamente comparados con los datos del ICP-OES, sin embargo, hay que tener en cuenta que los metales con bajo peso molecular ($Z<11$) no se pueden cuantificar mediante ED-XRF. Otro parámetro a tener en cuenta es el efecto matriz de este equipo, este problema se ha minimizado en estas determinaciones con la realización de calibrados en matriz de muestra. Como conclusión se puede decir que se han mejorado las metodologías ya existentes de la ED-XRF para determinar el perfil mineral en muestras de alimentos.

En el bloque de análisis de muestras mediante Smartphone se ha conseguido la determinación del contenido de clorofila en hojas y de compuestos polares en aceite de girasol usado mediante la toma de fotografías directamente de la muestra. En el primer estudio, si fue necesario un tratamiento de la muestra previo a la medida de la clorofila para poder extraer toda la clorofila presente en las hojas mediante el método de referencia. En el segundo estudio no se realizó ningún tipo de tratamiento de muestra ni para obtener las concentraciones mediante el método de referencia ni para la

determinación mediante Smartphone. Cabe destacar que estas determinaciones son más simples a nivel experimental, pero más complejas a nivel del tratamiento de los datos. Concluyendo este bloque, se puede afirmar que se ha conseguido con un dispositivo Smartphone junto con los métodos de referencia, la cuantificación correcta del contenido de clorofila con la mínima manipulación y tratamiento de la muestra y la determinación de compuestos polares totales en aceite de girasol usado para freír patatas fritas sin ningún tipo de tratamiento de muestra.

6. Bibliografía

1. Anastas, P.T., Warner, J.C. Green Chemistry: Theory and Practice, Oxford Univ. Press. New York. **1998**.

2. Tang, S.L.Y., Smith, R.L., Poliakoff, M. Principles of green chemistry: PRODUCTIVELY," Green Chem. **2005**, 7, 761-762.

3. Namiesnik, J. Trends in Environmental Analytics and Monitoring. Anal. Chem. **2010**, 30, 37–41.

4. Gałuszka, A., Migaszewski, Z., Namiesnik, J. The 12 principles of green analytical chemistry and the SIGNIFICANCE mnemonic of green analytical practices. TrAC-Trends Anal. Chem. **2013**, 50, 78–84.

5. Keith, L.H., Gron, L.U., Young, J.L. Green analytical methodologies. Chem. Rev. **2007**, 107, 2695-2708.

6. National Environmental Methods Index (NEMI). **2002**. http://www.nemi.gov/home/. Última fecha de acceso: 01/12/2020.

7. de la Guardia, M., Armenta, S. Green Analytical Chemistry: Theory and Practice. Ed. Elsevier, Amsterdam. **2011**.

8. Galuszka, A., Konieczka, P., Migaszewski, Z.M., Namiesnik, J. Analytical EcoScale for assessing the greenness of analytical procedures. TrAC-Trends Anal. Chem. **2012**, 37, 61-72.

9. Armenta, S., de la Guardia, M., Namiesnik, J. Green Microextraction, in Analytical Microextraction Techniques. Ed. M. Valcárcel, Betham Science. 2015.

10. Faus, J., Garcia-España, E., Moratal, J. Introducción a la Química bioinorgánica. Capítulo 1. Editorial Síntesis. Madrid. **2003**.

11. Libro blanco sobre seguridad alimentaria de la comisión de las Comunidades Europeas. https://eur-lex.europa.eu/legal-content/EN/TXT/PDF/?uri=CELEX:51999DC0719&from=ES. Última fecha de acceso: 01/12/2020.

12. BOE-A-2011-11604. Ley 17/2011, de 5 de julio, de seguridad alimentaria y nutrición. https://www.boe.es/buscar/pdf/2011/BOE-

A-2011-11604-consolidado.pdf. Última fecha de acceso: 01/12/2020.

13. Reglamento (CE) Nº 1881/2006 de la Comisión de 19 de diciembre de 2006 por el que se fija el contenido máximo de determinados contaminantes en los productos alimenticios. https://www.boe.es/doue/2006/364/L00005-00024.pdf. Última fecha de acceso: 01/12/2020.

14. Reglamento (CE) Nº 629/2008 de la comisión de 2 de julio de 2008 que modifica el Reglamento (CE) nº 1881/2006 por el que se fija el contenido máximo de determinados contaminantes en los productos alimenticios. https://www.boe.es/doue/2008/173/L00006-00009.pdf. Última fecha de acceso: 01/12/2020.

15. Reglamento (UE) Nº 420/2011 de la comisión de 29 de abril de 2011 que modifica el Reglamento (CE) nº 1881/2006, por el que se fija el contenido máximo de determinados contaminantes en los productos alimenticios. https://eur-lex.europa.eu/LexUriServ/LexUriServ.do?uri=OJ:L:2011:111:0003:0006:ES:PDF. Última fecha de acceso: 01/12/2020.

16. Reglamento (UE) Nº 488/2014 de la comisión de 12 de mayo de 2014 que modifica el Reglamento (CE) nº 1881/2006 por lo que respecta al contenido máximo de cadmio en los productos alimenticios. https://www.boe.es/doue/2014/138/L00075-00079.pdf. Última fecha de acceso: 01/12/2020.

17. Reglamento (UE) 2015/1006 de la comisión de 25 de junio de 2015 por el que se modifica el Reglamento (CE) nº 1881/2006 en cuanto al contenido máximo de arsénico inorgánico en los productos alimenticios. https://eur-lex.europa.eu/legal-content/ES/TXT/PDF/?uri=CELEX:32015R1006&from=es. Última fecha de acceso: 01/12/2020.

18. Codex Alimentarius de la OMS y FAO. http://www.fao.org/3/a-a0369s.pdf. Última fecha de acceso: 01/12/2020.

19. Reglamento (UE) Nº 1169/2011 del Parlamento Europeo y del Consejo de 25 de octubre de 2011 sobre la información alimentaria

facilitada al consumidor y por el que se modifican los Reglamentos (CE) nº 1924/2006 y (CE) no 1925/2006 del Parlamento Europeo y del Consejo, y por el que se derogan la Directiva 87/250/CEE de la Comisión, la Directiva 90/496/CEE del Consejo, la Directiva 1999/10/CE de la Comisión, la Directiva 2000/13/CE del Parlamento Europeo y del Consejo, las Directivas 2002/67/CE, y 2008/5/CE de la Comisión, y el Reglamento (CE) nº 608/2004 de la Comisión. https://eur-lex.europa.eu/LexUriServ/LexUriServ.do?uri=OJ:L:2011:304:0018:0063:es:PDF. Última fecha de acceso: 01/12/2020.

20. Organización Mundial de la Salud (OMS) y la Organización de las Naciones Unidas para la Agricultura y la Alimentación (FAO). Vitamins and mineral requirements in human nutrition. Segunda edición. Geneva. **2004**.

21. Organización Mundial de la Salud (OMS). Guía: Ingesta de potasio en adultos y niños. Geneva. **2012**.

22. Organización Mundial de la Salud (OMS). Guía: Ingesta de sodio en adultos y niños. Geneva. **2012**.

23. Dietary Guidelines Advisory Committee. The report of the Dietary Guidelines Advisory Committee on Dietary Guidelines for Americans. Washington, D.C., Department of Health and Human Services and Department of Agriculture, **2005**.

24. Whelton, P.K., He, J., Cutler, J.A., Brancati, F.L., Appel, L.J., Follmann, D., Klag, M.J. Effects of oral potassium on blood pressure. Meta-analysis of randomized controlled clinical trials. JAMA. **1997**, 277 (20), 1624–1632.

25. World Health Organization (WHO). Prevention of recurrent heart attacks and strokes in low and middle income populations: Evidence-based recommendations for policy makers and health professionals. Geneva. **2003**. http://www.who.int/cardiovascular_diseases/resources/pub0402/en/. Última fecha de acceso: 01/12/2020.

26. Bibbins-Domingo, K., Chertow, G.M., Coxson, P.G., Moran, A., Lightwood, J.M., Pletcher, M.J., Goldman, L. Projected effect of dietary salt reductions on future cardiovascular disease. N. Engl. J. Med. **2010**, 362 (7), 590–599.

27. World Health Organization (WHO). Preventing chronic disease: a vital investment. Geneva. 2005. http://www.who.int/chp/chronic_disease_report/contents/en/index.html. Última fecha de acceso: 01/12/2020.

28. World Health Organization (WHO). Global health risks: Mortality and burden of disease attributable to selected major risks. Geneva, 2009. https://www.who.int/healthinfo/global_burden_disease/GlobalHealthRisks_report_full.pdf. Última fecha de acceso: 01/12/2020.

29. de la Guardia, M., Garrigues, S. X-ray in Handbook of Mineral Elements. M. de la Guardia, S. Garrigues. John Wiley & Sons, Inc. Chichester, UK. **2015**.

30. https://wpo-altertechnology.com/es/xrf-x-ray-fluorescence-spectroscopy-hi-rel-parts/. Última fecha de acceso: 01/12/2020.

31. Hall, M. X-ray fluorescence-energy dispersive (ED-XRF) and wavelength dispersive (WD-XRF) spectrometry. Oxford University Press. **2015**.

32. Vanhoof, C., Bacon, J.R., Ellis, A.T., Fittschen, U.E.A., Vincze, L. 2019 atomic spectrometry update - a review of advances in X-ray fluorescence spectrometry and its special applications. JAAS. **2019**, 1-18.

33. Dao, L., Zeller, M.P., Wainman B.C., Farquharson, M.J. Feasibility of the use of a handheld XRF analyzer to measure skin iron to monitor iron levels in critical organs J. Trace Elem. Med. Biol. **2018**, 50, 305–311.

34. Pashkova, G.V., Smagunova A.N., Finkelshtein, A.L. X-ray fluorescence analysis of milk and dairy products: A review. TrAC-Trends Anal. Chem. **2018**, 106**,** 183–189.

35. Padilla, J.T., Hormes, J., Selim, H.M. Use of portable XRF: effect of thickness and antecedent moisture of soils on measured concentration of trace elements. Geoderma. **2019**, 337, 143–149.

36. Styburski, D., Janda, K., Baranowska-Bosiacka, I., Lukomska, A., Dec, K., Goschorska, M., Michalkiewicz, B., Zietek P., Gutowska, I. Beer as a potential source of macroelements in a diet: the analysis of calcium, chlorine, potassium, and phosphorus content in a popular low-alcoholic drink. Eur. Food Res. Technol. **2018**, 244 (10), 1853–1860.

37. Rawal, A., Chakraborty, S., Li, B., Lewis, K., Godoy, M., Paulette L., Weindorf, D.C. Determination of base saturation percentage in agricultural soils via portable X-ray fluorescence spectrometer. Geoderma. **2019**, 338, 375–382.

38. Afzal, F.S.M., Al-Ebraheem, A., Chettle, D.R., Desouza, E.D., Farquharson, M.J., O'Meara, J.M., Pidruczny, A., Wainman, B.C., McNeill, F.E. Feasibility of chromium measurements in skin using a portable hand-held XRF system. Nucl. Instrum. Methods Phys. Res., Sect. B. **2018**, 433, 1-9.

39. Fleming, D.E.B., Bennett S.R., Frederickson, C.J. Feasibility of measuring zinc in human nails using portable x-ray fluorescence. J. Trace Elem. Med. Biol. **2018**, 50, 609–614.

40. Rebiere, H., Kermaïdic, A., Ghyselinck, C., Brenier, C. Inorganic analysis of falsified medical products using X-ray fluorescence spectroscopy and chemometrics. Talanta. **2019**, 195, 490–496.

41. Mandal, A.C., Santra, S., Mitra, D., Sarkar, M., Bhattacharya, D. EDXRF as a Routine Tool for Numismatic Studies. Curr. Sci. **2003**, 85 (2), 134–135.

42. Héberger, K. Medical Applications of Mass Spectrometry, chapter 7: Chemoinformatics-multivariate mathematical-statistical methods for data evaluation. Elsevier. **2008**, 141-169.

43. Li, C-Q., Fang, Z., Xu, Q-S. A partition-based variable selection in partial least squares regression. Chemometr. Intell. Lab. Syst. **2020**, 198, 103935.

44. Statista. Number of smartphone users worldwide from 2016 to 2021 (in millions). https://www.statista.com/statistics/330695/number-of-smartphone-usersworldwide/. Última fecha de acceso: 01/12/2020.

45. Yang, K., Peretz-Soroka, H., Liu, Y., Lin, F. Novel developments in mobile sensing based on the integration of microfluidic devices and smartphones. Lab Chip. **2016**, 16, 943-958.

46. Nieuwenhuijsen, M.J., Donaire-Gonzalez, D., Rivas, I., de Castro, M., Cirach, M., Hoek, G., Seto, E., Jerrett, M., Sunyer, J. Variability in and agreement between modeled and personal continuously measured black carbon levels using novel smartphone and sensor technologies. Environ. Sci. Technol. **2015**, 49, 2977-2982.

47. Cherbuin, M., Zelder, F., Karlen, W. Quantifying cyanide in water and foodstuff using corrin-based CyanoKit technologies and a smartphone. Analyst. **2019**, 144, 130-136.

48. Rico-Yuste, A., González-Vallejo, V., Benito-Peña, E., Engel, T.C., Orellana, G., Moreno-Bondi, M.C. Furfural determination with disposable polymer films and smartphone-based colorimetry for beer freshness assessment. Anal. Chem. **2016**, 88, 3959-3966.

49. Wei, Q., Nagi, R., Sadeghi, K., Feng, S., Yan, E., Ki, S.J., Caire, R., Tseng, D., Ozcan, A. Detection and spatial mapping of mercury contamination in water samples using smart-phone. ACS Nano. **2014**, 8, 1121-1129.

50. Lopez-Molinero, A., Liñan, D., Sipiera, D., Falcon, R. Chemometric interpretation of digital image colorimetry. Application for titanium determination in plastics. Microchem. J. **2010**, 96, 380-385.

51. Soponar F., Moţ A.C, Sârbu C. Quantitative determination of some food dyes using digital processing of images obtained by thin-layer chromatography. J. Chromatogr. A. **2008**, 1188 (2), 295-300.

52. Franco, M., Suarez, W.T., dos Santos, V.B. Digital image method smartphone-based for furfural determination in sugarcane spirits. Food Anal. Methods. **2017**, 10, 508-515.

53. Ravazzi, C.G., Franco, M., Vieira, M.C.R., Suarez, W.T. Smartphone application of captopril determination in dosage forms and synthetic urine employing digital imaging. Talanta. **2018**, 189, 339-344.

54. Lima, M.J.A., Nascimento, C.F., Rocha, F.R.P. Feasible photometric measurements in liquid-liquid extraction by exploiting smartphone-based digital images. Anal. Methods. **2017**, 9, 2220-2225.

55. Aguirre, M.A., Long, K.D., Cunningham, B.T. Spectrometric smartphone-based system for ibuprofen quantification in commercial dosage tablets. J. Pharm. Sci. **2019**, 108, 2593-2598.

56. Böck, F.C., Helfer, G.A., da Costa, A.B., Dessuy, M.B., Ferrão, M.F. Rapid determination of ethanol in sugarcane spirit using partial least squares regression embedded in smartphone. Food Anal. Methods. **2018**, 11, 1951-1957.

57. Puangpila, C., Jakmunee, J., Pencharee, S., Pensrisirikul, W. Mobile-phone-based colourimetric analysis for determining nitrite content in water. Environ. Chem. **2018**, 15, 403-410.

58. http://artisticomiranda.blogspot.com/2013/11/modelo-rgb.html. Última fecha de acceso: 01/12/2020.

59. Nguyen, H., Sung, Y., O'Shaughnessy, K., Shan, X., Shih, W. Smartphone nanocolorimetry for on-demand lead detection and quantitation in drinking water. Anal. Chem. **2018**, 90, 11517-11522.

60. Lopez-Ruiz, N., Curto, V.F., Erenas, M.M., Benito-Lopez, F., Diamond, D., Palma, A.J., Capitan-Vallvey, L.F. Smartphone-based simultaneous pH and nitrite colorimetric determination for paper microfluid devices. Anal. Chem. **2014**, 86, 9554-9562.

61. Jung, Y., Kim, J., Awofeso, O., Kim, H., Regnier, F., Bae, E. Smartphone-based colorimetric analysis for detection of saliva alcohol concentration. Appl. Opt. **2015**, 54, 9183-9189.

62. https://www.freepng.es/png-g6gfm4/. Última fecha de acceso: 01/12/2020.

63. Wei, J., Yang, L., Luo, M., Wang, Y., Li, P. Nanozyme-assissted technique for dual mode detection of organophosphorus pesticide. Ecotox. Environ. Safe. **2019**, 179, 17-23.

64. Pla-Tolós, J., Moliner-Martínez, Y., Verdú-Andrés, J., Casanova-Chafer, J., Molins-Legua, C., Campíns-Falcó, P. New optical paper sensor for in situ measurement of hydrogen sulphide in waters and atmospheres. Talanta. **2016**, 156-157, 79-86.

65. https://99designs.es/blog/tips/c.orrect-file-formats-rgb-and-cmyk/ Última fecha de acceso: 01/12/2020.

66. Capitán-Vallvey, L. F., Lopez-Ruiz, N., Martinez-Olmos, A., Erenas, M. M., Palma, A. J. Recent developments in computer vision-based analytical chemistry: A tutorial review. Anal. Chim. Acta. **2015**, 899, 23-56.

67. https://www.aquateknica.com/conoce-el-espacio-de-color-cie-lab/. Última fecha de acceso: 01/12/2020.

68. Cherbuin, M., Zelder, F., Karlen, W. Quantifying cyanide in water and foodstuff using corrin-based CyanoKit technologies and a smartphone. Analyst. **2019**, 144, 130-136.

69. Sumriddetchkajorn, S., Chaitavon, K., Intaravanne, Y. Mobile-platform based colorimeter for monitoring chlorine concentration in water. 2014. Sens. Actuators B Chem. **2014**, 191, 561-566.

70. Shahvar, A., Saraji, M., Gordan, H., Shamsaei, D. Combination of paper-based thin film microextraction with smartphone-based sensing for sulfite assay in food samples. Talanta. **2019**, 197, 578-583.

71. Franco, M.O.K., Suarez, W.T., Maia, M.V., dos Santos, V.B. Smartphone application for methanol determination in sugarcane spirits employing digital image-based method. Food Anal. Methods. **2016**, 10, 2102-2109.

72. Levin, S., Krishnan, S., Raijkumar, Halery, N., Balkunde, P. Monitoring of fluoride in water samples using a smartphone. Sci. Total Environ. **2016**, 551-552, 101-107.

73. Soares, S., Torres, K.G., Pimentel, E.L., Martelli, P.B., Rocha, F.R.P. A novel spot test based on digital images for determination of methanol in biodiesel. Talanta. **2019**, 195, 229-235.

74. Muñoz-Serra, M., Serra-Mora, P., Herráez-Hernández, R., Verdú-Andrés, J., Campíns-Falcó, P. A new tool for direct non-invasive evaluation of chlorophyll *a* content from diffuse reflectance measurements. Sci. Total Environ. **2017,** 609, 370-376.

75. Evans, J.R. Photosynthesis and nitrogen relationships in leaves of C3 plants. Oecologia. **1989**, 78 (1), 9-19.

76. Hu, X., Tanaka, A., Tanaka, R. Simple extraction methods that prevent the artifactual conversion of chlorophyll to chlorophyllide during pigment isolation from leaf samples. Plant Methods. **2013**, 9, 19-32.

77. Jifon, J.L., Syvertsen, J.P., Whaley, E. "Growth environment and leaf anatomy affect nondestructive estimates of chlorophyll and nitrogen in Citrus sp. Leaves", J. Amer. Soc. Hort. Sci. **2005**, 130, 152-158.

78. Putra, M.D., Darmawan, A., Wahdini, I., Abasaeed, A.E. "Extraction of chlorophyll from pandan leaves using ethanol and mass transfer study", J. Serb. Chem. Soc. **2017**, 82, 921-931.

79. Delegido, J., Van Wittenberghe, S., Verrelst, J., Ortiz, V., Veroustraete, F., Valcke, R., Samson, R., Rivera, J.P., Tenjo, C., Moreno, J. "Chlorophyll content mapping of urban vegetation in the city of Valencia based on the hypersepectral NAOC index", Ecol. Indic. **2014**, 40, 34-42.

80. Peng, F., Liu, S., Xu, H., Li, Z. A comparative study on the analysis methods for chlorophyll-a. Adv. Mater. Res. **2013**, 726-731, 1411-1415.

81. Richardson, A.D., Duigan, S.P., Berlyn, G.P. "An evaluation of non-invasive methods to estimate foliar chlorophyll content", New Phytol. **2002**, 153, 185-194.

82. Wang, D., Fan, W., Guan, Y., Huang, H., Yi, T., Ji, J. Oxidative stability of sunflower oil flavored by essential oil from *Coriandrum sativum* L. during accelerated storage. LWT-Food Sci. Technol. **2018**, 98, 268-275.

83. BOE-A-1989-2265. Orden de 26 de enero de 1989 por la que se aprueba la Norma de Calidad para los Aceites y Grasas Calentados.

BLOQUE I

ANÁLISIS MEDIANTE ED-XRF

CAPÍTULO 1

Determinación directa del perfil mineral en muestras de cacao en polvo mediante ED-XRF portátil

Food Chemistry, 278 (2019) 373-379

Direct determination by portable ED-XRF of mineral profile in cocoa powder samples

L. Herreros-Chavez, M.L. Cervera, A. Morales-Rubio

Department of Analytical Chemistry, University of Valencia, 50 Dr. Moliner St., 46100 Burjassot, Valencia, Spain

ABSTRACT

The present study has exploited the rapidity of the analysis and the multi-elemental capability of the energy dispersive X- ray fluorescence (ED-XRF) technique for the mineral profile determination in cocoa powder. A fast, cheap and environmental sustainable method without reagent consumption or toxic waste generation has been proposed. The samples can be prepared in the form of pellets of 13 mm in diameter and 2-3 mm thickness. The different internal calibrations used by ED-XRF equipment did not provide accurate results when comparing the mineral profile with the concentration obtained by Inductively Couple Plasma Optical Emission Spectroscopy (ICP-OES) after microwave assisted digestion of samples. For direct ED-XRF analysis of the cocoa samples, an external calibration using as standards the cocoa samples diluted with sugar was prepared. The analytical parameters of Relative Standard Deviation and Limit of Detection for the determined elements are adequate to the concentration levels found in the samples.

Keywords: ED-XRF, cocoa powder, mineral profile, ICP-OES, direct analysis.

1. Introduction

Cocoa is a currently food in the diet of the vast majority of humans, consumed by a vast majority of people due to its taste, texture and excellent organoleptic properties (Villa, Pereira & Cadore, 2015). Cocoa powder is obtained from the cocoa beans, which can be from three different varieties of *Thebroma cacao L*. namely Forastero, Criollo and Trinitario (Afoakwa,

Quao, Takrama, Budu & Saalia, 2013). After harvest, the beans are released from their husks to obtain the seeds and from these, once roasted and pressed, cocoa liquor is produced. Finally, cocoa powder is obtained by partially defatting the liquor (Jacquot et al., 2016).

Cocoa powder contains most of the essential elements for our diet, such as calcium, cobalt, copper, chromium, potassium, iron, zinc (Paredes, Maestre, Prats & Todolí, 2006; Grivetti & Shapiro, 2009). Thus it is important to know the multi-element content including the heavy metal composition of cocoa powder present in the market today. Moreover, the consumption of chocolate and its derivatives have beneficial effects on health such as reducing the risk of cancer, hypertension and diabetes, which are associated with the presence of flavonoids and polyphenols (Fernández-Murga, Tarín, García-Perez & Cano, 2011; Mursu et al., 2004; Romagnolo & Selmin, 2012).

Usually, atomic spectrometric techniques are used for the determination of the mineral profile in cocoa powder and chocolate samples, including Flame Atomic Absorption Spectroscopy (FAAS) (Dahiya, et al., 2005; Ferreira et al., 2008; Güldas, 2008; Shittu & Badmus, 2009; Ieggli, Bohrer, do Nascimento & de Carvalho, 2011; Rehman & Husnain, 2012; Alagić & Huremović, 2015), Graphite Furnace Atomic Absorption Spectroscopy (GFAAS) (Güldas, 2008; Rehman & Husnain, 2012, Sepe, Constatini, Ciaralli, Ciprotti & Giordano, 2001; Jalbani et al., 2007; Ieggli, Bohrer, do Nascimento, de Carvalho & Gobo, 2011; Peixoto, Devesa, Vélez, Cervera, 2016), Inductively Coupled Plasma Optical Emission Spectroscopy (ICP-OES) (Villa et al., 2015; Peixoto et al., 2016; Anthemidis & Pliatsika, 2005; Pedro, de Oliveira & Cadore, 2006; Sager, 2012) and Inductively Coupled Plasma Mass Spectrometry (ICP-MS) (Villa et al., 2015; Sager, 2012; Yanus et al., 2014; Mounicou et al., 2003). However, the use of these techniques usually involves the solubilisation of the samples, including the partial or total destruction of the matrix, with high time analysis, and they are not direct methods. The literature reported methods for cocoa powder and chocolate sample treatment employ microwave assisted digestion (Güldas, 2008; Peixoto et al., 2016; Pedro et al., 2006; Sager, 2012), ultrasound assisted extraction (Jalbani et al., 2007), acid digestion/extraction (Villa et al., 2015; Dahiya et al., 2005; Shittu & Badmus, 2009; Rehman & Husnain, 2012; Alagić & Huremović, 2015; Yanus et al., 2014), dry ashing (Sepe et al., 2001), and emulsion/slurry formation (Ieggli, Bohrer, do Nascimento & de Carvalho, 2011; Ieggli, Bohrer, do Nascimento, de Carvalho & Gobo, 2011; Anthemidis & Pliatsika, 2005).

All these procedures involve a lot of steps, with the drawbacks of contamination and losses during hanging (Viñas et al., 2000).

X-ray fluorescence is an analytical technique of atomic spectroscopy that is highly recommended for the determination of the elemental composition in solid samples and it is also used for the direct analysis of mineral elements in liquids (Beckoff, KanngieBerb, Langhoff, Wedell & Wolff, 2006). This technique involves the bombardment of the samples with high energy radiation, which results in the ionization of the elements of interest and the detection of the corresponding emission of fluorescent energy, being the emitted photon characteristic of a transition between specific electrons in a particular element. The resulting fluorescence can be used to determine the elements present in the sample from Na to U. One of the advantages of the ED-XRF technique is that the analysis can be carried out directly on solid samples and, in case of the portable equipment, in situ analyses are possible. In addition, the required time to measure a sample is relatively low (~ 1 min), avoiding the laborious task of sample digestion and minimizing the possible loss of analytes and/or contamination (Gallardo et al., 2016). Thus, this equipment can be used for quality food control analysis.

Several studies have been published in recent years for the mineral profile determination by ED-XRF in different matrix using green and other methods as an alternative to the conventional ones (Brito, Teixeira & Korn, 2017; Guild, Paltridge, Andersson & Stangoulis, 2017; Mir-Marqués, Martínez-García, Garrigues, Cervera & de la Guardia, 2016; Fernández et al., 2017; Kaur & Kumar, 2016; Bull, Brown & Turner, 2017; Sosa, Guild, Burgos, Bonierbale & Felde, 2018).

The present contribution details the effectiveness of the portable ED-XRF technique for direct quantification of mineral profile in cocoa powder samples and the use of external calibrations employing these samples in order to provide accuracy results.

2. Materials and methods

2.1. Samples

In order to determine the mineral profile of cocoa powder, 19 different samples were purchased in local supermarkets of Valencia. Two powder cocoa-based food preparation original type (brands A and D), two powder

cocoa-based food preparation instant solution in hot and cold milk (brands B and C) and three powder cocoa-based food preparation for consumption after cooking (brands E, F and G). The samples of each brand were acquired in different stores and they were from different lot numbers (2 or 3). A detailed description of the analyzed cocoa powder samples is presented in **Table 1**, including the mineral profile. This data was included in the label of package. Also, a Certified Reference Material Rice flour unpolished Nº10c (National Institute for Environmental Studies, NIES) was employed for quality control and reliability of the method.

2.2. ED-XRF analysis

The analysis of the samples by ED-XRF was performed on pellets of the different pure cocoa samples, and also diluted ones by using glucose or sucrose as inert material. To prepare the pellet, 0.8 g of mass sample were weighed directly into a glass mortar and homogenized with the pistil for 2 minutes. The homogenous samples were introduced into an evacuable pellet die (Specac GS03000, Orpington, UK), pressing at 200 kg cm^{-2} for 2 minutes, after that 13 mm in diameter and 2-3 mm thick pellets were obtained. Three pellets were prepared from each lot of the different commercial brands and diluted ones with the inert sugar, finally all pellets were stored in a desiccator.

For the multi-elemental quantitative analysis of different samples, a portable ED-XRF (Bruker S1TITAN LE SMA-1402, Kennewick, WA, USA) equipped with a rhodium X-ray tube and an X-flash silica detector (50 kV, 15 μA) was used. The equipment has two internal calibrations, namely GeoChem Trace and Restricted Materials Plastic Low Density, which are used depending on the nature of the sample. Each pellet was measured in triplicate by varying its position and orientation between readings which were carried out in 60 seconds, the first 30 s for measure the lowest atomic number elements and the further 30 s to measure the elements with high atomic number.

Table 1. Label information of the different samples analyzed.

Sample type	Brand	Composition
Cocoa based food preparation	A	Ingredients: sugar, skimmed cocoa powder, kola-malted cereal cream, mineral salts, aromas and salt. [Ca]:300 mg/100 g; [Fe]: 15 mg/100 g
	D	Ingredients: sugar, skimmed cocoa powder (25%), dicalcium phosphate, vanilla flavor, salt and cinnamon powder.
Cocoa based food preparation instant solution in hot or cold milk	C	Ingredients: sugar, skimmed cocoa (21.6%), vitamins, minerals, aroma, cinnamon, salt, sunflower oil and emulsifier. [Fe]: 14.7 mg/100 g; [Zn]: 5.5 mg/100 g
	B	Ingredients: sugar, defatted cocoa powder, wheat flour, emulsifier (soy lecitin), aromas and salt.
Cocoa-based food preparation for consumption after cooking	E	Ingredients: sugar, low fat cocoa powder, wheat flour, emulsifier and flavourings.
	F	Ingredients: sugar, skimmed cocoa powder (19%), corn starch and vanilla flavour.
	G	Ingredients: sugar, thickeners, defatted cocoa powder, aromas and salt.

2.3. Reference procedure

For the determination of the mineral profile in the cocoa samples, ICP-OES after microwave assisted digestion was employed. As the microwave digester ("Ethos Sel" Milestone, Sorisole, Italy) carousel has 10 positions, each batch of digestion contains nine sample reactors, three samples in triplicate, and one reactor with the reagent blank.

In a clean TFM polytetrafluoroethylene (PTFE) vessel, 0.5 g of sample was weighed (with an accuracy of 0.1 mg), 4 mL of 69 % nitric acid from Scharlau, (Barcelona, Spain) was added and were predigested inside an ultrasound bath (Selecta, Barcelona, Spain) for 30 min. After that time, 1 mL of 30 % hydrogen peroxide (VWR Prolabo, Equator) was added in 0.25 mL portions and sonicated, leaving 10 minutes between each addition, nitrous oxide vapors (brown) and the formation of foam was observed. In order to reduce the foam, every 2 minutes the reactors were removed from the ultrasound bath and shaken manually for a few seconds until the foam disappears. Finally, 4 mL of ultrapure water (Adrona System, Riga, Latvia) was added. The vessels were introduced in their respective protection shield, closed hermetically and transferred inside the microwave oven. The program consists in 25 minutes to reach 200°C and 15 minutes at 200°C for digestion.

Once the digestion had completed, the reactors were removed from the microwave, cooled and opened inside the fume hood. The liquid was quantitatively transferred to 50 mL polypropylene tubes, collecting the sample drops with ultrapure water and diluting to a final volume of 15 mL.

For the multi-elemental quantitative analysis of the samples, an ICP-OES ("Optima 5300 DV" Perkin-Elmer, Norwalk, CT, USA) spectrometer equipped with AS93-plus automatic sampler was used. A radio frequency power of 1300 W; a plasma Ar flow of 15 L min^{-1}, an auxiliary Ar flow of 0.2 L min^{-1}, a nebulizer Ar flow of 0.8 L min^{-1} and a sample flow of 1.1 mL min^{-1} were employed. 1 mg L^{-1} Rhenium solution (Fluka, Neu-Ulm, Switzerland) was employed as internal standard. All the elements were measured in axial mode (except for Ca and K which were measured in radial mode). The most sensitive emission line, free of spectra interferences, was selected for each element. For the background correction two points were used. Control standards were measured for every series of 10 independent sample measurements. A multielement calibration standard solution containing 26

elements in HNO_3 5 % (Scharlau) was employed. Calibration standard was prepared daily by diluting in the range from 0.005 to 0.5 mg L^{-1}. Additional calibrations for Ca and K from 20 to 200 mg L^{-1} were done using 1000 mg L^{-1} Ca solution (Scharlau) and 1000 mg L^{-1} K solution (Scharlau).

3. Results and discussion

The ED-XRF measurements of the different sample pellets were carried out using the two internal calibration methods incorporated into the portable ED-XRF equipment, named GeoChem method and Low Density method, quantifying metal and non-metal elements. GeoChem method is indicated to analyze geological type samples and Low Density method is suitable for measuring low density plastics.

ED-XRF results were compared with those provided by the ICP-OES determination and none of the concentrations obtained by the two internal calibration methods of ED-XRF resembled those found by ICP-OES. This difference in the results may be due to the fact that the food sample matrix did not fitt into any of the two calibration methods used for the quantification of analytes. This behavior was observed for all the analyzed elements and, as an example, the results for calcium is shown in the **Table 2**. Nevertheless, a certain linearity was observed between the concentration quantified by the ED-XRF (using the GeoChem method) and the concentration measured by reference procedure ICP-OES (See **Fig. 1** in *supplementary material*).

Table 2. Comparison of Ca concentration provided by ED-XRF and ICP-OES.

Samples	[ED-XRF GeoChem] [a] (%, m/m)	[ED-XRF Low Density] [a] (%, m/m)	[ICP-OES] [b] (%, m/m)
A1	0.68 ± 0.02	0.74 ± 0.03	0.258 ± 0.004
A2	0.66 ± 0.03	0.72 ± 0.02	0.252 ± 0.004
A3	0.638 ± 0.016	0.70 ± 0.02	0.27 ± 0.02
B1	0.107 ± 0.006	0.226 ± 0.007	0.0356 ± 0.0014
B2	0.104 ± 0.005	0.212 ± 0.006	0.0363 ± 0.0009
B3	0.117 ± 0.004	0.217 ± 0.005	0.0446 ± 0.0012
C1	0.121 ± 0.009	0.194 ± 0.004	0.037 ± 0.009
C2	0.104 ± 0.004	0.188 ± 0.008	0.0374 ± 0.0006
C3	0.116 ±0.004	0.202 ± 0.005	0.04 ± 0.02
D1	0.40 ± 0.06	0.48 ± 0.06	0.186 ± 0.007
D2	0.44 ± 0.02	0.519 ± 0.012	0.188 ± 0.009
E1	0.128 ± 0.004	0.228 ± 0.009	0.0392 ± 0.0015
E2	0.133 ± 0.007	0.251 ± 0.004	0.0421 ± 0.0018
F1	0.118 ± 0.010	0.204 ± 0.016	0.0359 ± 0.0009
F2	0.155 ± 0.014	0.246 ± 0.018	0.050 ± 0.003
F3	0.147 ± 0.004	0.249 ± 0.005	0.042 ± 0.003
E1	0.316 ± 0.013	0.409 ± 0.012	0.128 ± 0.005
E2	0.347 ± 0.008	0.430 ± 0.011	0.1550 ± 0.0009
E3	0.370 ± 0.009	0.443 ± 0.010	0.1574 ± 0.0012

Notes:

a: the concentration corresponding to the analysis of nine replicates of each sample (three pellets measured by triplicate).

b: the concentration corresponding to the analysis of three replicates of each sample.

Compared to other techniques, the main disadvantages of ED-XRF systems are the high detection limits and the matrix effects (Brito, Teixeira & Korn, 2017). In order to counteract the matrix effect, two external calibration employing sample A1 as standard diluted with glucose or sucrose at different proportions (0, 25, 50, 75 and 100%) were elaborated. The signal intensities of the analytes obtained employing both measurement methods fit very well with the percentage of mass of the samples. The linearity provided by the GeoGhem method was better than that by Low Density one. Both the inert materials (glucose and sucrose) were suitable for diluting the powder cocoa samples, the linearity of the calibration equations were similar. Medium infrared spectroscopy (MIR) analysis of the powder cocoa samples showed sucrose in their composition and, therefore glucose was chosen as inert material for performing the calibrations.

Three external calibrations were performed using the sample A (Lot 1), B (Lot 3) and C (Lot 1) as standard: one cocoa powder original type and two cocoa instant type from two different trademark, employing the concentration of the elements of interest those provided by ICP-OES.

The three different external calibration lines for Ca, K, Fe, Cu and Zn are shown in **Fig. 1**. The signal intensity obtained by the ED-XRF GeoChem method is related to the known concentration of the analyte measured by ICP-OES. As it can be seen in all calibrations a linear relation has been found, regardless of a cocoa powder was used as standard. However, the calibration for Ca presents a higher slope when using sample A than those in which samples B or C were used as standards. This slope difference, corresponding to the analytical signal vs concentration, may be due to the different calcium concentration range in the sample A (273-2600 mg L^{-1}) being 6 times higher than the calcium concentration range found in the other cocoa samples, B and C (51-390 mg L^{-1}).

A statistical study was done for the three calibrations performed. These calibrations are statistically comparable because the intervals overlap for K, Fe, Cu and Zn. In the case of Ca (**Fig 1a**), the two calibrations in the low Ca concentration range were also comparable.

Therefore, for K (**Fig 1b**), Fe (**Fig 1c**), Cu (**Fig 1d**) and Zn (**Fig 1e**) the three calibrations performed were combined in a merged calibration and the signals of the different samples were interpolated on them. In the case of Ca, as mentioned above, it was not possible to perform a merged calibration with

the 3 individual calibrations, but it was possible to perform a merged calibration equation employing the two instant samples (B and C) for quantifying the samples containing low Ca concentration, and the calibration equation provided by sample A for samples containing Ca concentration higher than 400 mg L^{-1}.

Fig. 2 shows the concentration values of the different elements obtained by interpolating the ED-XRF fluorescence intensity in the external calibration lines shown in **Fig. 1** for Ca (**Fig 2a** and **Fig 2b**), K (**Fig 2c**), Fe (**Fig 2d**), Cu (**Fig 2e**) and Zn (**Fig 2f**) versus the concentrations obtained by ICP-OES reference procedure. The difference between the concentrations obtained by ICP-OES and the ED-XRF is minimal, taking into account the low sensitivity of the ED-XRF. As can be seen, the error made when interpolating the samples was relatively low and therefore, it could be concluded that these calibrations would serve for quantifying the cocoa powder samples.

The statistical parameters of the intercepts and the slopes from **Fig. 2** for the five studied analytes show that the intercepts were not different from 0 and the slopes not different from 1. The corresponding means and confidence intervals for the intercepts were Ca: 67 [-48 to 181]; K: 818 [-270 to 1907]; Fe: -11 [-29 to 6]; Cu: 1.4 [-0.2 to 3.1]; Zn: -2.0 [-2.8 to -1.2]. The corresponding means and confidence intervals for the slopes were Ca: 0.82 [0.73 to 0.90]; K: 0.89 [0.73 to 1.04]; Fe: 1.04 [0.90 to 1.17]; Cu: 0.85 [0.70 to 1.01]; Zn: 1.04 [1.00 to 1.07], only in the case of Ca the intercept was slightly lower than 1.

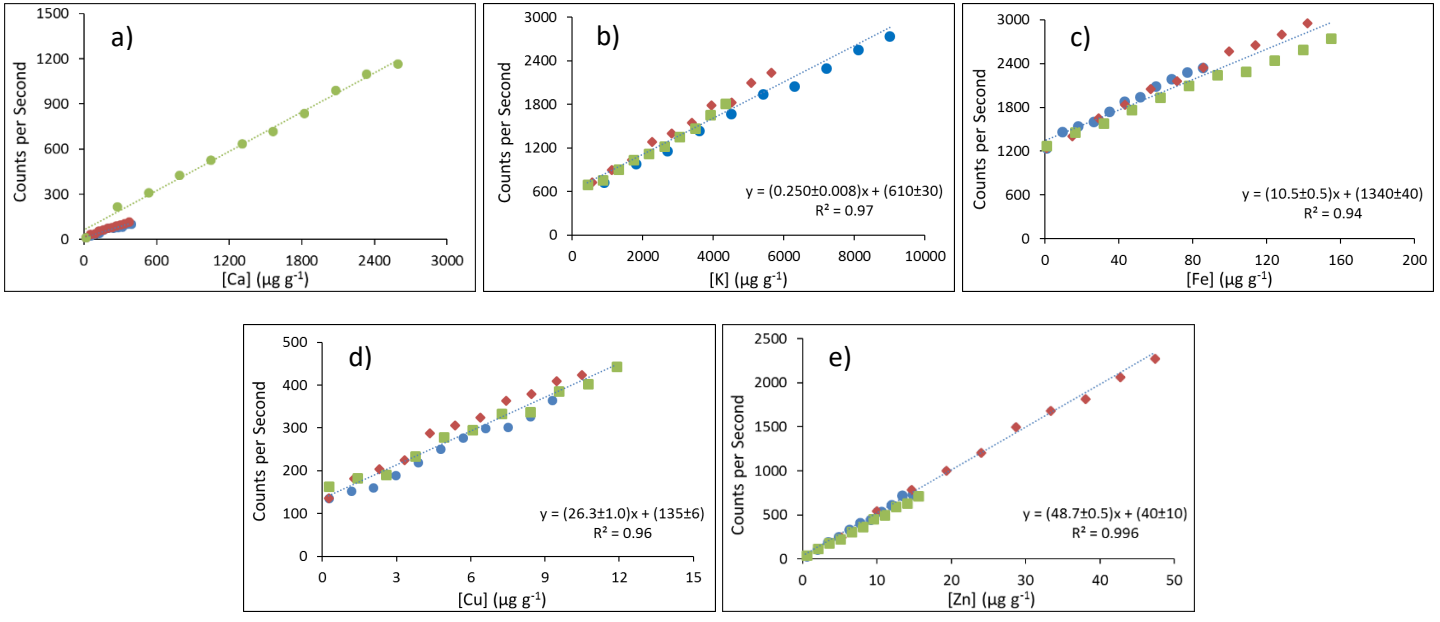

Fig. 1. Representation of the calibrations made from three different cocoa samples (a cocoa based food preparation type original and two cocoa based food preparation instant solution). In the case of K, Fe, Cu and Zn the merged calibration equation were presented. Legend: brand A (Green); brand B (Blue); brand C (Red).

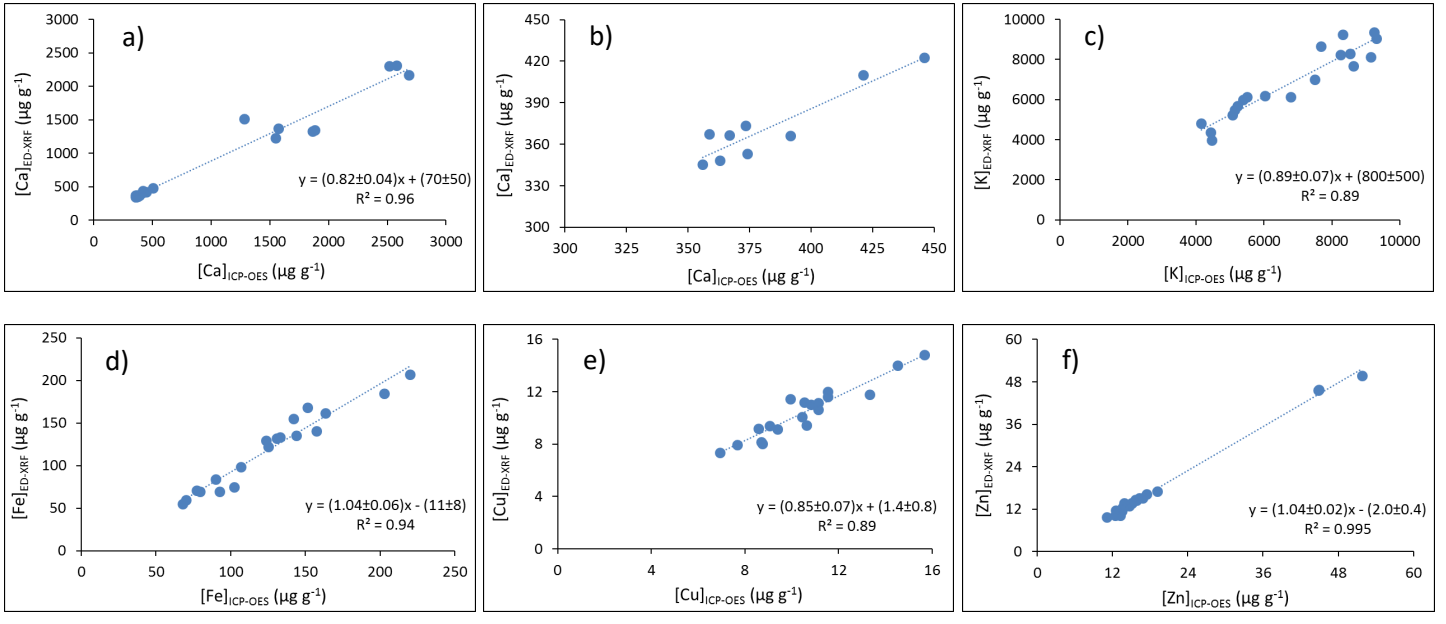

Fig. 2. Relation between ED-XRF concentrations obtained through interpolated intensities in the merged calibration for each analyte and concentration obtained by reference procedure ICP-OES. Additionally, in the case of calcium the low level concentration samples were presented in a more detailed graph.

The reliability of the method was performed analyzing a Certified Reference Material No 10c Rice Flour-Unpolished from National Institute for Environmental Studies (NIES). **Table 3** shows the good agreement between the results found and the certified values for each element. The limits of detection of the proposed method, calculated from 3σ-criterion with the reagent blank (glucose), were significantly lower than their concentration in cocoa powder samples (see **Table 3**). The RSD for the samples was lower than 8 % for all the elements with exception of Ca, in which a mean value of 10 % was obtained in a range of 1.4 to 26 % (see **Table 3**).

Table 3. Limit of detection, relative standard deviation (RSD) and certified reference material values.

Analytes	**Limit of Detection (μg g^{-1})**	**RSD (%)**	**NIES Nº10 Rice Flour-Unpolished Concentration (μg g^{-1})**	
Ca	114[a] 37.7[b]	10 (1.4-26)	**Observed** 96.2 ± 1.1	**Certified** 95 ± 2
K	178	0.9-3	2771 ± 3	2750 ± 100
Fe	14.4	0.7-3	< LOD	11.4 ± 0.8
Cu	1.9	3-8	4.2 ± 0.2	4.1 ± 0.3
Zn	1.7	0.5-6	21.29 ± 0.14	23.1 ± 0.9

Notes: a: Brand A Calibration; b: Join Calibration (Brand B and Brand C)

The suitability of the developed external calibrations for the determination of any cocoa powder samples at any concentration was studied by comparing the concentration obtained for the samples directly analyzed by ED-XRF and the one after the dilution using glucose at different dilution ratio. As can be seen in **Fig. 3**, there is a high correlation between both concentration values, the corresponding equation line was y= (0.971±0.011) x – (23±35), with a correlation coefficient r= 0.991. The confidence interval for the slope [0.95 to 0.99] was around 1, and the confidence interval for the intercept [-93 to 48] included the 0 value. Therefore, no systematic error was carried out when the samples were diluted.

The concentration ranges in the samples of cocoa powder were for K from 4000 to 9300 μg g^{-1}, for Fe from 55 to 207 μg g^{-1}, for Cu from 7 to 15 μg g^{-1} and for Zn from 10 to 50 μg g^{-1}.

In the case of Ca, the ED-XRF signal intensity of the samples were interpolated in the corresponding calibration equation as a function of the Ca content in the sample, being the concentration range from 350 to 2600 µg g^{-1}.

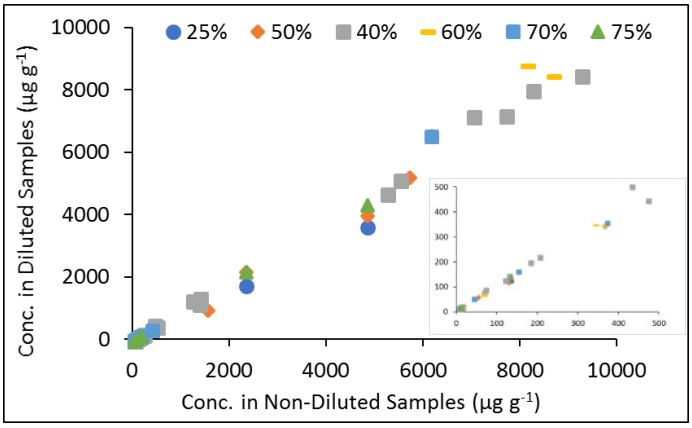

Fig. 3. Relation between the concentration in diluted samples with glucose and non-diluted samples analyzed by ED-XRF.

The mineral profile of chocolate samples depends on the type of sample (white, milk and dark) and also on the percentage of cocoa in the chocolate (Villa et al., 2015; Ieggli, Bohrer, do Nascimento & de Carvalho, 2011). Thus, it was compared our results with contents reported in the literature for powdered cocoa and chocolate for cooking which were closer to our samples. For Ca the concentrations determined by us were very close to literature values for powdered cocoa beverages (median =187, range 149-5723 µg g^{-1}) (Shittu & Badmus, 2009), cocoa powder (1586 µg g^{-1}) (Anthemidis & Pliatsika, 2005), chocolate flavored beverages (559, 116-1680 µg g^{-1}) (Pedro et al., 2006), and cocoa samples (1554, 1298-1741 µg g^{-1}) (Sager, 2012). However, in one literature study on chocolate drink powders the concentrations (11100, 598-18500 µg g^{-1}) (Peixoto et al., 2016) were much higher than in our study. In the case of K, the quantified concentrations were also of the same order than the ones cited in bibliography for chocolate drink powders (8590, 5600-11700 µg g^{-1}) (Peixoto et al., 2016) and chocolate flavored beverages (4640, 1340-6662 µg g^{-1}) (Pedro et al., 2006).

The concentrations obtained for Fe were agree with those found in the literature for powdered cocoa beverages (203, 95-652 µg g^{-1}) (Shittu &

Badmus, 2009), cocoa powder (57-145 μg g^{-1}) (Alagić & Huremović, 2015), chocolate for cooking (21-39 μg g^{-1}) (Alagić & Huremović, 2015), chocolate drink powder (248, 110-340 μg g^{-1}) (Peixoto et al., 2016), cocoa powder (170 μg g^{-1}) (Anthemidis & Pliatsika, 2005), chocolate flavored beverages (54, 44-93 μg g^{-1}) (Pedro, de Oliveira & Cadore, 2006), and cocoa samples (167, 111-450 μg g^{-1}) (Sager, 2012).

Copper contents are in accordance with those found in the literature for powdered chocolate (3.3 μg g^{-1}) (Ferreira et al., 2008), powdered cocoa beverages (9.9, 3.9-25.8 μg g^{-1}) (Shittu & Badmus, 2009), chocolate for cooking (1.2-9.4 μg g^{-1}) (Alagić & Huremović, 2015), chocolate drink powder (9.1, 6-14.9 μg g^{-1}) (Peixoto et al., 2016) and chocolate flavored beverages (4.5, 2.6-6.6 μg g^{-1}) (Pedro et al., 2006). Lower values than reported for cocoa powder (31-38 μg g^{-1}) (Alagić & Huremović, 2015), cocoa powder (52 μg g^{-1}) (Anthemidis & Pliatsika, 2005), and cocoa samples (56, 45-56 μg g^{-1}) (Sager, 2012).

The samples contain a wide concentration range of Zn for both the analyzed samples and data in the literature, namely powdered chocolate (9.0 μg g^{-1}) (Ferreira et al., 2008), cocoa powder (36-80 μg g^{-1}) (Alagić & Huremović, 2015), chocolate for cooking (6-13 μg g^{-1}) (Alagić & Huremović, 2015), chocolate drink powder (18, 11-125 μg g^{-1}) (Peixoto et al., 2016), cocoa powder (75 μg g^{-1}) (Anthemidis & Pliatsika, 2005), chocolate flavored beverages (9, 4-119 μg g^{-1}) (Pedro et al., 2006) and cocoa samples (79, 76-82 μg g^{-1}) (Sager, 2012).

Regarding the origin of the powder cocoa samples, no other data of mineral profile from Spain were found but, on comparing with contents reported in other countries like Brazil (Fe: 44 - 340; Cu: 2.6 - 15, and Zn 4 - 125 mg kg^{-1}) (Ferreira et al., 2008; Peixoto et al., 2016; Pedro et al., 2006), Nigeria (Fe: 95 - 652 and Cu: 4 -26 mg kg^{-1}) (Shittu & Badmus, 2009), Austria (Fe: 111 - 450; Cu: 45 - 56, and Zn: 76 - 82 mg kg^{-1}) (Sager, 2012), Greece (Fe: 170; Cu: 52, and Zn: 75 mg kg^{-1}) (Anthemidis & Pliatsika, 2005), and Bosnia and Herzegovina (Fe: 57 - 144; Cu: 31 - 38, and Zn: 36 - 80 mg kg^{-1}) (Alagić & Huremović, 2015), it was found similar values of Fe similar values of Cu to Brazil and Nigeria and lower than the other countries for Zn similar contents to Bosnia and Herzegovina and lower than the rest of territories.

The concentrations obtained by ED-XRF and ICP-OES were similar to the values reported in the package for brand A (Ca: 3000 μg g^{-1}; in front of 2260

± 80 for ED-XRF and 2590 ± 80 for ICP-OES; Fe: 150 μg g^{-1} in front of 146 ± 14 and 155 ± 10, respectively) and for brand C (Fe: 147 μg g^{-1}; in front of 150 ± 18 and 142 ± 9, respectively; Zn: 55 μg g^{-1} in front of 47 ± 2 and 47 ± 4, respectively).

4. Conclusions

A direct method for mineral profile of cocoa samples by portable ED-XRF has been developed, providing accurate results for Ca, K, Fe, Cu and Zn, in agreement with certified values for Rice flour CRM. The LOD and RSD obtained were adequate for the common concentration of these elements in cocoa powder samples.

Portable ED-XRF has been calibrated employing as standards pellets of cocoa samples diluted with glucose, with high correlation between ED-XRF signal intensity and concentration provided by ICP-OES. The regression between the results found by ED-XRF to the one obtained by ICP-OES provides slope close to 1 with r^2 from 0.89 to 0.995.

The direct and non-destructive developed method was a faster, greener and simpler alternative than conventional acid digestion methods for multielemental determination and can be used in routine analysis due to the high analytical frequency and low cost, without reagent consumption that means no residue generation, in accordance with Green Analytical Chemistry.

5. Acknowledgements

The authors gratefully acknowledge the financial support of the Ministerio de Economia y Competitividad-Feder Project CTQ2016-78053 and CTQ2014-52841.

6. Conflict of interest

There are not conflict of interest between the authors.

Appendix A. Supplementary data

Supplementary data associated with this article can be found in the online version, at doi: 10.1016/j.foodchem.2018.11.065.

7. References

Afoakwa, E. O., Quao, J., Takrama, J., Budu, A. S., & Saalia, F. K. (2013). Chemical composition and physical quality characteristics of Ghanaian cocoa beans as affected by pulp pre-conditioning and fermentation. *Journal of Food Science and Techonology, 50(6)*, 1097-1105.

Alagić, N., & Huremović, J. (2015). Determination of metals contents in various chocolate samples. *Bulletin of the Chemists and Technologists of Bosnia and Herzegovina, 45,* 39-42.

Anthemidis, A. N., & Pliatsika, V. G. (2005). On-line slurry formation and nebulization for inductively coupled plasma atomic spectrometry. Multi-element analysis of cocoa and coffee powder samples. *Journal of Analytical Atomic Spectrometry, 20,* 1280-1286.

Beckoff, B., KanngieBerb, B., Langhoff, N., Wedell, R., & Wolff, H. (2006). *Handbook of Practical X-Ray Fluorescence Analysis*. (1st Ed.) Heidelberg:Springer-Verlag. (Chapter 6).

Brito, G. B., Teixeira, L. S. G., & Korn, M. G. A. (2017). Direct analysis of marine macroalgae for determination of macro minerals by energy dispersive X-ray fluorescence. *Microchemical Journal, 134,* 35-40.

Bull, A., Brown, M. T., & Turner, A. (2017). Novel use of field-portable-XRF for the direct analysis of trace elements in marine macroalgae. *Environmental Pollution, 220*, 228-233.

Dahiya, S., Karpe, R., Hegde, A. G., & Sharma, R. M. (2005). Lead, cadmium and nickel in chocolates and candies from suburban areas of Mumbai, India. *Journal of Food Composition and Analysis, 18(6),* 517-522.

Fernández, Z. H, dos Santos Junior, J. A., dos Santos Amaral, R., Alvarez, J. R. E, da Silva, E. B., de França, E. J., … do Nascimento Santos, J. M. (2017). EDXRF as an alternative method for multielemental analysis of topical soils and sediments. *Environmental Monitoring Assessment, 189 (9),* 447-456. Fernández-Murga, L., Tarín, J. J., García-Perez, M. A., & Cano, A. (2011). The impact of chocolate on cardiovascular health. *Maturitas, 69(4),* 312-321.

Ferreira, H. S., Santos, A. C. N., Portugal, L. A., Costa, A. C. S., Miró, M., & Ferreira, S. L. C. (2008). Pre-concentration procedure for determination of copper and zinc in food samples by sequential multi-element flame atomic absorption spectrometry. *Talanta, 77(1),* 73-76.

Gallardo, H., Queralt, I., Tapias, J., Guerra, M., Carvalho, M. L., & Marguí, E. (2016). Possibilities of low-power X-ray fluorescence spectrometry methods for rapid multielemental analysis and imaging of vegetal foodstuffs. *Journal of Food Composition and Analysis, 50,* 1-9.

Grivetti, L. I., & Shapiro, H. (2009). *Chocolate: history, culture and heritage*. (1st ed.) Hoboken: Wiley (Chapter 1).

Guild, G. E., Paltridge, N. G., Andersson, M. S., & Stangoulis, J. C. R. (2017). An energy-dispersive X-ray fluorescence method for analysing Fe and Zn in common bean, maize and cowpea biofortification programs. *Plant and Soil, 419(1-2)*, 457-466.

Güldas, M. (2008). Comparison of digestion methods and trace elements determination in chocolates with pistachio using atomic absorption spectrometry. *Journal of Food and Nutrition Research, 47(2),* 92-99.

Ieggli, C. V. S., Bohrer, D., do Nascimento, P. C., & de Carvalho, L. M. (2011). Determination of sodium, potassium, calcium, magnesium, zinc and iron in emulsified chocolate samples by flame atomic absorption spectrometry. *Food Chemistry, 124(3),* 1189-1893.

Ieggli, C. S. V., Bohrer, D., do Nascimento, P. C., de Carvalho, L. M., & Gobo, L. A. (2011). Determination of aluminum, copper and manganese content in chocolate samples by graphite furnace atomic absorption spectrometry using a microemulsion technique. *Journal of Food Composition and Analysis, 24(3),* 465-468.

Jacquot, C., Petit, J., Michaux, F., Chávez Montes, E., Dupas, J., Girard, V., & Gaiani, C. (2016). Cocoa powder surface composition during aging: A focus on fat. *Powder Technology, 292,* 195-202.

Jalbani, N., Kazi, T. G., Jamali, M. K. Arain, M. B., Afridi, H. I., Sheerazi, S. T. & Ansari, R. (2007). Application of fractional design and Doehlert matrix in the optimization of experimental variables associated with the ultrasonic-

assisted digestion of chocolate samples for aluminum determination by atomic absorption spectrometry. *Journal of AOAC International, 90(6)*, 1682-1688.

Kaur, J., & Kumar, A. (2016). Element analysis of different varieties of rice samples using XRF technique. *AIP Conference Proceedings, 1728,* 020350-1-4.

Mir-Marqués, A., Martínez-García, M., Garrigues, S., Cervera, M. L., & de la Guardia, M. (2016). Green direct determination of mineral elements in artichokes by infrared spectroscopy and X-ray fluorescence. *Food Chemistry, 196,* 1023-1030.

Mounicou, S., Szpunar, J., Andrey, D., Blake, C., & Lobinski, R. (2003). Concentrations and bioavailability of cadmium and lead in cocoa powder and related products. *Food Additives and Contaminants, 20(4),* 343-352.

Mursu, J., Voutilainen, S., Nurmi, T., Rissanen, T. H., Virtanen, J. K., Kaikkonen, J., & Salonen J. T. (2004). Dark chocolate consumption increases HDL cholesterol concentration and chocolate fatty acids may inhibit lipid peroxidation in healthy humans. *Free Radical Biology and Medicine. 37(9),* 1351-1359.

Paredes, E., Maestre, S. E., Prats, S., & Todolí, J. L. (2006). Simultaneous determination of carbohydrates, carboxylic acids, alcohols, and metals in foods by high-performance liquid chromatography inductively coupled plasma atomic emission spectrometry. *Analytical Chemistry, 78(19),* 6774-6782.

Pedro, N. A. R., de Oliveira, E., & Cadore, S. (2006). Study of mineral content of chocolate flavoured beverages. *Food Chemistry, 95(1)*, 94-100.

Peixoto, R. R. A., Devesa, V., Vélez, D., & Cervera, M. L. (2016). Study of the factors influencing the bioaccessibility of 10 elements from chocolate drink powder. *Journal of Food Composition and Analysis, 48*, 41-47.

Rehman, S., & Husnain, S. M. (2012). Assessment of trace metal contents in chocolate samples by Atomic Absorption Spectrometry. *Journal of Trace Element Analysis, 1(1),* 1-11.

Romagnolo, D. F., & Selmin, O. I. (2012). Flavonoids and Cancer Prevention: A Review of the Evidence. *Journal of Nutrition Gerontology and Geriatrics, 31(3),* 206-238.

Sager, M. (2012). Chocolate and cocoa products as a source of essential elements in nutrition. *Journal of Nutrition Food Science, 2(1),* 1-10.

Sepe, A., Constantini, S. Ciaralli, L., Ciprotti, M., & Giordano, R. (2001). Evaluation of aluminum concentrations in samples of chocolate and beverages by electrothermal atomic absorption spectrometry. *Food Additives and Contaminants. 18(9),* 788-796.

Shittu, T. A., & Badmus, B. A. (2009). Statistical correlations between mineral element composition, product information and retail price of powdered cocoa beverages in Nigeria. *Journal of Food Composition and Analysis, 22(3),* 212-217.

Sosa, P., Guild, G., Burgos, G., Bonierbale, M., & Felde, T. (2018). Potential and application of X-ray fluorescence spectrometry to estimate iron and zinc concentration in potato tubers. *Journal of Food Composition and Analysis. 70,* 22-27.

Villa, J. E. L., Pereira, C. D., & Cadore, S. (2015). A novel and simple acid extraction for multielemental determination in chocolate bars. *Microchemical Journal, 121,* 199-204.

Viñas. P, Pardo-Martínez M, & Hernánadez-Córdoba M. (2000). Rapid determination of selenium, lead and cadmium in baby food samples using electrothermal atomic absorption spectrometry and slurry atomization. *Analytica Chimica Acta, 412(1-2)*, 121-130.

Yanus, R. L., Sela, H., Borojovich, E. J., Zakon, Y., Saphier, M., Nikolski, A., & Karpas, Z. (2014). Trace elements in cocoa solids and chocolate: An ICPMS study. *Talanta, 119,* 1-4.

Appendix A. Supplementary Material

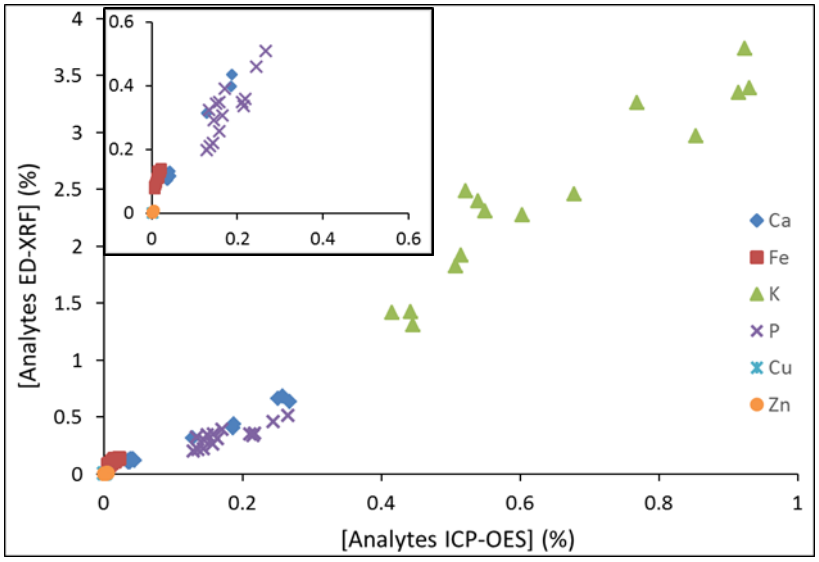

Fig. SM-1. Relation between the concentration obtained by ED-XRF and ICP-OES in cocoa powder samples.

CAPÍTULO 2

Metodología verde para el control de calidad del contenido elemental en leches infantiles en polvo

LWT – Food Science and Technology, 111 (2019) 484-489

Green methodology for quality control of elemental content of infant milk powder

L. Herreros-Chavez, A. Morales-Rubio, M.L. Cervera

Department of Analytical Chemistry, University of Valencia, 50 Dr. Moliner St., 46100 Burjassot, Valencia, Spain

ABSTRACT

A green methodology for the direct determination of elemental content in infant milk powder samples from 0-3 years was developed. A portable energy dispersive X-ray fluorescence (ED-XRF) tool has been used as a direct method for the quantification of five essential elements (Ca, K, Fe, Cu and Zn). For analysis pellets from 0.8 g of each sample weight were made and analyzed. Due to the high dependence of the ED-XRF signal with the sample matrix, external calibrations using cocoa powder diluted with glucose were performed. Infant milk samples were diluted with lactose and the signals were interpolated in the external calibrations. Concentrations obtained by ED-XRF were compared with the concentration found by Inductively Coupled Plasma Optical Emission Spectroscopy (ICP-OES) determination and those indicated in the package label of the corresponding milk samples. Direct determination by ED-XRF provides accurate results, and shows a good correlation with ICP-OES with r^2 values ranging between 0.80 till 0.95. Limits of detection (LOD) were 114, 178, 14, 0.9 and 1.7 µg/g for Ca, K, Fe, Cu and Zn, respectively, being relative standard deviation (RSD) for real milk powder sample analysis lower than 10% for most of the elements.

Keywords: Infant formula, food analysis, essential elements, ED-XRF, ICP-OES.

1. Introduction

Milk is a basic food for humans along the live, being the main source of food in the first months of the baby. Several studies recognize the importance of milk and its derivatives for newborns and children feeding. The World Health Organization (WHO) recommends breast milk as the ideal food for children under 6 months of age (WHO, 2018). Although it is recommended as an ideal food and provides the most health benefits to the infant, many mothers use infant formula due to various factors such as health problems in the mother that can be transmitted to the baby (like human immunodeficiency viruses, mastitis or leukemia), difficulties in producing breast milk, work, or social acceptance of nursing in public (Gruttman & Zimmerman, 2000). The growth and development of infants in the first months depend directly on the ingested diet (Gokhale & Kirschner, 2003; Hulzebos & Sauer, 2007; Zand, Chowdhry, Wray, Pullen & Snowden, 2012; Zand et al., 2011) and a correct feeding in the early stages of life is very important.

The term infant milk powder includes both infant formula and follow-on formula for healthy children. They can be presented as liquid or powdered food and provide most of the nutrients for infants. Therefore, it is important to know the mineral composition of these foods, including essential and toxic elements such as heavy metals (Ikem, Nwankwoala, Odueyungb, Nyavor & Egiebor, 2002; Lesmiewicz, Wroz, Wojcik & Zyrnicki, 2010). It is also of interest to know the trace elements concentration because, they may be essential or toxic to the infants depending on the concentration in which they are found. Regarding the content of metals in foods, the current Spanish legislation (Real Decreto 867/2008, 2008) establishes the composition, labeling and advertising requirements for infant formulas and follow-on formulas, and the European Union sets maximum levels for certain contaminants in foodstuffs (Commission Regulation Nº 1881/2006, 2006).

For the determination of mineral content in milk powder, it is important to perform an efficient digestion of the sample in order to obtain low LODs (Limit of detection) and quantitative, accurate and precise results. For this reason, the most used procedure for analysis of these samples is microwave digestion (Ikem, Nwankwoala, Odueyungb, Nyavor & Egiebor, 2002; Zand, Chowdhry, Wray, Pullen & Snowden, 2012; Zand et al., 2011; Lesmiewicz, Wroz, Wojcik & Zyrnicki, 2010; Oreste et al., 2016; Pereira, Pereira, Schmidt & Moreira, 2013; Sola-Larrañaga & Navarro-Blasco, 2009; Cava-Montesinos, Cervera, Pastor & de la Guardia, 2005; Bu-Hamdi, Al-Harbi & Anderson, 2016)

followed by analyte determination of digested samples using a spectroscopic technique. Among the detection techniques, Flame Atomic Absorption Spectroscopy (FAAS) (Sola-Larrañaga & Navarro-Blasco, 2009; Zamir & Hussain, 2001; Yaman & Çokol, 2004), Electrothermal Atomic Absorption Spectroscopy (ETAAS) (Campillo, Viñas, López-Garcia & Hernández-Córdoba, 1998; Miller-Ihli, 1997), Inductively Coupled Plasma Optical Emission Spectroscopy (ICP-OES) (Badgat, Baran & Tokay, 2014; Ikem, Nwankwoala, Odueyungb, Nyavor & Egiebor, 2002; Zand, Chowdhry, Wray, Pullen & Snowden, 2012; Zand et al., 2011; Oreste et al., 2016; Pereira, Pereira, Schmidt & Moreira, 2013; Durovic et al., 2017; Dolan & Capar, 2002) or Inductively Coupled Plasma Mass Spectrometry (ICP-MS) (Zand, Chowdhry, Wray, Pullen & Snowden, 2012; Zand et al., 2011, Cava-Montesinos, Cervera, Pastor & de la Guardia, 2005; Bu-Hamdi, Al-Harbi & Anderson, 2016; Pozebon, Dressler & Curtius, 1998) have been employed. The microwave treatment is time consuming and requires the use of concentrated acids for complete destruction of the matrix.

A greener alternative to those techniques is the direct determination of the mineral content using X-ray fluorescence by both energy dispersive (ED-XRF) and wavelength dispersive (WD-XRF) methods. This equipment allows the direct measurement of the samples, which minimizes the sample preparation. The minimal manipulation of the samples reduces the risk of analyte loss, and the use of corrosive and toxic reagent is avoided. Moreover, it does not generate residues of any type and the energy consumption employed is relatively low.

In the last few years, numerous studies of the mineral profile in samples of infant milk powder using both WD-XRF (Fernandes, Brito & Gonçalves, 2015; Perring & Andrey, 2004; Perring, Andrey, Basic-Dvorzak & Blanc, 2005; Perring & Blanc, 2008a; Pashkova, 2009) and ED-XRF (Gunicheva, 2010; Jolly et al., 2017; Perring & Andrey, 2003; Perring, Andrey, Basic-Dvorzak & Hammer, 2005; Perring & Blanc, 2008b) have appeared.

The aim of this work is the development of a direct and fast methodology to quantify the elemental content of Ca, K, Fe, Cu and Zn in infant milk powder using ED-XRF. Twenty infant milk samples were analyzed and X-ray line counting rates obtained by ED-XRF measurement were interpolated in an external calibration. On the other hand, these concentrations were compared to those obtained by ICP-OES and with the values labeled in the package of the different analyzed samples.

2. Materials and methods

2.1. Samples

Twenty infant milk powder samples from 8 different brands were analyzed in this study. The samples were classified in three groups, from 0 to 6 months (Brand A, B, C, D, E, F, G and H), from 6 to 12 months (Brand I, J, K, L, M and N) and from 1 to 3 years old (Brand O, P, Q, R, S and T). Four lots of each brand sample were acquired in different stores (Lots 1 to 4). Additionally, a standard reference material Non-Fat Milk Powder (NIST-1549, National Institute of Standards and Technology, Gaithersburg, MD, USA) was analysed. A description of the infant milk powder samples and their mineral composition indicated in the package label is presented in the **Table 1**.

2.2. Statistical analysis

The statistical analysis was done employing analysis of data tool (regression) from Microsoft Excel software. The regression analysis tool performs linear regression analysis using the "least squares" method to fit a line to a set of observations. It can analyze the way in which the values of one or more independent variables affect a dependent variable.

The uncertainties were calculated employing the function “desvest” from Microsoft Excel software. The standard deviation is calculated with “n-1” method. “Desvest” uses the following formula:

$$\sqrt{\frac{\sum(x-\bar{x})^2}{(n-1)}}$$

Where “x” is each value of the sample, “$\bar{x}$” is the average of the sample and “n” is the size of the samples.

2.3. ED-XRF analysis

For the determination of elemental content by ED-XRF analysis, pellets from pure milk powder and pellets from milk diluted using lactose as inert material were made. To prepare the sample pellets, 0.8 g of milk powder were weight directly into a glass mortar and homogenized with the pestle for 2 minutes. The homogenous sample was introduced into an evacuable pellet die Specac

GS03000 (Orpington, UK) pressed at 1961.3 Pa for 2 minutes, and 13 mm of diameter and 2-3 mm of thickness pellets were obtained. Three pellets were prepared from each lot of the different commercial brands diluted ones with lactose (0.8 g of milk powder plus lactose), which were stored in a desiccator. Each pellet was analyzed three times by changing the position and orientation between readings.

The equipment used in the multi-elemental quantitative analysis was a portable ED-XRF from Bruker S1 TITAN LE SMA-1402 (Kennewick, WA, USA) with a rhodium tube (maximum voltage of 50 kV and maximum amperage of 15 μA, employing in the analysis 50 kV and 7 μA, respectively) and a X-FLASH Silicon drift detector (SDD) with a high energy resolution of 147 eV at Mn KαGeoChem Trace internal application was chosen for milk powder samples analysis. Each measurement takes 60 seconds: during the first 30 s the lowest atomic number elements (from Mg with 12 till Cr with 24 atomic number) are measured, while the elements with higher atomic number (from Mn with 25 till U with 92 atomic number) are measured in the last 30 s.

Table 1. Description and mineral composition of infant milk powder samples, values reported in the package label of each brand.

Age Group	Type	Brand	Ca (µg/g)	Cu (µg/g)	Fe (µg/g)	K (µg/g)	Zn (µg/g)
0-6 months	Milk-based	A	3380	3.10	31	4620	31
	Milk-based	B	3720	3.72	58	5690	45
	Milk-based	C	5040	3.60	50	5510	40
	Lactose-free formula	D	3850	3.85	60	5000	46
	Designed to avoid regurgitation formula	E	4200	3.80	61	6400	51
	Regular milk	F	3300	3.20	32	5250	39
	Designed to avoid regurgitation formula	G	3530	4.40	49	5500	50
	Designed to avoid regurgitation formula	H	3570	3.00	40	5500	36
6-12 months	Milk-based	I	5000	3.00	80	6200	40
	Lactose-free formula	J	6200	3.60	80	5900	53
	Milk-based	K	5810	4.02	84	5630	53
	Milk-based	L	5030	3.52	91	6220	40
	Milk-based	M	4800	4.00	73	5550	47
	Milk-based	N	82*	0.57*	1.2*	83*	0.75*
	Milk-based	O	5770	3.80	78	5700	57
	Milk-based	P	5400	1.83	73	6000	29
1-3 years	Milk-based	Q	5750	3.70	76	5500	53
	Milk-based	R	6400	NI	83	NI	55
	Milk-based	S	5350	1.45	73	6010	29
	Milk-based	T	7900	3.45	80	8600	50

Note: values * in mg/100 mL of reconstituted product; NI: concentration not indicated in the package label.

2.4. Reference method

A microwave-assisted acid digestion system "Ethos Sel" Milestone (Sorisole, Italy), equipped with a temperature probe, was used to digest the samples. As the microwave digester carousel has 10 positions, each batch of digestion contains nine sample reactors, three samples in triplicate, and one reactor with a reagent blank.

Approximately 0.5 g of sample was weighed, with a precision of 0.1 mg, in a polytetrafluoroethylene modified (TFM) vessel and 4 mL of 15.4 mol/L HNO_3 from Scharlau (Barcelona, Spain) was added, then the vessel was placed into an ultrasound bath from Selecta (Barcelona, Spain) for 30 min. After this time, 1 mL of 12.3 mol/L H_2O_2 from Scharlau (Barcelona, Spain) was carefully added and placed again in the ultrasound bath, observing the evolution of nitrous oxide vapors (brown) and the foam formation. In order to reduce the foam, every 5 minutes the reactors were removed from the ultrasound bath and shaken manually for a few seconds until the foam disappears. Finally, 4 mL of ultrapure water Adrona System (Riga, Latvia) was added. The vessels were introduced in their respective protection shield, closed hermetically and transferred to the microwave oven digester. The digestion program consists of a progressive increase of temperature up to reach 200 °C for 25 minutes with a maximum exit power of 500 W and the digestion at 200 °C for 15 minutes with a maximum exit power of 900 W.

Once the digestion had completed, the reactors were removed from the microwave oven, cooled and opened inside a fume hood. The liquid was quantitatively transferred to 50 mL polypropylene tubes, collecting all the sample drops with ultrapure water and diluting to a final volume of 15 mL.

An ICP-OES spectrometer “Optima 5300 DV” from Perkin-Elmer (Norwalk, CT, USA) equipped with AS93-plus automatic sampler was used to analyze the elements in the digested samples. A radio frequency power of 1300 W; a plasma Ar flow of 15 L/min, an auxiliary Ar flow of 0.2 L/min, a nebulizer Ar flow of 0.8 L/min and a sample flow of 1.1 mL/min were employed. A 1 mg/L Rhenium solution from Fluka (Neu-Ulm, Switzerland) was used as an internal standard. All the elements were measured in axial mode (except for Ca and K which were measured in radial mode). The most sensitive emission line, free of spectral interferences, was selected for each element. For the background correction, two points were used. Control standards were measured for every series of 10 independent sample measurements. A

multielement calibration standard solution containing 26 elements in HNO_3 of 1.20 mol/L from Scharlau (Barcelona, Spain) was employed. Calibration standard was prepared daily by dilution in the range 0.025 to 5 mg/L. Additionally, a calibration for Ca from 20 till 200 mg/L and for K from 50 till 500 mg/L was prepared from 1000 mg/L solution from Scharlau (Barcelona, Spain).

3. Results and discussion

3.1. ED-XRF results

Previous studies carried out for the determination of elemental content in food matrices by ED-XRF concluded that the values of the concentration obtained by ED-XRF using the available internal applications (GeoChem Trace and Restricted Materials Plastic Low Density) did not agree with the concentrations obtained through the reference method by ICP-OES. Nevertheless, a linear regression between the ED-XRF counts per second and the concentration of sample in cocoa pellets diluted with glucose was found (Herreros-Chavez, Morales-Rubio & Cervera, 2019).

For this reason, an external calibration with a cocoa based food preparation diluted with glucose was done. The signals (counts per second) obtained by the ED-XRF GeoChem application versus the known concentration of the analyte measured by ICP-OES were shown in **Fig. 1**. The ranges of concentrations determined in the performed external calibration were from 0 to 2600 μg/g for Ca, from 0 to 4400 μg/g for K, from 0 to 160 μg/g for Fe, from 0 to 12 μg/g for Cu and from 0 to 15 μg/g for Zn.

The signals counts per second obtained by ED-XRF were interpolated in these calibration equations for sample analysis. Due to the high concentrations of Ca, K and Zn in milk samples (Ca: 3300-7900 μg/g; K: 4600-8600 μg/g; Zn: 29-57 μg/g) which were out of the calibration ranges, those were diluted with an inert sugar (lactose) in order to be inside of the external calibration.

Table 2 shows the comparison among the concentrations of the five elements quantified by ED-XRF, the concentration obtained by ICP-OES and the concentration labeled in the package of each sample, respectively.

As it can be seen in **Table 2**, the concentrations obtained by the three different ways, the concentrations quantified by external calibration and those obtained by reference method and the contents indicated in the package label, agreed between them.

Spanish legislation establishes the minimum and the maximum value of the five elements analyzed in infant formulas. For Ca the values are between 50 till 140 mg, for K values are between 60 till 160 mg, for Fe values are between 0.3 till 1.3 mg, for Cu values are between 35 till 100 μg and for Zn the values are between 0.5 till 1.5 mg, respectively, per 100 kcal of infant milk powder. Taking into account the range from 449 to 519 kcal per 100 g of the analyzed milk powder in the present study, with a mean value of 486, for conversion the mineral content in μg/g to mg per 100 kcal multiply by 10 and divide by 486 the μg/g values. It should be noted that in the present work, all the analyzed samples are inside these ranges of concentration.

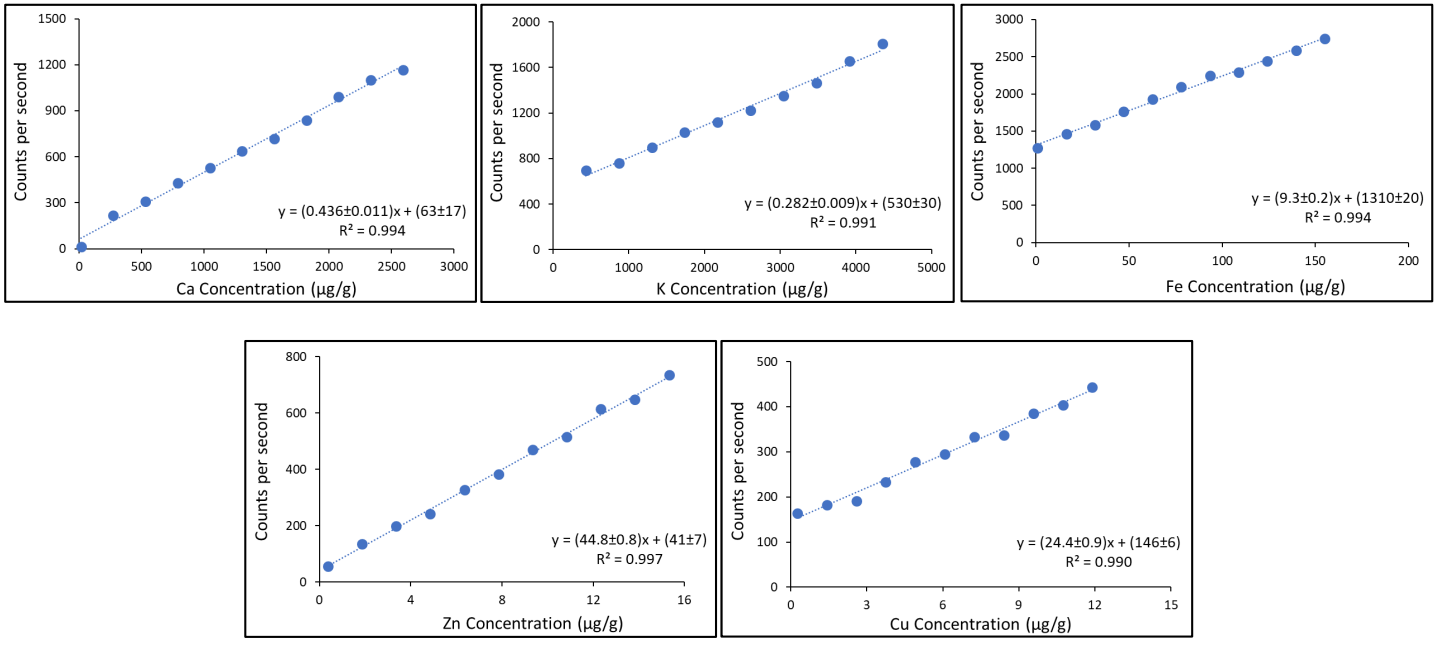

Fig. 1. Representation of ED-XRF GeoChem method signal (in counts per second) in front of ICP-OES analyte concentration employing a cocoa based food preparation.

Table 2. Concentration obtained by external calibration ED-XRF, ICP-OES and package label of each sample analyzed, expressed in µg/g as m ± s.

Samples	Ca			K		
	ED-XRF	**ICP-OES**	**Label**	**ED-XRF**	**ICP-OES**	**Label**
A	4150 ± 40	3900 ± 100	3380	4500 ± 100	4840 ± 90	4620
B	4160 ± 30	4000 ± 100	3720	4940 ± 90	5100 ± 100	5690
C	5240 ± 60	5000 ± 100	5040	4800 ± 100	4900 ± 100	5510
D	3150 ± 5	3020 ± 10	3580	4510 ± 70	4532 ± 5	5000
E	4830 ± 40	4400 ± 200	4200	7020 ± 80	7300 ± 300	6400
F	3560 ± 30	3070 ± 40	3300	4630 ± 60	5100 ± 200	5250
G	3180 ± 60	3090 ± 40	3530	5010 ± 50	5000 ± 100	5500
H	3330 ± 20	3230 ± 60	3570	4850 ± 90	4880 ± 70	5500
I	4730 ± 80	4600 ± 100	5000	5110 ± 60	5500 ± 100	6200
J	6800 ± 200	6300 ± 200	6200	5800 ± 100	6300 ± 200	5900
K	6360 ± 30	6200 ± 100	5810	4960 ± 30	5300 ± 100	5630
L	5300 ± 500	4950 ± 40	5030	6300 ± 700	6500 ± 70	6220
M	5000 ± 100	4820 ± 60	4800	4700 ± 400	5200 ± 100	5550
N	6580 ± 40	6280 ± 80	6900	5000 ± 50	5410 ± 10	5000
O	5990 ± 40	5470 ± 40	5770	5200 ± 100	5420 ± 40	5700
P	5590 ± 30	5700 ± 100	5400	4730 ± 70	5350 ± 70	6000
Q	5830 ± 100	5500 ± 200	5750	5000 ± 200	5700 ± 200	5500
R	6600 ± 50	6630 ± 20	6400	6300 ± 200	7000 ± 30	NI
S	6500 ± 400	6400 ± 200	5350	5470 ± 40	5500 ± 100	6010
T	6700 ± 400	7000 ± 100	7900	7300 ± 600	7800 ± 200	8600

Table 2. Continuation.

Samples	Fe			Cu			Zn		
	ED-XRF	**ICP-OES**	**Label**	**ED-XRF**	**ICP-OES**	**Label**	**ED-XRF**	**ICP-OES**	**Label**
A	56.7 ± 0.2	57.9 ± 0.3	31	3.6 ± 0.2	3.37 ± 0.07	3.1	43.1 ± 1.0	40.5 ± 0.7	31
B	57.5 ± 0.4	56.8 ± 1.2	58	3.6 ± 0.3	3.78 ± 0.03	3.72	45.28 ± 0.08	43.5 ± 1.5	45
C	47.5 ± 0.7	47.9 ± 0.9	50	3.9 ± 0.3	3.88 ± 0.08	3.6	37.9 ± 1.2	35.3 ± 0.8	40
D	57.2 ± 0.5	56.0 ± 0.8	60	4.17 ± 0.16	4.06 ± 0.02	3.85	47.17 ± 0.05	42.2 ± 0.7	46
E	49.6 ± 0.2	55 ± 4	61	4.4 ± 0.4	4.8 ± 0.3	3.8	51 ± 4	49.8 ± 1.0	51
F	27.4 ± 0.8	25.3 ± 1.0	32	2.80 ± 0.09	2.91 ± 0.13	3.2	34.9 ± 0.6	31.4 ± 0.7	39
G	43.7 ± 1.4	44.00 ± 0.14	49	3.7 ± 0.4	3.87 ± 0.07	4.4	38.9 ± 0.7	37.4 ± 0.2	50
H	35.5 ± 1.6	38.0 ± 0.6	40	3.0 ± 0.2	3.14 ± 0.04	3	35.5 ± 0.9	35.6 ± 0.3	36
I	72.7 ± 0.8	71.7 ± 1.8	80	2.98 ± 0.03	3.43 ± 0.05	3	33.58 ± 0.12	32.9 ± 0.8	40
J	70.4 ± 1.0	82 ± 4	80	3.32 ± 0.19	4.028 ± 0.003	3.6	52 ± 2	50 ± 2	53
K	78.5 ± 0.5	79.8 ± 1.4	84	4.06 ± 0.07	3.89 ± 0.08	4.02	44.4 ± 0.9	46.4 ± 1.4	53
L	73.7 ± 0.7	76.4 ± 0.7	91	3.0 ± 0.2	2.96 ± 0.05	3.52	46 ± 4	44.5 ± 0.2	40
M	63.1 ± 0.6	61 ± 2	73	4.02 ± 0.10	3.99 ± 0.14	4	43 ± 3	40.0 ± 1.2	47
N	77.4 ± 1.1	82.2 ± 0.6	80	3.96 ± 0.13	4.24 ± 0.04	4.1	43.82 ± 0.12	47.7 ± 0.9	50
O	67.1 ± 0.9	69.6 ± 1.0	78	3.8 ± 0.3	3.81 ± 0.11	3.8	49.8 ± 0.3	46.0 ± 1.2	57
P	67.6 ± 0.5	69.0 ± 0.6	73	1.8169 ± 0.0016	1.46 ± 0.02	1.83	25.67 ± 0.15	26.6 ± 0.4	29
Q	67.3 ± 0.9	73 ± 4	76	3.4 ± 0.5	4.2 ± 0.2	3.7	52.6 ± 0.9	48.5 ± 1.4	53
R	69.2 ± 1.6	70.1 ± 0.4	83	1.4 ± 0.2	2.09 ± 0.07	NI	45.1 ± 0.3	51 ± 2	55
S	66.4 ± 0.2	71.2 ± 1.1	73	1.23 ± 0.04	1.24 ± 0.02	1.45	29.6 ± 0.5	27.6 ± 0.4	29
T	66.90 ± 0.09	75 ± 2	80	4.46 ± 0.12	4.53 ± 0.12	3.45	46 ± 7	44.7 ± 1.1	50

Note: average corresponding to 9 and 3 replicates in the case of ED-XRF (energy dispersive x-ray fluorescence) and ICP-OES (inductively coupled plasma optical emission spectroscopy), respectively. NI: no indicated in the package label.

The correlation between the concentration obtained by interpolation of the ED-XRF signal in the external calibration and the concentration obtained by ICP-OES (**Fig. SM-1** shown in supplementary material) was also determined. **Table 3** shows the statistical parameters for the correlation between the concentrations obtained by the proposed method in front of the concentrations obtained by ICP-OES for the five studied analytes. For Ca and Zn, the 1 value was included inside the confidence intervals of the slope, and for K, Fe and Cu which were very close. No significant differences were found between both methodologies, with high correlations between the concentrations obtained by the proposed method and those given by the reference method.

Table 3. Statistical parameters of the values obtained by ED-XRF in comparison with the results obtained by reference procedure ICP-OES.

Analyte	Determination coefficient (R^2)	Slope (b)	Confidence interval (95%)
Ca	0.95	1.027 ± 0.009	[1.009;1.046]
K	0.85	0.947 ± 0.010	[0.927;0.968]
Fe	0.95	0.964 ± 0.007	[0.949;0.979]
Cu	0.88	0.955 ± 0.016	[0.921;0.988]
Zn	0.80	1.018 ± 0.013	[0.991;1.046]

3.2. Comparison ICP-OES and package label concentrations

The concentrations measured by ICP-OES after microwave assisted digestion for Ca, Cu, Fe, K, Mg, Mn, Na, P, Se and Zn were compared with the mineral content labeled on the packages (see supplementary material **Fig. SM-2**). There is a high correlation between both concentrations, corresponding to the equation line y = (0.980 ± 0.008) x, with a determination coefficient r^2 = 0.990 for the ten elements. The confidence interval for the slope was from 0.964 to 0.995, very close to 1, which shows the agreement between both values (ICP-OES and package label).

3.3. Sample dilution with inert sugar lactose

The suitability of the developed external calibration for the determination of any infant milk powder sample at any concentration was studied by comparing the concentrations obtained for the samples directly measured by ED-XRF and after dilution using lactose at different dilution ratio. As it can be seen in **Fig. 2**, there is a high correlation between both concentration values, corresponding to the equation line y= (1.05 ± 0.02) x for Fe (Fig 2a), with a determination coefficient r^2 = 0.99 and y = (1.18 ± 0.08) x for Cu (Fig 2b), with a determination coefficient r^2 = 0.85. The confidence interval for the slope were 1.01 to 1.09 and 1.00 to 1.35 for Fe and Cu, respectively, both close to 1. Therefore, no systematic error was carried out when the samples were diluted with lactose.

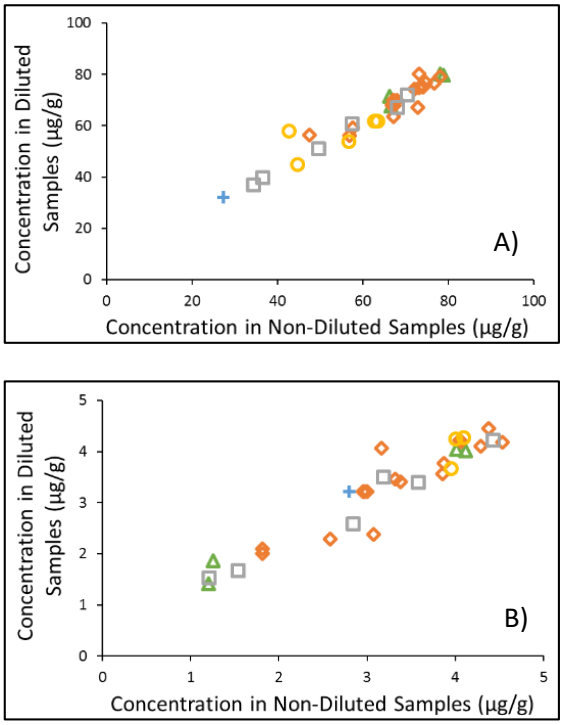

Fig. 2. Relation between the concentration in diluted samples with lactose and non-diluted samples analyzed by ED-XRF for iron (2A) and copper (2B). Note: ▲: 25 % diluted (green); ♦: 30 % diluted (orange); ■: 35 % diluted (grey); ●: 40 % diluted (yellow); +: 50 % diluted (blue).

3.4. Analytical parameters of developed procedure

The accuracy of the method was confirmed by analyzing a Standard Reference Material (SRM) 1549 Non-Fat Milk Powder from NIST. **Table 4** shows the good agreement between the results found and the certified values of each element; only in the case of K the confidence intervals did not overlap. As it can be seen in **Table 4**, the limits of detection of the proposed method for the elements, calculated from 3σ-criterion with the reagent blank (lactose), were significantly lower than their concentration in infant milk powder. Relative standard deviation (RSD) for the samples was lower than 10 % for all the elements except for Cu, in which a mean value of 9 % was obtained in a range from 2 till 14 % (see **Table 4**), being the mean values of RSD 3, 3, 1.5 and 4 % for Ca, K, Fe and Zn, respectively. The RSD values prove the high precision of the proposed methodology of direct analysis.

Table 4. Limit of detection (LOD), relative standard deviation (RSD) for analyzed samples and standard reference material values.

Analytes	Limit of Detection (μg/g)	RSD (%) (n=20)	NIST 1549 Non-Fat Milk Powder Concentration (μg/g)	
			Observed (n=9)	Certified
Ca	114	0.7-7	13000 ± 600	13000 ± 500
K	258	0.8-5	15300 ± 200	16900 ± 300
Fe	0.2	0.4-3	1.60 ± 0.15	1.78 ± 0.10
Cu	0.09	2-14	0.6 ± 0.2	0.70 ± 0.10
Zn	2	1.1-10	47 ± 4	46 ± 2

Note: values calculated from 9 measurements per sample.

4. Conclusions

ED-XRF using external calibration permits the direct quantification of Ca, K, Fe, Cu and Zn in infant milk powder with RSD lower than 10% and results in agreement with certified concentrations in non-fat milk powder SRM. The linear regression between the results found by ED-XRF to results obtained by ICP-OES in the twenty-studied infant milk powder provides r^2 values from 0.80 to 0.95 for the five analytes. The concentrations obtained by ICP-OES were comparable with the concentrations indicated in the package label.

The direct and green developed method is faster, cheaper and simpler than the conventional acid digestion ones for multielemental determination. This green methodology can be used for quality control and routine analysis in milk powder samples with no reagent consumption that means no residue generation, in accordance with Green Analytical Chemistry.

5. Conflict of interest

There are not conflicts of interest between the authors. The authors declare no competing financial interest.

6. Acknowledgments

Authors gratefully acknowledge the financial support of the Ministerio de Ciencia, Innovacion y Universidades-Agencia Estatal de Investigación-FEDER (EU) (Project CTQ2016-78053-R).

Appendix A. Supplementary data

Supplementary data associated with this article can be found in the online version, at doi: 10.1016/j.lwt.2019.05.055

7. References

Bagdat, S., Baran, E. K., & Tokay, F. (2014). Element fractionation analysis for infant formula and food additives by inductively coupled plasma optical emission spectrometry. *International Journal Food Science and Technology*, *49*, 392-398.

Bu-Hamdi, M. A., Al-Harbi, M., & Anderson, A. K. (2016). Assessment of the nutritionally essential minerals and physiochemical properties of infant milk food commercially available in Kuwait. *International Journal of Agricultural Science and Food Technology*, *2 (1)*, 1-8.

Campillo, N., Viñas, P., López-Garcia, I., & Hernández-Córdoba, M. (1998). Direct determination of copper and zinc in cow milk, human milk and infant formula samples using electrothermal atomization atomic absorption spectrometry. *Talanta*, *46,* 615-622.

Cava-Montesinos, P., Cervera, M. L., Pastor, A., & de la Guardia, M. (2005). Room temperature acid sonication ICP-MS multielemental analysis of milk. *Analytica Chimica Acta*, 531, 111-123.

Commission Regulation (EC) No 1881/2006 of 19 December 2006 and amendments. Setting maximum levels for certain contaminants in foodstuffs, https://eur-lex.europa.eu/legal-content/EN/TXT/PDF/?uri=CELEX:02006R1881-20140901&from=ES/ Accessed 6 November 2018.

Dolan, S. P., & Capar, S. G. (2002). Multi-element analysis of food by microwave digestion and inductively coupled plasma-atomic emission spectrometry. *Journal of Food Composition and Analysis, 15,* 593-615.

Durovic, D., Milisavljevic, B., Nedovic-Vukovic, M., Potkonjak, B., Spasic, S., & Vrvic, M. M. (2017). Determination of microelements in human milk and infant formula without digestion by ICP-OES. *Acta Chimica Slovenica, 64*, 276-282.

Fernandes, T. A. P., Brito, J. A. A., & Gonçalves, L. M. L. (2015). Analysis of micronutrients and heavy metals in Portuguese infant milk powders by Wavelength Dispersive X-Ray Fluorescence Spectrometry (WD-XRF). *Food Analytical. Method*s, *8,* 52-57.

Gokhale, R., & Kirschner, B. S. (2003). Assessment of growth and nutrition. *Best Practice and Research: Clinical Gastroenterology, 17,* 153-162.

Gunicheva, T. N. (2010). Advisability of X-ray fluorescence analysis of dry residue of cow milk applied to monitor environment. *X-Ray Spectrometry*, *39*, 22-27.

Gruttman, N., & Zimmerman, D. R. (2000). Low-income mothers' views on breastfeedings. *Social Science & Medicine, 50*, 1457-1473.

Herreros-Chavez, L., Morales-Rubio, A., & Cervera, M.L. (2019). Direct Determination by Portable ED-XRF of Mineral Profile in Cocoa Powder Samples. *Food Chemistry, 278, 373-379*.

Hulzebos, C. V., & Sauer, P. J. J. (2007). Energy requirements. *Seminary in Fetal and Neonatal. Medicine*, *12*, 2-10.

Ikem, A., Nwankwoala, A., Odueyungb, S., Nyavor, K., & Egiebor, N. (2002). Levels of 26 elements in infant formula from USA, UK and Nigeria by microwave digestion and ICP-OES. *Food Chemistry, 77,* 439-447.

Jolly, Y. N., Iqbal, S., Rahman, M. S., Kabir, J., Akter, S., & Ahmad, I. (2017). Energy dispersive X-ray fluorescence detection of heavy metals in Bangladesh cows' milk. *Heliyon*, *3 (9),* 1-22.

Lesmiewicz, A., Wroz, A., Wojcik, A., & Zyrnicki, W. (2010). Mineral and nutritional analysis of Polish infant formulas. *Journal of Food Composition and Analysis, 23,* 424-431.

Miller-Ihli, N. J. (1997). Slurry sampling electrothermal atomic absorption spectrometry: results from the second phase of an international collaborative study. *Journal of Analytical Atomic Spectrometry, 12,* 205-212.

Oreste, E.Q., de Souza, A., Pereira, C. C., Lisboa, M. T., Cidade, M. J. A., Vieira, … & Ribeiro, A. S. (2016). Evaluation of sample preparation methods for the determination of Ca, Cu, Fe, K and Na in milk powder samples by ICP-OES. *Food Analytical Methods*, *9*, 777-784.

Pashkova, G. V. (2009). X-ray fluorescence determination of element contents in milk and dairy products. *Food Analytical Methods, 2*, 303-310.

Pereira, J. S. F., Pereira, L. S. F., Schmidt, L., & Moreira, C. M. (2013). Metals determination in milk powder samples for adult and infant nutrition after focused-microwave induced combustion. *Microchemical J*ournal, *109*, 29-35.

Perring, L., & Andrey, D. (2003). ED-XRF as a tool for rapid minerals control in milk-based products. *Journal of Agricultural and Food Chemistry*, *51,* 4207-4212.

Perring, L., & Andrey, D. (2004). Wavelength-dispersive x-ray fluorescence measurements on organic matrices: application to milk-based products. *X-Ray Spectrometry, 33*, 128-135.

Perring, L., Andrey, D., Basic-Dvorzak, M., & Blanc, J. (2005). Rapid multimineral determination in infant cereal matrices using wavelength dispersive X-ray fluorescence. *Journal of Agricultural and Food Chemistry*, *53,* 4696-4700.

Perring, L., Andrey, D., Basic-Dvorzak, M., & Hammer, D. (2005). Rapid quantification of iron, copper and zinc in food premixes using energy dispersive X-ray fluorescence. *Journal of Food Composition and Analysis*, *18*, 655-663.

Perring, L., & Blanc, J. (2008a). Faster measurement of minerals in milk powder: comparison of a high power wavelength dispersive XRF system with ICP-AES and potentiometry reference methods. *Food Analytical Method*s, *1,* 205-213.

Perring, L., & Blanc, J. (2008b). Validation of quick measurement of mineral nutrients in milk powders: comparison of energy dispersive X-ray fluorescence with inductively coupled plasma-optical emission spectroscopy and potentiometry reference methods. *Sensing and Instrumentation for Food Quality*, *2*, 254-261.

Pozebon, D., Dressler, V. L., & Curtius, A. J. (1998). Determination of trace elements in biological materials by ETV-ICP-MS after dissolution or slurry formation with tetramethylammonium hydroxide. *Journal of Analytical Atomic Spectrometry*, *13,* 1101: 1105.

Real Decreto 867/2008, de 23 de mayo, por el que se aprueba la reglamentación técnico-sanitaria especifica de los preparados para lactantes

y de los preparados de continuación. BOE num131, de 30 de mayo de 2008 [Original language]. Royal Decree 867/2008, of May 23, which approves the technical-sanitary regulations specific to preparations for infants and follow-on formulas. BOE num 131, of May 30, 2008.

Sola-Larrañaga, C., & Navarro-Blasco, I. (2009). Optimization of a slurry dispersion method for minerals and trace elements analysis in infant formulae by ICP-OES and FAAS. *Food Chem*istry, *115,* 1048-1055.

WHO, World Health Organisation. Global strategy for infant and young child feeding.
http://apps.who.int/iris/bitstream/handle/10665/42590/9241562218.pdf;jsessionid=F654699EA06E3DCE388EDB215FFE2D01?sequence=1 /Accessed on 6 November 2018.

Yaman, M., & Çokol, N. (2004). Determination of trace elements in human milk, cows' milk and baby foods by flame AAS using wet ashing and microwave oven sample digestion procedures. *Atomic Spectroscopy*, *25 (4),* 185-190.

Zamir, T., & Husssain, A. (2001). Determination of lead and cadmium level in powdered milk Quetta (Pakistan) by atomic absorption spectroscopy. *Journal of Biological Science*, *1 (5),* 412-413.

Zand, N., Chowdhry, B. Z., Zotor, F. B., Wray, D. S., Amuna, P., & Pullen, F. S. (2011). Essential and trace elements content of commercial infant foods in the UK. *Food Chem*istry, *128*, 123-128.

Zand, N., Chowdhry, B. Z., Wray, D. S., Pullen, F. S., & Snowden, M. J. (2012). Elemental content of commercial 'ready to-feed' poultry and fish based infant foods in the UK. *Food Chemistry*, *135,* 2796-2801.

Appendix A. Supplementary Material

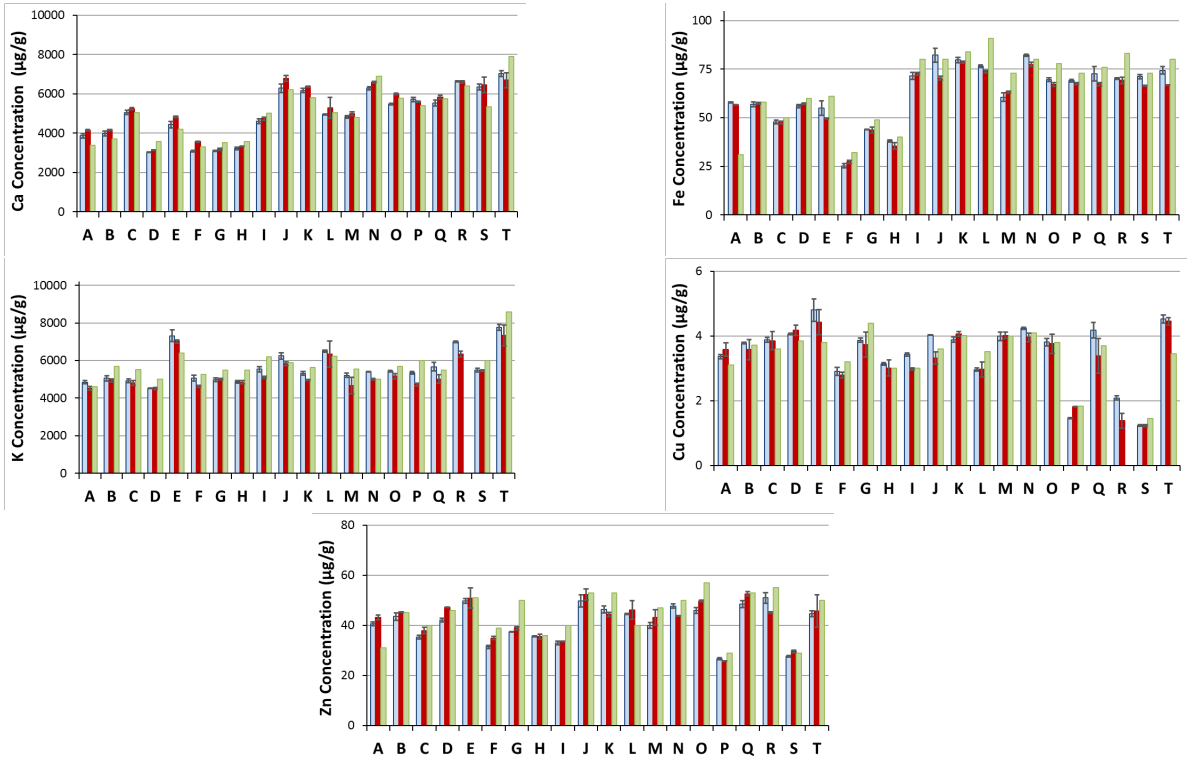

Fig. SM-1. Comparison between the concentration obtained by ICP-OES (Blue), concentration obtained by external calibration ED-XRF (Red), and the package label concentration (Green) for Ca, K, Fe, Cu and Zn.

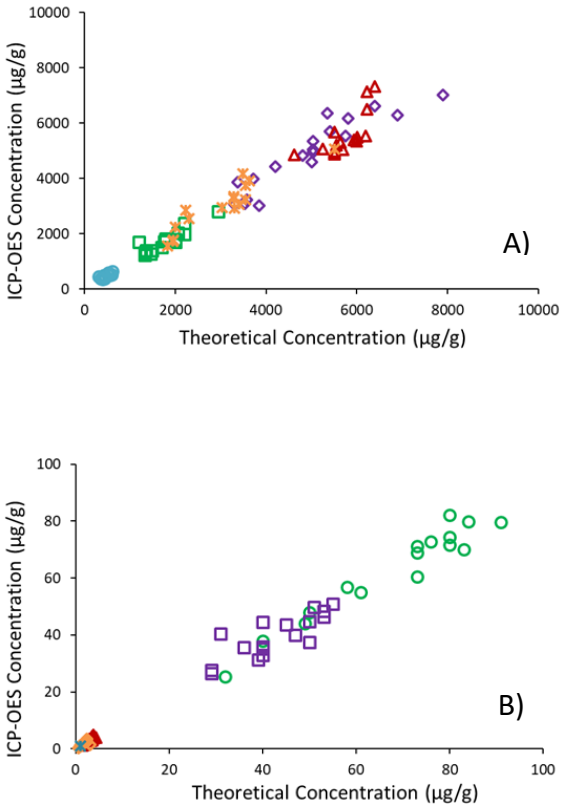

Fig. SM-2. Comparison between the concentration obtained by ICP-OES and the concentration stipulated in the package label in infant milk samples. Figure SM-2A shows the comparison for the ten elements, and Figure SM-2B shows the comparison for Cu, Fe, Mn, Se and Zn (elements with low contents).

Note: In Fig 2A: ▲: K (red); ♦: Ca (purple); ■: Na (green); ●: Mg (blue); *: P (orange).

In Fig 2B: ▲: Cu (red); ♦: Mn (orange); ■: Zn (purple); ●: Fe (green); *: Se (blue).

CAPÍTULO 3

Modelización mediante mínimos cuadrados parciales de fluorescencia de rayos X con dispersión de energía

Talanta, 194 (2019) 158-163

Partial least squares modelization of energy dispersive X-ray fluorescence

L. Herreros-Chavez, A. Morales-Rubio, M.L. Cervera, M. de la Guardia

Department of Analytical Chemistry, University of Valencia, 50 Dr. Moliner St., 46100 Burjassot, Valencia, Spain

ABSTRACT

As a proof of concept, a green methodology has been developed for the energy dispersive X-ray fluorescence (ED-XRF) determination of calcium, potassium, iron, magnesium, aluminium, chromium, strontium, phosphorus and nickel in the peel of untreated kaki fruit (*Diospyros kaki*. L) samples. ED-XRF spectra of fifty-six kakis purchased in the local area of LLombay (Valencia) were obtained directly from samples without any previous treatment and without sample damage just after cleaning the fruit with distilled water. Inductively Couple Plasma Optical Emission Spectrometry (ICP-OES) was used as a reference method to determine the mineral elements after microwave assisted acid digestion. XRF spectra and concentration values obtained by ICP-OES were processed using partial least squares (PLS) data treatment to build the corresponding chemometric models for prediction of mineral profile of samples. PLS-ED-XRF permits a direct and accurate determination of Ca and K in kaki peel. For Al, Fe, Mg, Ni and Sr screening semiquantitative results were obtained. Concentrations obtained directly by the internal calibration of instrument, using GeoChem Trace model, were also compared with data predicted by chemometric models being found that PLS models must replace the calibration of the instrument for thus kind of analysis.

Keywords: ED-XRF, kaki fruit peel, mineral profile, ICP-OES, direct analysis, PLS.

1. Introduction

Quality control of fruit products is a serious concern for food industry and human consum [1]. Direct determination of mineral profile of fruits is commonly made by atomic spectroscopy and mass spectrometry techniques, like Inductively Coupled Plasma Optical Emission (ICP-OES) [2-7], Inductively Coupled Plasma Mass Spectrometry (ICP-MS) [2,8] and Atomic Absorption Spectrophotometry (AAS) [9]. However, these techniques involve the use of relatively expensive instrumentation and a previous sample digestion which could cause contaminations or losses. A greener and fast alternative to the aforementioned procedures for the quantification of mineral elements in food samples is the use of energy dispersive X-ray fluorescence (ED-XRF) which permits the direct obtention of spectra from untreated samples with a relative low cost and portable instrumentation in less than 1 minute [10]. This technique could be extremely useful for monitoring of mineral elements in relation with the quality of tools [11-14].

The main disadvantage of ED-XRF is its low sensitivity and strong matrix effects. Due to the high dependence of the XRF measurements from the matrix it is not easy to calibrate the signals and, in general, samples of the same type than those to be analyzed must be used. However, it is possible to modelize ED-XRF spectra through the use of chemometric models based on reference data found by ICP-OES. Partial least squares (PLS) as a multicalibration strategy employed in food mineral profile determination can be employed to create quantitative models from XRF signals [1, 6, 15, 16].

Kaki (*Diospyros kaki.* L) is a fruit originated in China and introduced in Europe in the nineteen century, [17]. Nowadays, the national production in Spain is focused in the Comunidad Valenciana, where there is a protected designation of origin (PDO) 'Kaki Ribera del Xúquer' [18].

The concentration of mineral elements in kaki fruits depends on the soil, weather and harvest season, being also different in the peel and flesh of the fruit. For example, the concentration of Ca in peel could be greater and that of P smaller than corresponding values in flesh. Concentrations of Mg, Mn and Zn in flesh only exceeded those in the peel during early fruit development. In ripe fruits, the highest concentrations were found in seeds for all elements except Ca, which remains particularity high in the peel due to its association to pectin [19].

Portable ED-XRF instruments are provided with an associated internal calibration for several types of samples. However, in many cases the aforementioned models do not provides accuracy results due to the matrix effects. So, the objective of this study has been to evaluate PLS models for calibration of ED-XRF signals based on the use of a sensitive and accurate reference procedure, as it is ICP-OES, for building sample specific models; being in this study the development of a green analytical procedure for mineral profile determination of kaki fruit peel as a proof of concept.

2. Materials and methods

2.1. Samples

Fifty-six samples of kaki fruits were collected from the area of LLombay (Valencia) produced under the PDO 'Kaki Ribera del Xúquer'. Samples were washed with Adrona (Riga, Latvia) system ultrapure water with a resistivity of 18.2 MΩ cm, and ED-XRF spectra directly measured from the sample. For the ICP-OES analysis, the peel of samples was removed, with a scalpel, dried in an oven for 8 hours at 60°C and digested inside a microwave oven before dilution and determination.

2.2. Reference method

Reference mineral element data were obtained using an ICP-OES Optima 5300 DV Perkin Elmer (Norwalk, CT, USA), equipped with an auto sampler AS 93-plus and a crossflow nebuliser, after microwave assisted digestion employing a Milestone 'Ethos Sel' microwave (Sorisole, Italy), with thermocouple probe for automatic temperature control, using high pressure TFM polytetrafluorethylene (PTFE) 100 mL vessels. For sample digestion, 0.5 g of dry peel sample were accurately weight inside TFM rectors and 4 mL of concentrated HNO_3 69 % from Scharlau (Barcelona, Spain) were added. Acidified samples were treated inside an ultrasound water bath (Selecta, Barcelona, Spain) for 30 min. After that, 1 mL of 35 % hydrogen peroxide (Scharlau) was added, being observed the evolution of brown nitrous oxide vapors and the formation of foam. In order to reduce foam formation, every 2 minutes the reactors were removed from the ultrasound bath and shaken manually for a few seconds until the foam disappears. Finally, 4 mL of ultrapure water was added, the vessels closed and introduced in their respective protection shield inside the microwave oven. The digestion program followed the steps of 25 minutes to reach 200°C and digestion in 15

minutes at 200°C. After digestion, samples were diluted till 15 mL and analyzed by ICP-OES; 1 mg L^{-1} Rhenium solution (Fluka, Neu-Ulm, Switzerland) was employed as internal standard. All the elements were measured in axial mode; except for Ca and K which were measured in radial mode. The most sensitive emission line, from interferences free spectra, was selected for each element, two points for background correction were used. Control standards were measured for every series of 10 independent sample measurements. A multielement calibration standard solution containing 26 elements in HNO_3 5 % (Scharlau) was employed to prepare calibration standards daily by diluting the stock one in the range from 0.005 to 5 mg L^{-1}. Additional calibration was done from 1000 mg L^{-1} Ca solution and 1000 mg L^{-1} K solution both from (Scharlau) in a range from 20 till 200 mg L^{-1}.

2.3. ED-XRF analysis

ED-XRF spectra were obtained directly from samples. Each sample was measured eight times in different positions located in the equator region and spectra obtained at 50 kV and 15μA, with 60 s acquisition time (30 s for high atomic number elements and another 30 s for low atomic number elements). The equipment used was a Bruker S1TITAN LE SMA-1402 (Kennewick, WA, USA) equipped with a rhodium X-ray tube and a X-flash silica detector.

2.4. Chemometric treatment

Models for the prediction of mineral profile of kaki fruit peel samples from their ED-XRF spectra were built using partial least squares (PLS) chemometric treatment employing a Matlab 2014a software from Mathworks (Natick, MA, USA) and PLS Toolbox 6.2 from Eigenvector Research Inc. (Wenatchee, WA, USA). The calibration set was composed by sample spectra of known composition, determined by ICP-OES. It should be representative of the entire range of concentrations and contain possible interferences from other components present in the samples that may affect the recorded spectra. The most appropriated PLS model was selected considering the energy range, the best number of latent variables and signal preprocessing most appropriate in order to found the lowest calibration and cross validation errors. In all the cases, venetian blinds with 3 splits cross validation (CV) was employed for the selection of models with the minimum root mean square error of cross validation (RMSECV). Mean centering (MC), first derivate (FD), second derivate (SD) and orthogonal signal correction (OSC), were assayed as signal pretreatments.

3. Results and discussion

3.1. X-ray fluorescence spectra of kaki peel samples

Fig. 1 shows a typical spectra of a kaki fruit peel sample. As can be seen in the figure, lines corresponding to mineral elements present in the sample were located between 0 and 15 keV.

Kα lines of Al, Ca, Cr, Fe, K, Mg, Ni, P and Sr could be seen at 1.49, 3.69, 5.41, 6.41, 3.31, 1.25, 2.01, 7.48, 14.17 keV, respectively.

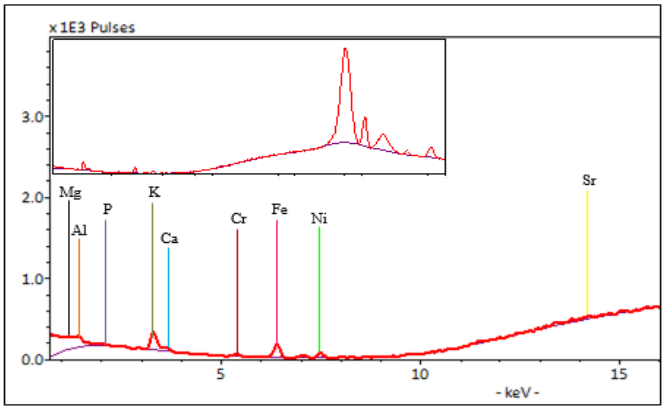

Fig. 1. Detailed ED-XRF spectra of a kaki fruit peel simple in the energy range between 0 and 15 keV. Inset: The whole spectra of sample with XRF primary lines.

3.2. ICP-OES data of selected samples

Table 1 shows the mean and standard deviation of Al, Ca, Cr, Fe, K, Mg, Ni, P and Sr concentration in samples selected to build the calibration models. These data were used to calibrate the ED-XRF signals. Samples were classified according to the non-astringency treatment performed. Samples marked as 'C' underwent a common treatment with CO_2 (concentrations as high as 95 to 98 % for 24 h) [20]. Samples marked as 'A' were non-astringency untreatment and those marked as 'R' were allowed to mature in the tree.

3.3. PLS-ED-XRF model selection

3.3.1. Spectral range

To build the PLS models, 15 kaki fruit samples were used to perform the calibration set. The spectral range from 0 to 40 keV, 0 to 15 keV and the specific line corresponding to each target element were assaged to build PLS models. As an example for Ca, the RMSECV found from 360 μg g^{-1} for the whole range or 370 μg g^{-1} for the Kα line at 3.69 keV till 300 μg g^{-1} on using the spectra range from 0 to 15 keV. So, a total of 686 variables of the total from 0 to 15 keV were selected.

Table 1. ICP-OES concentration (μg g^{-1}) of target elements determined in kaki peel samples employed to build the PLS-ED-XRF model.

Samples	[Al]	[Ca]	[Cr]	[Fe]	[Mg]	[K]	[Ni]	[P]	[Sr]
C4	4.4 ± 0.3	1300 ± 300	<LOD	5.38 ± 0.12	550 ± 20	12900 ± 500	0.9 ± 0.2	800 ± 100	13.5 ± 0.7
C8	6 ± 3	1500 ± 20	0.22 ± 0.06	5.7 ± 0.3	545 ± 3	9800 ± 300	0.55 ± 0.09	596 ± 17	16.3 ± 0.2
C17	4.0 ± 0.7	1210 ± 100	0.029 ± 0.012	5.4 ± 1.8	515 ± 3	11200 ± 300	2.26 ± 0.19	800 ± 80	10.8 ± 1.0
C22	5.2 ± 0.9	1210 ± 60	0.26 ± 0.06	7.1± 0.6	540 ± 8	13600 ± 100	0.55 ± 0.04	900 ± 45	14.4 ± 0.7
C26	5.9 ± 0.5	1454.2 ± 1.1	0.34 ± 0.15	7.2 ± 1.1	575 ± 8	9900 ± 100	1.23 ± 0.12	900 ± 30	18.5 ± 0.4
C32	5.4 ± 0.6	1000 ± 100	0.020 ± 0.007	6.8 ± 0.4	519 ± 6	12710 ± 80	0.73 ± 0.06	800 ± 90	11.3 ± 1.6
C33	3.7 ± 0.5	1140 ± 30	0.10	6.5 ± 0.7	604 ± 12	15000 ± 300	1.25 ± 0.14	1010 ± 70	12.8 ± 0.6
C35	4.4 ± 1.1	1080 ± 60	<LOD	5.9 ± 0.6	570 ± 40	13400 ± 900	1.10 ± 0.17	920 ± 90	13.2 ± 0.7
A1	3.4 ± 1.0	710 ± 70	0.012 ± 0.002	5.6 ± 0.6	652 ± 17	11400 ± 500	0.73 ± 0.07	960 ± 80	12.3 ± 1.4
A2	3.2 ± 1.0	890 ± 130	0.05	5.5 ± 0.9	690 ± 30	11800 ± 600	0.86 ± 0.19	900 ± 100	15 ± 2
A3	2.2 ± 0.5	870 ± 130	0.03	4.4 ± 0.3	660 ± 20	10600 ± 500	0.6 ± 0.04	1000 ± 100	15.8 ± 1.0
A4	2.8 ± 1.2	1170 ± 80	<LOD	4.6 ± 0.4	620 ± 30	10700 ± 500	0.46 ± 0.07	1000 ± 100	156 ± 0.8
A5	3.3 ± 0.8	1130 ± 50	0.05	5.09 ± 0.15	690 ± 20	11100 ± 500	0.583 ± 0.015	1160 ± 20	18.6 ± 1.3
A6	2.2 ± 0.3	730 ± 40	0.03	5.0 ± 0.2	710 ± 30	12400 ± 5200	0.82 ± 0.06	970 ± 40	12.4 ± 0.9
R1	6.3 ± 0.6	1710 ± 15	0.02	7.5 ± 0.4	520 ± 20	8700 ± 200	1.39 ± 0.03	730 ± 20	28.2 ± 0.5

Notes: Limit of detection (LOD) for chromium: 0.07 μg g^{-1}; C: kaki samples treated with CO_2 to avoid astringency; A: kaki samples without non-astringency treatment; R: kaki samples with natural maturation.

3.3.2. Latent variables (LV)

Fig. 2 shows as an example the relation between the root mean square error of cross validation (RMSECV) and the root mean square error of calibration (RMSEC) in front of the number of LV. As it can be seen in **Fig 2a**, errors for Ca determination fall down on increasing the LVs being found that 4 LVs would be enough to describe the relationship between ED-XRF spectra and Ca concentration. In this case the explained variance for signals (X) was 78 % and 99.7 % for Ca

concentration (Y). In the case of K (see **Fig. 2b**) 3 LVs provided low root mean square errors with explained variance of 76 % and 98 % for X and Y, respectively.

For phosphorus 3 latent variables (LV) were necessary to build the PLS models. The variance explained for X and Y were 73 % and 95 %. For aluminum, calcium, iron, magnesium, nickel and strontium 4 LV were necessary to build the models. For chromium 5 LV were necessary to build the models with explained variance for X and Y of 92 % and 99 %, respectively.

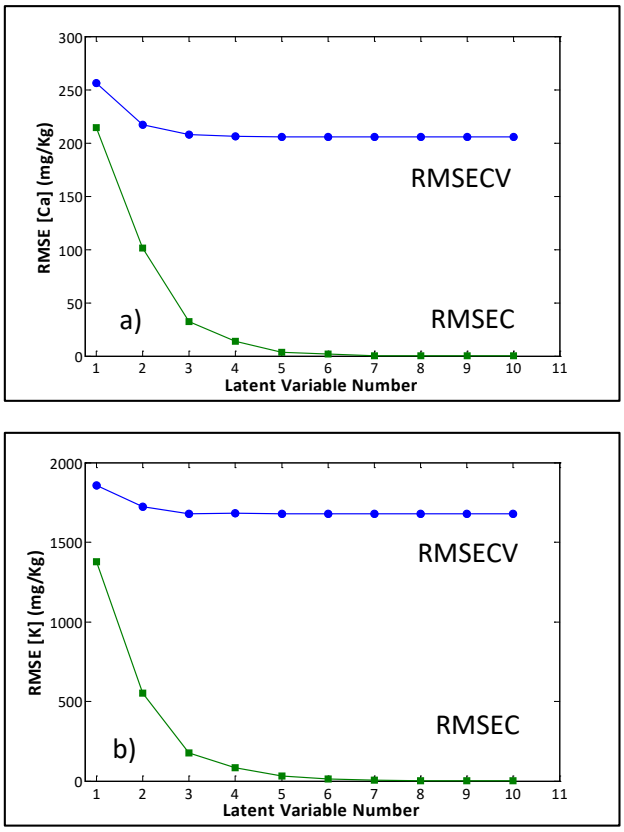

Fig. 2. Effect of the number of latent variables on the root mean square error of calibration (RMSEC) and the root mean square error of cross validation (RMSECV) for Ca (2a) and K (2b) determinate.

3.3.3. Pre-process

Different preprocessing method were assayed as indicated in the experimental part. As an example, **Table 2** summarizes RMSECV found for K determination by using different preprocessing strategies both, only or combined, as it can be seen the use of SD plus MC provided the best model. Additionally, it must be indicated than the errors found also depends on the orders of application of preprocessing treatments.

Table 2. Root mean square error of cross validation (RMSECV) of pre-process studied for built PLS model for K.

Pre-process	RMSECV (μg g^{-1})
OSC	1479
FD	1422
SD	1508
MC	1821
OSC + MC	1529
FD + MC	1416
SD + MC	1395
OSC + FD	1401
OSC + SD	1497
OSC + FD + MC	1908
OSC + SD + MC	1879

Notes:

- OSC: orthogonal signal correction
- FD: first derivate
- SD: second derivate
- MC: mean centering

For Al and Mg, OSC plus FD plus MC provided the best spectral preprocessing. For Ca, Fe, Ni and Sr, SD plus MC were selected as it was the same for K. For Cr, FD plus MC provided the best spectral preprocessing and for P, OSC plus SD plus MC were chosen for the spectral preprocessing.

3.3.4. Calibration PLS model

Fig. 3 shows the correlation between the calculated concentration of K in front of the concentration determined by ICP-OES. It provides a R^2 values of 0.98 and it can be seen that data from ED-XRF after PLS treatment were practically the same of those found by ICP-OES.

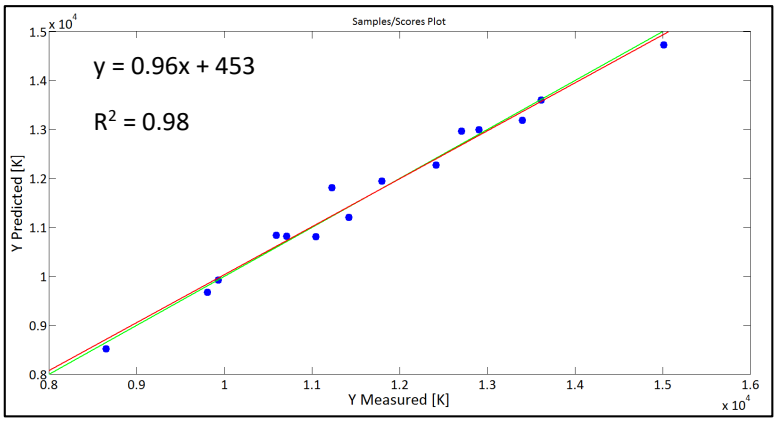

Fig. 3. Concentration calculated in front of the concentration of K determined by ICP-OES reference method ICP-OES.

3.3.5. PLS models

Table 3 shows the main characteristics of PLS-ED-XRF models selected for each considered element. For the whole range of 9 elements considered the best calibration models provided RMSC values from 0.012 till 230 µg g^{-1}, being strongly dependent these values on the concentration range of elements. So, a regression line y = 0.0198x – 0.373 with R^2 = 0.993 was found between RMSEC and mean concentration values.

It was also found that RMSE values increased one order of magnitude when moving from RMSEC to RMSECV. However, once again a good correlation was found between RMSECV and average values of y = 0.1409x + 10.405 with R^2 = 0.999.

RRMSECV from 0.5 for Fe till 15 % for Cr where found. However, on moving from calibration to cross validation the relative errors respect to the mean mineral element concentration were 137 % for Cr and 60 % for Ni evidencing that the aforementioned elements can not be predicted from kaki fruit peel ED-XRF spectra, probably on the low ED-XRF signals obtained and the low element concentrations. Al and Sr could be predicted which mean RRMESCV of 28 % and 24 %, respectively, which varied from 54 till 17 % in the case of Al and from 37 to 12 % in case of Sr. the five remaining elements (Ca, Fe, K, Mg and P) could be quantified with errors lower than 20 %.

Table 3. Characteristics of the selected PLS-ED-XRF models for the determination of target mineral elements in kaki peel.

Element	Range (µg g^{-1})	Mean (µg g^{-1})	SD (µg g^{-1})	Pre-process (µg g^{-1})	LV	R^2	RMSEC (µg g^{-1})	RRMSEC Mean (%)	RMSECV (µg g^{-1})	RRMSECV Mean (%)
Al	2.2-6.9	4.3	1.5	OSC+ FD+ MC	4	0.98	0.17	4	1.2	28
Ca	713-2184	1204	376	SD + MC	4	0.997	14	1.2	215	18
Cr	0-0.10	0.08	0.10	FD + MC	5	0.990	0.012	15	0.11	137
Fe	4.4-7.8	6.0	1.1	SD + MC	4	0.998	0.03	0.5	0.7	12
K	8656-15011	11622	1639	SD + MC	3	0.98	230	2.0	1643	14
Mg	493-711	591	71	OSC + FD+ MC	4	0.994	5	0.8	81	14
Ni	0.5-2.3	1.0	0.5	SD + MC	4	0.990	0.05	5	0.6	60
P	596-1162	894	140	OSC + SD+ MC	3	0.95	31	3	169	19
Sr	10.8-33.2	16.4	6.1	SD + MC	4	0.995	0.3	1.8	4	24

Notes:

- SD: standard deviation
- LV: latent variables
- RMSEC: root mean square error of calibration
- RRMSEC: relative root mean square error of calibration
- RMSECV: root mean square error of cross validation
- RRMSECV: relative root mean square error of cross validation

3.4. Comparison of ED-XRF and PLS-ED-XRF concentrations

The concentration provided by ED-XRF using GeoChem Trace model were compared with those predicted by PLS. **Fig. 4** shows as examples the regression between these data for Ca and K, being found regression line y = (1.03 ± 0.09) x - (104 ± 106) with R^2 = 0.72 for Ca and y = (0.89 ± 0.09) x + (2091 ± 1074), with R^2 = 0.65 for K. So, it can be concluded that both models are not coincident and the R^2 values are very poor. However, the statistical treatment of slope and intercept values show that for these two elements slopes are statistically comparable with 1 and intercepts with 0. In spite of that it is strongly recommended to do not use the GeoChem Trace model for kaki fruit spectra modelization, being thus preferable to modelate the signals by PLS.

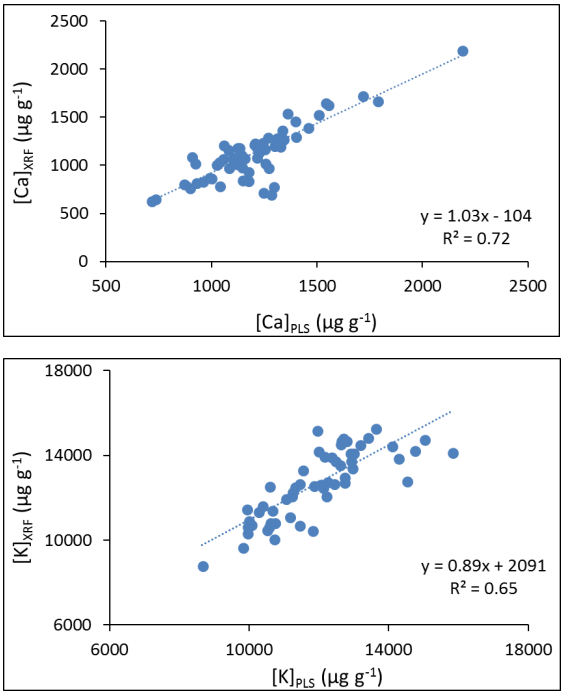

Fig. 4. Correlation between the concentration obtained directly by ED-XRF and the concentration obtained by PLS model for Ca and K.

3.5. Comparison ED-XRF intensities and PLS-ED-XRF concentrations

The regression between the number of counts per second obtained by ED-XRF and the predicted concentration of Al, Ca, Fe, K, Mg and Sr provided linear relationships summarized in **Table 4** from which it can be concluded the good analysis features of method developed. Only in case of P, there are not correlation between the intensity and the concentration predicted by PLS-ED-XRF model. **Fig. 5** shows, as an example the data distribution for Sr and Mg.

Table 4. Regression lines between peak height ED-XRF and predicted element concentrations in kaki fruit peel samples.

Analyte	Regression	R^2
Al	50.5x + 247	0.74
Ca	0.18x + 77	0.78
Fe	59.3x + 1234	0.77
K	0.10x + 549	0.80
Mg	1.07x + 405	0.79
Sr	30.1x + 754	0.86

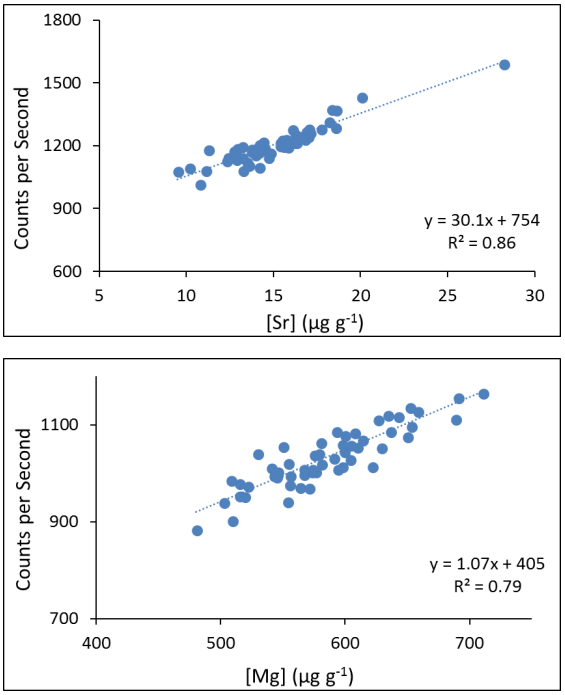

Fig. 5. Correlation between the peak height intensity of ED-XRF spectra and the predicted concentration for Sr and Mg.

4. Conclusions

A non-destructive and fast green method has been developed for the determination of Ca and K and this screening of Al, Fe, Mg and Sr in kaki fruit peel samples based on the sensitivity limitations of XRF to detect low atomic number elements. The method provided data without consumption of reagents nor the generation of wastes, as an alternative to atomic spectroscopy methods involving sample digestion. PLS treatment of ED-XRF spectra was based on the use of a reduced number of samples previously analyzed by ICP-OES and signals directly obtained from samples and it can be used to evaluate fruit disorders related to plant treatment with main mineral elements as Ca and K and other trace elements.

In short, the proposed procedure can be considered as an example of the potentiality of using PLS in combination with reference data for some samples, of the same type than those to be analyzed, to create ED-XRF models appropriate for each type of analysis.

5. Conflict of interest

There are not conflict of interest between the authors.

6. Acknowledgements

The authors gratefully acknowledge the financial support of Ministerio de Economia y Competitividad-Feder Project CTQ2016-78053-R and CTQ2014-52841-P.

7. References

[1] M. Khanmohammadi, F. Karami, A. Mir-Marqués, A.B. Garmarudi, S. Garrigues, M. de la Guardia, Classification of persimmon fruit origin by near infrared spectrometry and least squares-support vector machines, J Food Eng. 142 (2014) 17-22.

[2] A. Mir-Marqués, A. Domingo, M.L. Cervera, M. de la Guardia, Mineral profile of kaki fruits (*Diospyros kaki* L.), Food Chem. 172 (2015) 291-297.

[3] A.M.P. dos Santos, J.S. l.ima, D.S. Anunciação, A.S. Souza, D.C.M.B. dos Santos, G.D. Matos, Determination and evaluation employing multivariate analysis of the mineral composition of broccoli (*Brassica oleracea L*. var. *Italica*), Food Anal Methods. 6 (2013) 745-752.

[4] T. Mahmood, F. Anwar, T. Iqbal, I.A. Bhatti, M. Ashraf, Mineral composition of strawberry, mulberry and cherry fruits at different ripening stages as analyzed by inductively coupled plasma-optical emission spectroscopy, J Plant Nutr. 35 (2010) 111-122.

[5] S.S. Mitić, M.V. Obradović, M.N. Mitić, D.A. Kostić, A.N. Pavlović, S.B. Tošić, M.D. Stojković, Elemental composition of various sour cherry and table grape cultivars using inductively coupled plasma atomic emission spectrometry method (ICP-OES), Food Anal Methods. 5 (2012) 279-286.

[6] A. Mir-Marqués, M. Martínez-García, S. Garrigues, M.L. Cervera, M. de la Guardia, Green direct determination of mineral elements in artichokes by infrared spectroscopy and X-ray fluorescence, Food Chem. 196 (2016) 1023-1030.

[7] A. Mir-Marqués, M.L. Cervera, M. de la Guardia, A preliminary approach to mineral intakes in the Spanish diet established from analysis of the composition of university canteen menus, J Food Compost Anal. 27 (2012) 160-168.

[8] S.D. Kelly, A.S. Bateman, Comparison of mineral concentrations in commercially grow organic and conventional crops – Tomatoes (*Lycopersicon esculentum*) and lettuces (*Lactuca sativa*), Food Chem. 119 (2010) 738-745.

[9] C.H. Lescano, I.P. de Oliveira, F.F. de Lima, D.S. Baldivia, P.N. Justi, C.A.L. Cardoso, J.L.R. Júnior, E.J. Sanjinez-Argandoña, Nutritional and chemical characterizations of fruit obtained from *Syagrus romanzoffiana, Attalea dubia, Attalea phalerata and Mauritia flexuosa*, J Food Measurement Characterization. 12 (2018) 1284-1294.

[10] M. de la Guardia, S. Garrigues, Handbook of mineral elements in food, first ed. Wiley & Sons, UK, 2015.

[11] N.M. Hepp, I.C. James, Application of high-energy polarized energy-dispersive x-ray fluorescence spectrometry to the determination of trace levels of As, Hg, and Pb in certifiable color additives, X-Ray Spectrom. 45 (2016) 330-338.

[12] Y.H. Choi, C.K. Hong, G.Y. Park, C.K. Kim, J.H. Kim, K. Jung, J.H. Kwon, A non-destructive approach for discrimination of the origin of sesame seeds using ED-XRF and NIR spectrometry with chemometrics, Food Sci Biotechnol. 25 (2016) 433-438.

[13] A. Sussilini, A.G. Lima, E.C. Figueiredo, H.L. Fernandes, S.C.L. Pinheiro, S.C.L. Bueno, M.I.M.S. Pereira, X-ray scattering information of ED-XRF technique for powdered fruit juice mixes, X-Ray Spectrom. 38 (2009) 254-257.

[14] B. Tanaskovski, M. Jović, M. Mandić, L. Pezo, S. Degetto, S. Stanković, Element analysis of mussels and possible health risks arising from their consumption as a food: the case of Boka Kotorska Bay, Adriatic Sea, Ecotoxicol Environ Saf. 130 (2016) 65-73.

[15] A. dos S. Augusto, P.L. Barsanelli, F.M.V. Pereira, E.R. Pereira-Filho, Calibration strategies for the direct determination of Ca, K and Mg in commercial samples of powdered milk and soil diatery supplements using laser-induced breakdown spectroscopy (LIBS), Food Res Int. 94 (2017) 72-78.

[16] J. Moros, I. Llorca, M.L. Cervera, S. Garrigues, M. de la Guardia, Chemometric determination of arsenic and lead in untreated powdered red paprika by diffuse reflectance near-spectroscopy, Anal Chim Acta. 613 (2008) 196-206.

[17] K. Yonemori, A. Sugiura, M. Yamada, Persimmon genetics and breeding, Plant Bree Rev. 19 (2000) 191-225.

[18] CRDO (2011). Consejo Regulador de la Denominación de Origen "Kaki Ribera del Xúquer". Available from: http:// www.kakifruit.com.

[19] C.J. Clark, G.S. Smith, Season changes in the composition, distribution and accumulation of mineral nutrients in persimmon fruit, Sci Hort. 42 (1990) 99-111.

[20] L. Arnal, M.A. del Río, Removing astringency by carbon dioxide and nitrogen-enriched atmospheres in Persimmon fruit cv. "Rojo Brillante", J Food Sci. 68 (2003) 1-3.

CAPÍTULO 4

Perfil mineral de legumbres y frutos mediante fluorescencia de rayos X con dispersión de energía por mínimos cuadrados parciales

Journal of Food Composition and Analysis, 82 (2019) 103240

Mineral profile of legumes and fruits through partial least squares energy dispersive X-ray fluorescence

L. Herreros-Chavez[a], F. Oueghlani[b], A. Morales-Rubio[a], M.L. Cervera[a], M. de la Guardia[a]

[a] Department of Analytical Chemistry, University of Valencia, 50 Dr. Moliner St., 46100 Burjassot, Valencia, Spain

[b] Department of Biological Engineering Institute Polytechnique Privé de l'Université Libre de Tunis, Tunisia

ABSTRACT

Energy dispersive X-ray fluorescence (ED-XRF) has been employed for the determination of mineral elements in 15 varieties of legumes and 14 cherry samples. ED-XRF signals directly obtained from pulverized samples were modelized by partial least squares (PLS) using Inductively Coupled Plasma Optical Emission Spectrometry (ICP-OES) of a selected number of samples, after microwave assisted acid digestion, as reference data. Models were built to predict the concentration of Al, Ca, Cu, Fe, K, Mg, P, Sr and Zn. Average concentrations predicted were 6, 930, 7, 40, 6400, 990, 2100, 4 and 15 μg g^{-1} for Al, Ca, Cu, Fe, K, Mg, P, Sr and Zn, respectively with relative errors from 7 till 26 %. In the case of Al, the methodology proposed only provided screening data.

Keywords: food composition, direct food analysis, ED-XRF, mineral elements, PLS, ICP-OES, legumes, cherries.

1. Introduction

Food mainly contain carbohydrates, proteins, vitamins and minerals which are necessary for the correct function of the body. Food need to be analyzed for guarantee their nutritional values, mineral contribution and security due to consumers demand and in the last decades have been extensively

controlled, to obtain data about nutrition, health or toxicity (Perring and Andrey, 2004). Essential elements are important in the diet for a correct function of the human body and are classified in two categories: macroelements and microelements (de la Guardia and Garrigues, 2015). The presence of these mineral elements in food depends on many factors; such as the type of food, origin, agricultural and farming procedures and geographical location (Fairweather-Tait and Hurrell, 1996; Nielsen, 1981). Deficit intakes of essential elements caused deficiency syndromes, which must be avoided or reversed by the administration of supplements, while excessive intake can produce a negative impact on health (Goldhaber, 2003).

Determination of the mineral profile of food is often done using mass spectrometry and atomic spectroscopy methods such as Inductively Coupled Plasma Optical Emission Spectrometry (ICP-OES) (Mir-Marqués, 2012; Zand et al., 2011; Siemianowska et al., 2016: Porto et al., 2017; Stanimirović et al., 2018; Stojanović et al., 2017), Inductively Coupled Plasma Mass Spectrometry (ICP-MS) (Kelly and Bateman, 2010; Carbonell-Barrachina et al., 2012; Wheal et al., 2016) and Atomic Absorption Spectroscopy (AAS) (Lescano et al., 2018; Almela et al., 2006; Sarkar et al., 2017; Gliszczyńska-Świglo et al., 2018; Singh et al., 2016; Butkuté et al., 2017; Ramírez-Ojeda et al., 2018). However, these techniques involve the use of expensive and non-portable instrumentation. Additionally, they require a previous sample digestion, employing temperature and acids which could cause contaminations or losses of target analytes spent energy and time (Mir-Marqués et al., 2014).

A green and fast alternative for the analysis of minerals in foods could be based on direct measurements by energy dispersive X-ray fluorescence (ED-XRF). These equipments are less costly than classical atomic spectroscopy ones and permit a simple, portable and fast analysis of any type of solid samples (Mbaye et al., 2015; Mir-Marqués et al., 2016; Mir-Marqués et al., 2012; Palmer et al., 2009) without any chemical sample pre-treatment, thus deleting the consumption of reagents and the generation of toxic wastes, making these analyses easy, cheap and free from environmental side effects (de la Guardia and Garrigues, 2015). However, the main disadvantages of XRF are their relatively low sensitivity and high matrix effects (Mir-Marqués et al., 2016) which can difficult to perform accurate quantitative determinations. Food analysis by ED-XRF include bread improver (Ekinci et al., 2002), spices (Joseph et al., 1999), tea (Nas et al., 1993), flours (Saleh et al., 1986), milk powder (Alvarez et al., 1990), vegetables-fruit-grains (Nielson et al., 1991) and fast food menus (Nielson et al., 1991).

This technique has been used to quantify macro and micronutrient and contamination in food and feed industries (Perring and Andrey, 2003).

The main purpose of this study was the modelization of mineral profile of legumes and cherry samples, based on direct ED-XRF spectra of samples and PLS treatment. Calibration of ED-XRF signals was based on the use of a series of samples accurately analyzed by a reference ICP-OES procedure.

2. Material and methods

2.1. Samples

A total of twenty-nine samples: (15) legumes and (14) cherry samples were purchased from different local markets in Spain. In the case of cherry samples, the bones were used as reference value of the fruit mineral content (Matos-Reyes et al., 2013). Cherry bones were separated from the flesh, dried and pulverized in an agate mortar till to obtain a sample size lower than 425 μm. Legume samples were grounded in a domestic grinder till a size of 250 μm and kept in polypropylene tubes. For ICP-OES determinations, a representative set of samples from each two types considered, were selected to obtain reference values of their mineral profile. To do these analysis, samples were digested inside a microwave oven before dilution and measurement of the element emission.

A certified reference material of Spinach, NCS ZC73013 from NACIS was used to test the accuracy of the reference method.

2.2. Reference method

Reference values on the mineral composition of samples were determined by ICP-OES using an Optima 5300 DV, from Perkin Elmer (Norwalk, CT, USA), equipped with an auto sampler AS 93-plus and a cross flow nebuliser. The microwave assisted digestion of samples was made using a Milestone 'Ethos Sel' microwave (Sorisole, Italy) equipped with 100 mL high pressure polytetrafluorethylene modified (TFM) vessels and a thermocouple probe for automatic temperature control.

In a TFM reactor, 0.5 g of each sample were accurately weighted and it was added 4 mL of concentrated HNO_3 (69 % for trace analysis), from Scharlau (Barcelona, Spain), and 1 mL of 35 % hydrogen peroxide, from Scharlau. The mixture was sonicated in an ultrasound water bath for 30 min at room

temperature. Reactors were shaken manually for a few seconds to prevent foam formation and gas leakage during pressurized microwave digestion. After sonication, 4 mL of ultrapure water were added and the reactors were closed and placed inside the microwave oven. The digestion program was: 25 minutes to reach 200°C, a step of 15 minutes at 200°C and a cooling down step for 25 minutes. After digestion, samples were diluted till 15 mL with nanopure water before being analyzed by ICP-OES. Rhenium (1 mg L^{-1}), from Fluka (Neu-Ulm, Switzerland), was used as internal standard and added to all samples, blanks and standards.

All the elements were measured in axial mode except Ca, K, Mg, and Sr, which were measured in radial mode. The most sensitive emission line, free from spectral interferences, was selected for each considered element, using two points for background correction. Control standards were measured for every series of 10 independent sample measurements. A multi-element standard solution containing 26 elements (Al, As, Ba, Be, Bi, B, Cd, Ca, Cr, Co, Cu, Fe, K, Li, Mg, Mn, Mo, Na, Ni, Pb, Se, Sr, Ti, Tl, V and Zn) in 5 % HNO_3, from Scharlau, was used to prepare the calibration standards daily by diluting the stock one in the range from 0.05 to 5 mg L^{-1}. Additional calibration for Ca and K was carried out using 1000 mg L^{-1} Ca and K solutions from Scharlau in a range from 20 till 750 mg L^{-1}.

2.3. ED-XRF procedure

The equipment used to obtain XRF spectra was a portable energy dispersive X-ray fluorescence model S1 TITAN LE SMA-1402 from Bruker (Kennewick, WA, USA). The system was equipped with a rhodium X-ray tube and a X-flash silicon drift detector. For instrument control, S1 RemoteCtrl and S1Sync software, from Bruker, was employed, and spectra were treated by using the ARTAX software also from Bruker. Measurements were made at 50 kV and 7 µA, with 60 s acquisition time. During the first 30 s the lowest atomic number elements from Mg till Cr were measured. Elements with high atomic number; from Mn till U were measured in the last 30 s by using an automatic filter changer.

Approximately 0.8 g of sample was placed inside evacuable pellet die from Specac GS03000 (Orpington, UK). Samples were compacted and pressed at 200 kg cm^{-2} for 2 minutes and 13 mm diameter and 2-3 mm thick pellets were stored in a desiccator to prevent hydration. Three pellets were prepared for each sample. Each pellet was measured three times by ED-XRF changing their position and orientation after each measurement.

2.4. Chemometric data treatment

Models for prediction of the mineral element concentrations in cherry bones and legumes, employing their ED-XRF spectra, were performed using partial least squares (PLS), using Matlab 2014a software from Mathworks (Natick, MA, USA) and the PLS toolbox 6.2 from Eigenvector Research Inc. (Wenatchee, WA, USA). Calibration set was composed by 6 samples of cherry bones and 5 legume samples with known concentrations determined by ICP-OES. For each type of sample, it was built a model and it was also built a merged model for legumes plus cherry.

For building the best PLS models, different energy spectral ranges were selected considering also the best number of latent variables and signal pre-processing in order to found the lowest calibration and cross validation errors. In all the cases, venetian blinds with 2 (for individual models) and 3 (for models with combination of the two types of samples) split cross validation (CV) were employed for the selection of the optimum number of latent variables (LV) in order to minimize the root mean square error of cross validation (RMSECV).

Different data pre-treatment models assayed were: mean centering (MC), first derivate (FD), second derivate (SD), standard normal variation (SNV), smoothing (SMO), autoscale, normalization, multiplicative signal correction (MSC), variable alignment and orthogonal signal correction (OSC), also combination of them were assayed as signal pretreatments. The best model was selected for each element and matrix on the basis of the lowest root mean square error of calibration (RMSEC) and lowest root mean square error of cross validation (RMSECV).

3. Results and discussion

3.1. X-ray fluorescence spectra of analyzed samples

Fig. 1 inset shows typical ED-XRF spectra between 0 and 40 keV of samples and the detailed spectra of one cherry bone and one legume sample in the energy range from 0 till 15 keV. All the elements studied provided specific Kα peaks in this region.

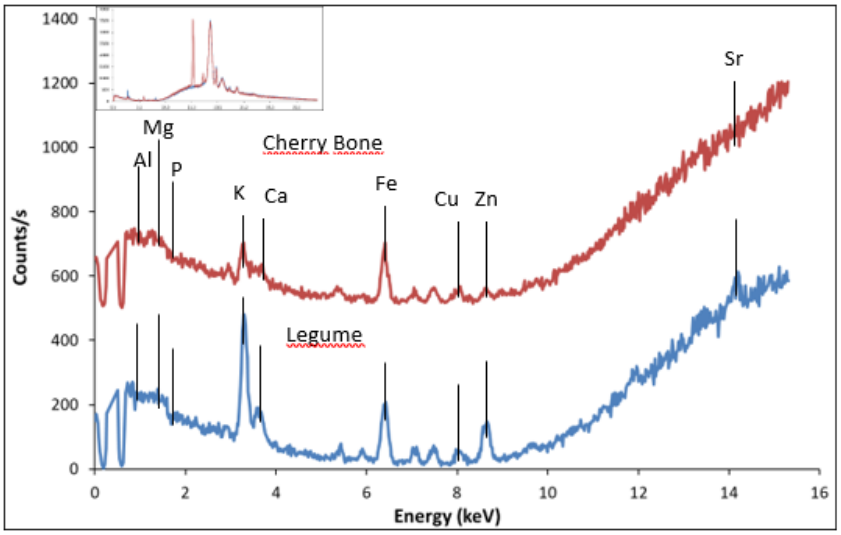

Fig 1. ED-XRF spectra of legumes and cherry bones in the energy range between 0 and 15 keV. NOTE: cherry bone spectrum was shift in the Y axis for clarity. Inset: complete spectrum of a legume sample.

3.2. ICP-OES data of selected samples

Table 1 shows the average and standard deviation of three independent ICP-OES determinations of Al, Ca, Cu, Fe, K, Mg, P, Sr and Zn in samples selected to build the ED-XRF-PLS models. These concentrations were employed to calibrate ED-XRF signals. Samples were marked according to the type of sample as 'CB' for cherry bones and 'L' for legumes.

Table 2 shows data found by ICP-OES for the analysis of six certified reference materials, in present study and previous ones (Ruiz de Cenzano et al., 2017; Mir-Marqués et al., 2015). As it can be seen in this table, the regression between data obtained by ICP-OES and certified values are in a good agreement, providing an equation y = (-79 ± 93) + (0.983 ± 0.009) x, with 0.997 determination coefficient. So, being obtained statistically values of 0 and 1 for the intercept and slope [0.964; 1.003] and thus, it can be concluded that no significant differences were found between these two sets of data.

Table 1. ICP-OES concentration in μg g^{-1} of target elements determined in cherry bone and legume samples employed to build the PLS-ED-XRF models.

Sample	[Al]	[Ca]	[Cu]	[Fe]	[K]	[Mg]	[P]	[Sr]	[Zn]
CB1	2.3 ± 1.2	1320 ± 20	4.68 ± 0.04	11.3 ± 0.7	1220 ± 60	600 ± 20	740 ± 30	6.67 ± 0.07	4.31 ± 0.06
CB2	10.5 ± 1.2	980 ± 40	5.7 ± 0.3	21.3 ± 0.4	1630 ± 60	500 ± 10	710 ± 20	4.05 ± 0.13	5.93 ± 0.17
CB3	2.1 ± 0.9	660 ± 40	6.7 ± 0.2	11.7 ± 0.8	1800 ± 100	620 ± 30	740 ± 40	1.91 ± 0.15	3.25 ± 0.10
CB4	3.2 ± 0.5	880 ± 30	7.0 ± 0.2	16.6 ± 0.6	2440 ± 70	760 ± 20	1110 ± 20	1.69 ± 0.05	7.3 ± 1.5
CB5	1.05 ± 0.05	620 ± 20	3.72 ± 0.07	9.70 ± 0.18	1720 ± 30	670 ± 10	730 ± 10	2.29 ± 0.12	3.83 ± 0.03
CB6	0.41 ± 0.11	770 ± 40	4.74 ± 0.12	18 ± 3	1710 ± 40	710 ± 20	880 ± 20	3.06 ± 0.08	4.42 ± 0.14
L1	7.7 ± 1.3	1550 ± 50	9.0 ± 0.1	60 ± 3	14200 ± 130	1580 ± 30	3710 ± 20	7.50 ± 0.17	27.0 ± 0.7
L2	15.4 ± 1.8	670 ± 50	7.9 ± 0.5	63 ± 3	14150 ± 1050	1530 ± 120	4270 ± 260	3.7 ± 0.4	32 ± 2
L3	2.5 ± 0.7	880 ± 50	8.1 ± 0.2	77 ± 5	12850 ± 570	1650 ± 70	3970 ± 120	2.33 ±0.09	31.3 ± 1.1
L4	13.0 ± 1.5	1230 ± 120	8.62 ± 0.11	52.7 ± 0.7	11500 ± 200	1450 ± 40	3400 ± 60	10.3 ± 1.1	30.2 ± 0.5
L5	9.1 ± 1.6	680 ± 15	7.4 ± 0.3	48 ± 2	6880 ± 60	850 ± 20	2320 ± 70	1.62 ± 0.05	19 ± 5

Notes: CB: cherry bones samples, L: legumes samples. Values are the average ± the standard deviation of three replicate analysis of each sample.

Table 2. Mineral content of six Certified Reference Material by means the ICP-OES reference procedure and their accuracy.

Element	NCS ZC73013 spinage (a)			NCS ZC73016 chicken (b)			NIST 1570a spinach leaves (b)		
	Conc. Found (μg g^{-1})	Certified Value (μg g^{-1})	Accuracy (%)	Conc. Found (μg g^{-1})	Certified Value (μg g^{-1})	Accuracy (%)	Conc. Found (μg g^{-1})	Certified value (μg g^{-1})	Accuracy (%)
Ca	5240 ± 120	6600 ± 300	79	---	---	---	14000 ± 1800	15270 ± 410	92
Cu	9.77 ± 0.07	8.9 ± 0.4	110	1.5 ± 1.5	1.46 ± 0.12	103	15 ± 3	12.2 ± 0.6	123
Fe	456 ± 4	540 ± 20	84	32 ± 9	31 ± 3	103	---	---	---
K	26100 ± 160	24900 ± 1100	105	14800 ± 160	14600 ± 700	101	27000 ± 3000	29030 ± 520	93
Mg	4860 ± 70	5520 ± 150	88	1230 ± 16	1300 ± 100	95	8400 ± 1000	8900	94
P	2850 ± 30	3600 ± 200	79	---	---	---	---	---	---
Sr	85.1 ± 0.6	87 ± 5	98	0.56 ± 0.10	0.64 ± 0.08	87	50 ± 7	55.6 ± 0.8	90
Zn	30.4 ± 0.3	35.3 ± 1.5	86	32 ± 6	26 ± 1	123	83 ± 16	82 ± 3	101
Element	NIST 1568a rice flour (b)			TORT-2 (lobster hepatopancreas)(c)			IAEA-359 cabbage (c)		
	Conc. Found (μg g^{-1})	Certified value (μg g^{-1})	Accuracy (%)	Conc. Found (μg g^{-1})	Certified value (μg g^{-1})	Accuracy (%)	Conc. Found (μg g^{-1})	Certified value (μg g^{-1})	Accuracy (%)
Ca	126 ± 9	118 ± 6	107	---	---	---	18200 ± 100	18500 ± 510	98
Cu	2.0 ± 0.3	2.4 ± 0.3	83	113 ± 5	106 ± 10	107	5.6 ± 0.2	5.67 ± 0.18	99
Fe	8.14 ± 1.08	7.4 ± 0.9	110	104 ± 10	105 ± 13	99	146 ± 1	148 ± 3.9	99
K	1220 ± 80	1280 ± 8	95	---	---	---	32500 ± 200	32500 ± 690	100
Mg	530 ± 40	560 ± 20	95	---	---	---	2160 ± 10	2160 ± 50	100
P	---	---	---	---	---	---	---	---	---
Sr	---	---	---	46 ± 4	45.2 ± 1.9	102	50.2 ± 0.4	49.2 ± 1.4	102
Zn	19 ± 4	19.4 ± 0.5	98	179 ± 7	180 ± 6	99	38.9 ± 0.5	38.6 ± 0.7	101

Note: (a): present study. (b): Ruiz de Cenzano et al. 2017. (c): Mir-Marqués et al. 2015.

3.3. PLS-ED-XRF models to determine the mineral profile of foods

3.3.1. Spectral range and latent variables

To build the PLS models, 6 cherry bones and 5 legume samples were used as calibration set. In all PLS-ED-XRF models only 761 variables corresponding to the signals between 0 till 15 keV of the spectra, from a total of 2048 variables, were selected.

To select the optimum number of latent variables (LV), RMSCV together with X and Y explained variances were evaluated. **Fig. 2** shows, as an example, the variation of RMSEC and RMSECV in front of the number of LV for potassium models corresponding to: **Fig 2A** merged model for legumes + cherry bones; **Fig 2B** legumes model and **Fig 2C** model only for cherry bones. As it can be seen in this figure, both, RMSEC and RMSECV, decrease on increasing the number of LV being the best number of LV 5 for the merged model and 2 and 3 for the individual food models. However, taking also into account the RRMSEC and explained variance, it can be concluded that in the case of legumes model 2 LV were enough and for cherry bones 3 LV were needed to build the best models. Explained variance for signal X values were 73.1, 97.9 and 97.9 % for legumes, cherry bones and merged models, respectively, for determination concentration of K. Explained variance for concentration (Y variable) were 99.9, 99.7 and 99.9 %, respectively, considering 5, 2 and 3 LV. The same behavior was found for all the elements considered.

3.3.2. Pre-processing

For the selection of the best model, different preprocessing methods were assayed as indicated in the experimental part. **Table 3** summarizes RRMSEC and RRMSECV of data found for the ED-XRF spectra modelized results. In all the cases, only the best models were selected for each element employing different pre-processing combined treatments.

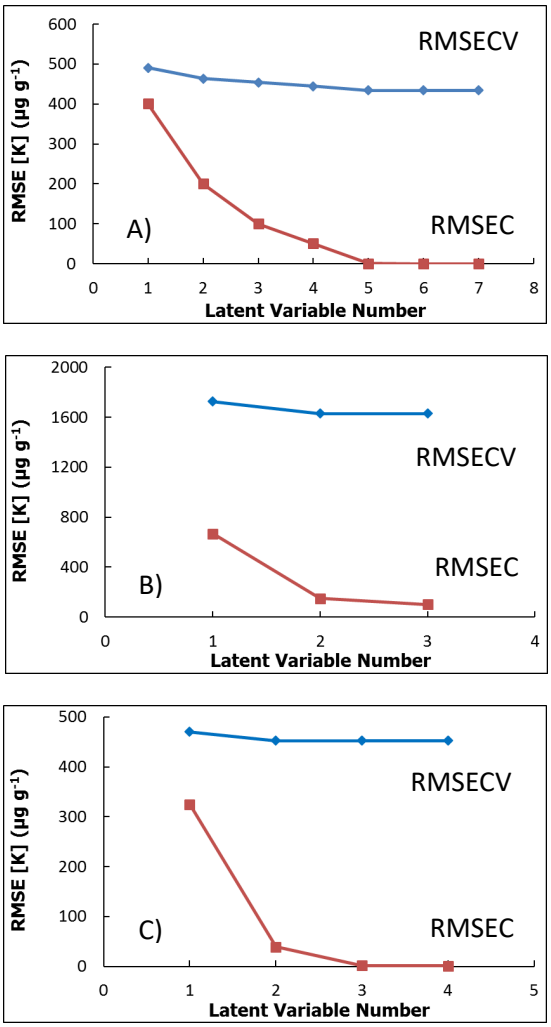

Fig. 2. Effect of the number of latent variables on the root mean square error of calibration (RMSEC) and the root mean square error of cross validation (RMSECV) for K. Note: **2A** correspond to the combined model with legumes + cherry bones, **2B** correspond to legumes model and **2C** correspond to cherry bones model.

Table 3. Conditions and characteristics of the best models for the determination of target mineral elements using different pre-processing treatments of ED-XRF spectra.

Element	Min (µg g^{-1})	Max (µg g^{-1})	Mean (µg g^{-1})	Pre-process	LV	R^2	RMSEC (µg g^{-1})	RRMSEC Mean (%)	RMSECV (µg g^{-1})	RRMSECV Mean (%)	RRMSEP (%)
Model for legumes + cherry bone samples											
Al	0.4	15	6	Autoscale + SD	5	0.99999	0.008	0.13	6	98	33
Ca	623	1554	933	SD + OSC + Autoscale	5	1	0.15	0.016	197	21	1.0
Cu	3.7	9.0	7	OSC + SMO + MC	5	0.99999	0.003	0.04	1.07	16	0.3
Fe	9.7	77	36	Normalize + SMO	5	0.992	2	6	6	17	8
K	1218	14156	6370	OSC + MC	5	1	0.10	0.0016	434	7	13
Mg	498	1655	994	Autoscale + OSC	5	1	0.007	0.0007	129	13	3
P	711	4267	2050	SNV + MC	5	0.99999	7	0.3	220	11	10
Sr	1.6	10	4	SMO + SNV + MC	5	0.994	0.2	5	1.08	26	23
Zn	3.2	32	15	Normalize + OSC + SNV	5	0.99998	0.06	0.4	3	19	16
Model for legume samples											
Al	2.5	13	10	FD + Autoscale	2	0.9994	0.11	1.1	7	70	9
Ca	675	1555	1006	Autoscale + SNV + MC	2	0.9999	4	0.4	332	33	2
Cu	7.4	8.6	8	Autoscale + SNV + MC	2	0.9997	0.009	0.11	0.5	6	2
Fe	48	77	61	Autoscale + MC	2	0.98	1.3	2	8	13	7
K	6881	14193	11912	Variable alignment + Autoscale	2	0.997	148	1.2	1628	14	0.17
Mg	850	1655	1414	Variable alignment + Autoscale	2	0.997	17	1.2	259	18	4
P	2316	4267	3529	SNV + SD + MC	2	0.992	59	1.7	398	11	13
Sr	1.6	10	5	MSC + FD	2	0.96	0.6	12	4	80	10
Zn	20	32	28	SNV + Autoscale + MC	2	0.9996	0.09	0.3	5	18	7

Table 3. Continuation.

				Model for cherry bone samples							
Al	0.4	10	3.3	OSC + SNV + MC	3	0.99999	0.011	0.3	4	121	102
Ca	623	1317	872	SD + OSC	3	0.99999	0.7	0.08	222	25	2
Cu	3.7	7.0	5.4	Autoscale + OSC	3	1	0.0002	0.004	1.3	24	10
Fe	9.7	21	15	SMO + OSC	3	0.998	0.17	1.1	7	47	36
K	1218	2442	1752	SD + OSC	3	0.99998	1.5	0.09	452	26	22
Mg	498	759	644	Autoscale + SD	3	0.99999	0.3	0.05	83	13	20
P	711	1107	817	SD + SNV	3	0.9993	4	0.5	205	25	2
Sr	1.7	6.7	3.3	SD + MC	3	0.99999	0.0006	0.018	1.6	48	15
Zn	3.2	7.4	4.8	SD + OSC	3	0.9996	0.03	0.6	2	42	38

Notes: LV: latent variables. R^2: determination coefficient. RMSEC: root mean square error of calibration. RRMSEC: relative root mean square error of calibration. RMSECV: root mean square error of cross validation. RRMSECV: relative root mean square error of cross validation. RRMSEP: relative root mean square error of prediction. SD: second derivate. OSC: orthogonal signal correction. SNV: standard normal variation. MC: mean centering. FD: first derivate. MSC: multiplicative signal correction. SMO: smoothing.

3.3.3. PLS model calibration

Fig. 3 shows, as an example for Zn, the correlation between the concentrations predicted by PLS-ED-XRF for cherry bone and legume models in front of the concentration obtained by ICP-OES. Models provided R^2 values of 0.9996 with a regression line y = 0.9996 x + 0.0013 for cherry bones, R^2 0.9996 value with a regression y = 0.9996 x + 0.0104 for legumes and R^2 0.99998 for a regression y = 1x + 0.0004 for the merged model for cherry bones + legumes. In these three models, values of 0 for the intercept and 1 for the slope were statistically included. So, no systematic error was found for PLS-ED-XRF predicted data in front of ICP-OES determined ones.

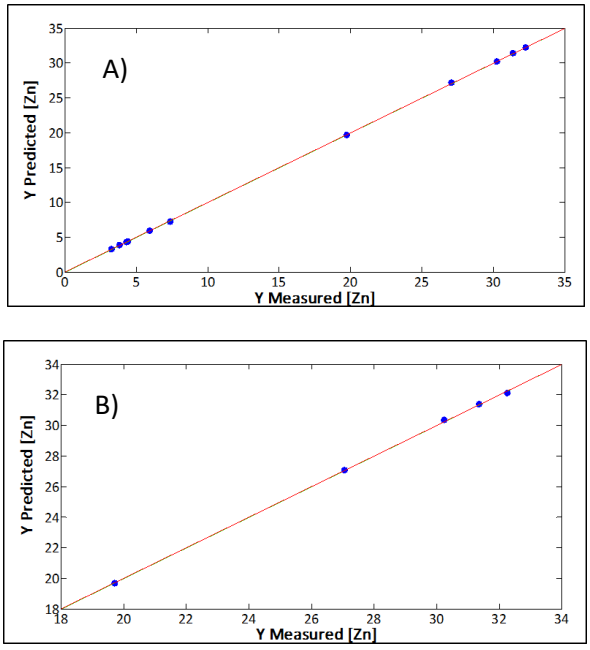

Fig. 3. Concentration predicted in front of concentration of Zn determined by reference method ICP-OES in µg g^{-1} using different models A: PLS merged model for cherry bones and legume samples. B: PLS model for legume samples. C: PLS model for cherry bone samples.

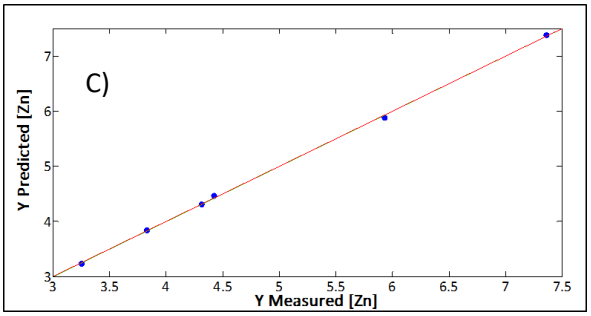

Fig. 3. Continuation.

3.3.4. PLS-ED-XRF model characteristics

Table 3 shows the main characteristics of PLS-ED-XRF models selected for each analyte. The lowest prediction errors were obtained for Cu using the merged model, K for legumes model and Ca and P for cherry bones model being the relative root mean square error of prediction (RRMSEP) 0.3 % for Cu, 0.17 % for K and 2 % for Ca and P. The merged model provided RRMSECV values from 7 till 26 % for K, Ca, Cu, Fe, Mg, P, Sr and Zn. For Al, the relative average error of cross validation was 98 % thus indicating that this element can not be predicted accurately. It is

probably due to the low concentration of Al in the samples and his low sensitivity in ED-XRF. RRMSEP values varied from 0.3 to 23 % for all the analytes excluding Al.

On the other hand, this model works better for cherry samples than that built only from this kind of samples and it could be due to the lowest homogeneity of cherry bones as compared with legumes and from the fact that an increase of the number of calibration objects and concentration ranges also improved the prediction robustness.

The legumes model provided RRMSECV values from 6 till 33 % for Ca, Cu, K, Mg, P and Zn. For Al and Sr RRMSECV values found were 70 and 80 %, respectively. Additionally, RRMSEP values from 0.17 till 13 % were obtained for Al, Ca, Cu, Fe, K, Mg, P, Sr and Zn, evidencing a good prediction capability. It can be concluded that this is the model with lowest prediction error for all the analytes considered.

The cherry bones model provided RRMSECV values from 13 till 48 % for Ca, Cu, Fe, K, Mg, P and Zn and RRMSEP values in the range from 2 till 38 %.

However, for Al, average RRMSECV value of 121 % and RRMSEP value of 102 % were obtained. So, this element can not be quantified by using the PLS-ED-XRF model. On the other hand, it can be concluded that the model established just from cherry bones predicted worse the concentration of considered elements that the merged model.

As compared with previous studies made on the mineral composition of foods by ED-XRF (Mir-Marqués et al., 2014 and 2016) it can be concluded that the use of data found by ICP-OES for samples of the same type that those to be analyzed permits to obtain accurate results also using a general merged model including different types of foods. The single limitations come from the reduced sensitivity of ED-XRF for many elements of interest and problems related to the homogeneity of solid samples which were directly analyzed by the proposed method.

4. Conclusions

A green, fast and non-destructive method was developed for the determination of Ca, Cu, Fe, Mg, P, Sr and Zn in cherry and legume samples by using ED-XRF measurements. PLS models built from ED-XRF spectra of a series of samples previously analyzed by ICP-OES allowed the determination of mineral profile with accurate results avoiding sample digestion and dissolution, without consumption of reagents and generation of wastes, thus offering an alternative to atomic spectroscopy techniques involving sample digestion. However, it must be noticed that reference data, obtained by atomic spectroscopy methodologies is required as the base to build the ED-XRF calibration models.

5. Conflict of interest

There is no conflict of interest between the authors.

6. Acknowledgements

The authors acknowledge the financial support of Ministerio de Ciencia, Innovación y Universidades-Agencia Estatal de Investigación FEDER (EU) (Project CTQ2016-78053-R and CTQ2014-52841-P).

7. References

Almela, C., Clemente, M. J., Vélez, D., Montoro, R., 2006. Total arsenic, inorganic arsenic, lead and cadmium contents in edible seaweed sold in Spain. Food Chem. Toxicol. 44, 1901-1908.

Alvarez, M., Mazo-Gray, V., 1990. Determination of potassium and calcium in milk powder by energy-dispersive x-ray fluorescence spectrometry. X-ray Spectrom. 19, 285-287.

Butkuté, B., Padarauskas, A., Cesevičiené, J., Pavilonis, A., Taujenis, L., Lemežiené, N., 2017. Perennial legumes as a source of ingredients for healthy food: proximate, mineral and phytoestrogen composition and antibacterial activity. J. Food Sci. Technol. 54 (9), 2661-2669.

Carbonell-Barrachina, Á.A., Ramírez-Gandolfo, A., Wu, X., Norton, G. J., Burló, F., Deacon, C., Meharg, A.A., 2012. Essential and toxic elements in infant foods from Spain, UK, China and USA. J. Environ. Monit. 14, 2447-2455.

de la Guardia, M., Garrigues, S., (eds.) 2015. Handbook of mineral elements in food. John Wiley & Sons (Oxford, UK).

Ekinci, N., Ekinci, R., Sahin, Y., 2002. Determination of iodine and calcium concentrations in the bread improver using EDXRF. J. Quant. Spectrosc. Radia. Transfer 74 (6), 783-787.

Fairweather-Tait, S. J., Hurrell, R. F., 1996. Bioavailability of minerals and trace elements. Nutr. Res Rev. 9 (1), 295-324.

Gliszczyńska-Świglo, A., Klimczak, I., Rybicka, I., 2018. Chemometric analysis of minerals in gluten-free products. J. Sci. Food and Agric. 98, 3041-3048.

Goldhaber, B. S., 2003. Trace elements risk assessment: essentiality vs toxicity. Regul. Toxicol. Pharmacol. 38, 232-242.

Joseph, D., Lal, M., Bajapi, H. N., Mathur, P. K., 1999. Levels of trace elements of few indian spices by energy dispersive X-ray fluorescence (EDXRF) method. J. Food Sci. Technol. 36, 264-265.

Kelly, S. D., Bateman, A. S., 2010. Comparison of mineral concentrations in commercially grown organic and conventional crops-Tomatoes (*Lycopersicon esculentum*) and lettuces (*Lactuca sativa*). Food Chem. 119, 738-745.

Lescano, C. H., de Oliveira, I. P., de Lima, F. F., Baldivia, D. S., Justi, P. N., Cardoso, C. A. L., Raposo Júnior, J. L., Sanjinez-Argandoña, E. J., 2018. Nutritional and chemical characterizations of fruits obtained from Syagrus romanzoffiana, Attalea dubia, Attalea phalerata and Mauritia flexuosa. J. Food Meas. Charac. 12, 1284-1294.

Matos-Reyes, M. N., Simonot, J., López-Salazar, O., Cervera, M. L. de la Guardia, M., 2013. Authentication of Alicante´s Mountain cherries protected designation of origin by their mineral profile. Food Chem. 141, 2191-2197.

Mbaye, M., Traore, A., Ndao, A. S., Wague, A., 2015. Multivariate statistical techniques to determine essential and toxic elements in biological samples by X-ray fluorescence. J. Instrum. Sci. Technol. 43, 369-378.

Mir-Marqués, A., Cervera, M. L., de la Guardia, M., 2012. A preliminary approach to mineral intake in the Spanish diet stablished from analysis of the composition of university canteen menus. J. Food Compos. Anal. 27, 160-168.

Mir-Marqués, A., Garrigues, S., Cervera, M. L., de la Guardia, M., 2014. Direct determination of minerals in human diets by infrared spectroscopy and X-ray fluorescence, Microchem. J. 117, 156–163.

Mir-Marqués, A., González-Masó, A., Cervera, M. L., de la Guardia, M., 2015. Mineral profile of Spanish commercial baby food. Food Chem. 172, 238-244.

Mir-Marqués, A., Martínez-García, M., Garrigues, S., Cervera, M. L., de la Guardia, M., 2016. Green direct determination of mineral elements in artichokes by infrared spectroscopy and X-ray fluorescence. Food Chem. 196, 1023-1030.

Nas, S., Gokalp, H., Sahin, Y. Z., 1993. K and Ca content of fresh green tea, black tea, and tea residue determined by X-ray fluorescence analysis. Z. Lebensm.-Unters.-Forsch. 196, 32-37.

Nielsen, F. H., 1998. Ultratrace elements in nutrition: current Knowledge and speculation J. Trace Elem. Exp. Med. 11, 251-274.

Nielson, K. K., Mahoney, A. W., Williams, L. S., Rogers, V. C., 1991. X-ray fluorescence measurements of Mg, P, S, Cl, K, Ca, Mn, Fe, Cu, and Zn in fruits, vegetables and grain products. J. Food Compos. Anal. 4, 39-51.

Nielson, K. K., Mahoney, A. W., Williams, L. S., Rogers, V. C., 1991. Mineral concentrations and variations in fast-food samples analyzed by X-ray fluorescence. J. Agric. Compos. Anal. 39, 887-892.

Palmer, P. T., Jacobs, R., Baker, P. E., Ferguson, K., Webber, S., 2009. Use of field-portable XRF analyzers for rapid screening of toxic elements in FDA-regulated products. J. Agric. Food. Chem. 57, 2605-2613.

Perring, L., Andrey, D., 2004. Wavelength-dispersive x-ray fluorescence measurements on organic matrices: application to milk-based products. X-Ray Spectrom. 33, 128-135.

Perring, L., Andrey, D., 2003. ED-XRF as a tool for rapid minerals control in milk-based products. J. Agric. Food Chem. 51, 4207-4212.

Porto, H. L. R., de Castro, A. C. L., Azevedo, J. W. J., Soares, L. S., Ferreria, C. F. C., Silva, M. H. L., Ferreira, H. R. S., 2017. Mineral content in the lower course of the itapecuru river in the state of Maranhão, Brazil. Korean J. Chem. Eng. 34 (7), 1985-1991.

Ramírez-Ojeda, A. M., Moreno-Rojas, R., Cámara-Martos, F., 2018. Mineral and trace element content in legumes (Lentils, Chickpeas and beans): Bioaccesibility and probabilistic assessment of the dietary intake. J. Food Compos. Anal. 73, 17-28.

Ruiz de Cenzano, M., Rochina-Marco, A., López-Salazar, Ó., Cervera, M. L., de la Guardia, M., 2017. Mineral profile of children´s fast food menu samples. J. AOAC Int. 100, 1879-1884.

Saleh, N. S., Al-Saleh, K. A., 1986. Combined XRF and PIXE analysis of flour. Appl. Phys. Communi. 6, 195-204.

Sarkar, A. P., Basumatary, S., Das, S., 2017. Determination of nutritional composition of some selected fishes from Hel River of North-East India. Asian J. Chem. 29 (11), 2493-2496.

Siemianowska, E., Barszcz, A. A., Skibniewska, K. A., Markowska, A., Polak-Juszczak, L., Zakrzewski, J., Woźniak, M., Szarek, J., Dzwolak, W., 2016. Mineral content of muscle tissue of rainbow trout. Journal of Elementol. 21 (3), 833-845.

Singh, P., Prasad, S., Aalbersberg, W., 2016. Bioavalibility of Fe and Zn in selected legumes, cereals, meat and milk products consumed in Fiji. Food Chem. 207, 125-131.

Stanimirović, B., Djordjević, J.P., Pejin, B., Maletić, R., Vujović, D., Raičević, P., Tešić, Ž., 2018. Impact of clonal selection on Cabernet Franc Grape and wine elemental profiles. Sci. Hortic. 237, 74-80.

Stojanović, B. T., Mitić, S. S., Stojanović, G. S., Mitić, M. N., Kostić, D. A., Paunović, D. Đ., Arsić, B. B., Pavlović, A. N., 2017. Phenolic profiles and metal ions analyses of pulp and peel of fruit and seeds of quince (*Cydonia oblonga* Mill.). Food Chem. 232, 466-475.

Wheal, M. S., DeCourcy-Ireland, E., Bogard, J. R., Thilsted, S. H., Stangoulis, J. C. R., 2016. Measurement of haem and total iron in fish, shrimp and prawn using ICP-MS: Implications for dietary iron intake calculations. Food Chem. 201, 222-229.

Zand, N., Chowdhry, B. Z., Zotor, F. B., Wray, D. S., Amuna, P., Pullen, F. S, 2011. Essential and trace elements content in commercial infant foods in the UK. Food Chem. 128, 123-128.

CAPÍTULO 5

Determinación de elementos esenciales y no esenciales en cacaos en polvo españoles mediante técnicas espectroscópicas

Determination of essential and non-essential elements in Spanish cocoa powder by spectroscopic techniques

L. Herreros-Chavez, A. Morales-Rubio, M.L. Cervera

Department of Analytical Chemistry, University of Valencia, 50 Dr. Moliner St., 46100 Burjassot, Valencia, Spain

ABSTRACT

Concentration of essential elements (B, Ca, Co, Cr, Cu, Fe, K, Mg, Mn, Mo, Na, Ni, P and Zn) and non-essential elements (Al, Ba, Cd, Pb, Sr and Ti) in 21 cocoa powder samples were determined by Inductively Coupled Plasma Optical Emission Spectroscopy (ICP-OES). For the determination of these elements, microwave assisted acid digestion were needed. The procedure requires the use of few mL of concentrated nitric acid and hydrogen peroxide for the digestion of the samples. Cocoa powder and hot chocolates from different Spanish brands with different concentration of those elements between them were analyzed. Employing the concentration obtained by ICP-OES as reference data, in combination with chemometric treatment and energy dispersive X-ray fluorescence spectra, it was built models for the prediction of the concentration in cocoa powder samples of 10 elements. A dendrogram was done in order to classify the samples analyzed in function of their elemental composition. Essential elements were assessed for their daily intake with the daily reference intakes (DRI) and compared these results with the values recommended for Union European. Accuracy of the procedure employed was checked by analysis of the Certified Reference Material rice flour-unpolished from National Institute for Environmental Studies (NIES).

Keywords: cocoa powder, essential elements, heavy metals, dietary reference intake (DRI), PLS.

1. Introduction

Cocoa powder is a food product obtained from three different varieties of cocoa beans *Theobroma cacao L*. as Forastero, Criollo and Trinitario (Afoakwa, Quao, Takrama, Budu & Saalia, 2013). Discovered by Mayan civilization approximately 2500 years ago, cocoa liquor is produced from roasted and pressed beans. Later, from partially defatted liquor, cocoa powder is obtained (Jacquot et al., 2016). Nowadays, cocoa powder is a high consumption food product in all the world due to it is flavor, texture and organoleptic properties (Villa, Pereira & Cadore, 2015). It contains most of the essential elements for the human diet and it is consumption has beneficial effects due to the intakes of flavonoids (specifically catechin and epicatechin) and polyphenols, that reduce the risk of cancer, and heart attack (Hertog et al., 1995; Geleijnse, Launer, Hofman, Pols & Witterman, 1999) and for it is antioxidant properties (Calatayud et al., 2013; Fernández-Murga, Tarín, García-Perez & Cano, 2011).

In the human body it can be found at least 25 essential chemical elements for the life, 13 metals and 12 non-metals, actively participating in a high variety of biological processes (Faus, García-España & Moratal, 2003). An insufficient intake of these elements can produce pathological effects, which can disappear with the adequate supply. In some cases, the margin that it exists between deficiency and toxicity of that one element is very small (Faus, García-España & Moratal, 2003). On the other hand, the presence of heavy metals in foods (like Cd and Pb) can have toxic effects in the human organism (Shittu & Badmus, 2009), being able to produce bioaccumulation of them in the body.

Different organisms of important relevance like World Health Organization (WHO), Institute of Medicine of the National Academies of United States of America (IoM) or European Food Safety Authority (EFSA) have established which are the dietary recommended intake (DRI) of essential elements.

Usually, atomic spectrometric techniques are the most used for the determination of the element profile in cocoa powder samples as Flame Atomic Absorption Spectrometry (FAAS) (Shittu & Badmus, 2009; Dahiya, Karpe, Hegde & Sharma, 2005; Ferreira et al., 2008; Güldas, 2008; Ieggli, Bohrer, do Nascimento & de Carvalho, 2011; Rehman & Husnain, 2012; Alagić & Huremović, 2015), Graphite Furnace Atomic Absorption Spectrometry (GFAAS) (Güldas, 2008; Rehman & Husnain, 2012; Sepe,

Constantini, Cirialli, Ciprotti & Giordano, 2001; Jalbani et al., 2007; Ieggli, Bohrer, do Nascimento, de Carvalho & Gobo, 2011; Peixoto, Devesa, Vélez & Cervera, 2016), Inductively Coupled Plasma Optical Emission spectrometry (ICP-OES) (Villa, Pereira & Cadore, 2015; Peixoto, Devesa, Vélez & Cervera, 2016; Anthemidis & Pliatsika, 2005; Pedro, de Oliveira & Cadore, 2006; Sager, 2012) and Inductively Coupled Plasma Mass Spectrometry (ICP-MS) (Villa, Pereira & Cadore, 2015; Sager, 2012; Yanus et al., 2014; Mounicou, Szpunar, Andrey, Blake & Lobinski, 2003).

All these techniques need the use of a previous digestion to eliminate the organic matter present in the sample and bring the elements to the solution. This treatment requires a few milliliters of concentrated acids and that enable the complete extraction of the bioaccesible elements for the human organism.

An alternative to conventional methods for the quantification of mineral profile is the employ of direct methodologies, as Energy Dispersive X-ray Fluorescence (ED-XRF) or infrared spectroscopy. These techniques no need sample treatment, or minimum treatment of them, and permit fast and direct analysis for quantify analytes in different matrix. ED-XRF can be used for a high type of matrix as geological (Sciuto et al., 2019), biological (Pouzar, Zvolská, Jarolím & Vavrušová, 2017) and food (Herreros-Chavez, Morales-Rubio & Cervera, 2019).

In the present contribution, it was determined the content of essential and non-essential elements in different brands of cocoa powder considering the type of cocoa. ICP-OES was the method used for the determination of the mineral profile in the samples and to establish the daily intakes from this food. ED-XRF spectra were employed for built models with chemometric treatment in combination of reference data provided by ICP-OES.

2. Material and methods

2.1. Samples

Twenty-one cocoa powder samples were purchased in local supermarkets of Valencia, Spain: two original type preparation cocoa powder (brands A and B), two preparations by instant solution in hot and cold milk cocoa powder (brands C and D) and three cocoa powders for consumption after cooking (brands E, F and G). In all brands, three lots of each one were analyzed. A

detailed description of the analyzed cocoa powder samples is presented in **Table 1**, including the mineral content and composition when this data has been included in the package label. For check the accuracy of the method, the Certified Reference Material rice flour-unpolished (NIES-1568a) from National Institute for Environmental Studies was analyzed.

2.2. Microwave digestion of samples

0.5 g with an accuracy of 0.1 mg of the cocoa powder samples were weighed into a polytetrafluoroethylene modified vessel (TFM) and 4 mL of 15.4 mol/L HNO_3 from Scharlau (Barcelona, Spain) were added into the TFM vessels. Then, vessels were introduced in an ultrasound water bath for 15 minutes. 1 mL of 12.3 mol/L H_2O_2 (Scharlau) was added and the vessels were shaken manually, outside de water bath, for reduce the foam produced by the reaction. 4 mL of ultrapure water from Adrona System (Riga, Latvia) were added. The predigestion ends when the brown vapors cease and the shaked samples were practically dissolved.

Vessels with the predigested samples were introduced in their respective protection shield, placed the covers, closed hermetically, and introduced them into the microwave oven “Ethos Sel” Milestone (Sorisole, Italy). The digestion program consists of a progressive increase of the temperature to reach 200 °C in 25 minutes with a maximum power exit of 500 W and another step maintaining the temperature at 200 °C for 15 minutes with a maximum power exit of 900 W.

When the digestion was completed, the reactors were removed from the microwave, cooled and opened inside the fume hood. The liquid was quantitatively transferred to 50 mL polypropylene tubes, collecting the sample droplets with ultrapure water and diluting to a final volume of 15 mL.

Table 1. Label information of the different samples.

Brand	Ingredients	Energetic Value (Kcal)	Mineral content (mg/100 g)	Recommended portion (g)
A	Sugar, skimmed cocoa powder, kola-malted cereal cream, mineral salts, aromas and salt.	376	[Ca]:300 [Fe]: 15	15
B	Sugar, skimmed cocoa powder (25%), dicalcium phosphate, vanilla flavour, salt and cinnamon powder.	377	Not indicated	18
C	Sugar, skimmed cocoa (21.6%), vitamins, minerals, aroma, cinnamon, salt, sunflower oil and emulsifier.	383	[Fe]: 14.7 [Zn]: 5.5	14
D	Sugar, skimmed cocoa powder, wheat flour, emulsifier (soy lecithin), aromas and salt.	394	Not indicated	15
E	Sugar, low fat cocoa powder, wheat flour, emulsifier and flavourings.	382	Not indicated	50
F	Sugar, skimmed cocoa powder (19%), corn starch and vanilla flavour.	380	Not indicated	50
G	Sugar, thickeners, skimmed cocoa powder, aromas and salt.	383	Not indicated	33

2.3. ED-XRF sample treatment

Sample analysis by ED-XRF was performed on pellets of the different cocoa samples. To prepare the pellets, 0.8 g of sample were weighed directly into a glass mortar and homogenized with the pestle for 2 min. The homogenous samples were introduced into an evacuable pellet die (Specac GS03000, Orpington, UK), pressing at 1961.3 Pa for 2 minutes and 13 mm in diameter and 2–3 mm thick pellets were obtained. Three pellets were prepared from each lot of the different commercial brands. All pellets were stored in a desiccator before and after their analysis.

2.4. Statistical analysis

Statistical analysis was performed employing the tool regression in data analysis from Excel Microsoft Office software. The uncertainties were calculated by the "desvest" function included in the software which calculates the standard deviation with "n-1" method. This function employs the following equation:

$$\sqrt{\frac{\sum(x-\tilde{x}^2)}{(n-1)}}$$

Where "x" is each value of the sample, "$\tilde{x}$" is the average of the sample and "n" is the size of the samples.

2.5. Instrumentation

Digested samples were analyzed by using an ICP-OES "Optima 5300 DV" Perkin-Elmer (Norwalk, CT, USA) spectrometer equipped with AS93-plus automatic sampler. A radio frequency power of 1300 W; a plasma Ar flow of 15 L/min, an auxiliary Ar flow of 0.2 L/min, a nebulizer Ar flow of 0.8 L/min and a sample flow of 1.1 mL/min were employed. All the elements were measured in axial mode (except for Ca, K, Mg, Na and Sr which were measured in radial mode). As internal standard a 1 mg/L Rhenium solution from Fluka (Neu-Ulm, Switzerland) was employed. The most sensitive emission line, free of spectra interferences, was selected for each element. For the background correction two points were used. Control standards were measured for every series of 10 independent sample measurements. A multielement calibration standard solution containing 26 elements in HNO3

1.20 mol/L (Scharlau) was employed. Calibration standards were prepared daily by diluting adequately the stock solution in the range 0.025 to 5 mg/L. For Ca (Scharlau), K (Scharlau) Mg (Scharlau), Na (Scharlau) and P (Scharlau), from their 1000 mg/L standard solutions additional calibration from 10 until 200 mg/L were done.

For ED-XRF analysis, a portable energy dispersive X-ray fluorescence S1 TITAN LE SMA-1402 from Bruker (Kennewick, WA, USA) equipped with a rhodium X-ray tube, employing the maximum voltage (50 kV) and the maximum amperage (7 μA) amperage, and with a X-flash silicon drift detector (SDD), with a high energy resolution of 147 eV at Mn Kα with automatic changer, was employed. Each measurement takes 60 second; during the first 30 s the low atomic number elements (from Mg till Cr) were measured and the next 30 s were used to mesure the high atomic number elements (from Mn till U).

2.6. Chemometric treatment

Models for the prediction of the mineral profile in cocoa powder employing their ED-XRF spectra were performing using partial least squares (PLS), employing Matlab 2014a software from Mathworks (Natick, MA, USA) and PLS Toolbox 6.2 from Eigenvector Research Inc. (Wenatchee, WA, USA). Calibration set was composed by 7 cocoa powder samples of known concentration of elements determined by ICP-OES and 13 samples were used for validation set. For built the best PLS models considering the energy range of the ED-XRF spectra, the number of latent variables and the most adequate signal pre-processing were employed in order to found the lowest calibration and cross validation errors. In all the cases, venetian blinds with 2 splits cross validation (CV) was employed for the selection of the optimum number of latent variables (LV) with the minimum root mean square error of cross validation (RMSECV). Mean centering (MC), first derivate (FD), second derivate (SD), smoothing (SMO), orthogonal signal correction (OSC) and multiplicative signal correction (MSC), were assayed as signal pretreatments alone and combined between them.

3. Results and discussion

3.1. Mineral profile of the samples

Fig. 1 shows the concentration of Ca, Fe, K, P, Mg, Na, Zn, Cu, Al, Mn, B, Ba, Ni, Sr, Ti, Cr, Cd, Co, Mo and Pb obtained by ICP-OES in cocoa powder samples after microwave assisted digestion. In all the cases the concentration, corresponding to the average of three independent analyses of each lot, were expressed in µg/g. As it can be seen in **Fig. 1**, there is a high repeatability between the three lots analyzed from each brand, concluding that there are no significant differences between them. Only in the cases of Cd and Pb there is a higher difference between lots, but this fact may be due to the small concentration of these elements in the samples.

K, P, Ca, Mg, Na and Fe were the most abundant elements in cocoa powder samples. Their composition ranged from 4160 to 9600 µg/g, from 1270 to 2660 µg/g, from 310 to 2680 µg/g, from 875 to 2550 µg/g, from 41 to 1340 µg/g and from 64 to 350 µg/g, respectively. Al, Cu, Mn and Zn are minority elements and were present in the samples in lower concentrations, being found concentrations from 31 to 78 µg/g, from 6.9 to 15.7 µg/g, from 8.8 to 16.7 µg/g and from 11 to 52 µg/g, respectively. B, Ba, Cd, Co, Cr, Mo, Ni, Pb, Sr and Ti were quantified in trace amount with concentration ranged from 3.5 to 6.4 µg/g, from 2.6 to 4.9 µg/g, from 0.0008 to 0.252 µg/g, from 0.18 to 1.19 µg/g, from 0.09 to 2.54 µg/g, from 0.04 to 0.26 µg/g, from 1.8 to 3.2 µg/g, from 0.013 to 0.090 µg/g, from 3.4 to 8.1 µg/g and from 0.8 to 51.8 µg/g respectively.

The concentration obtained for the non-essential elements, Al, Ba, Cd, Pb and Sr were very low values, so it can be concluded that the intakes of this food not presents a risk for consumers health. From them, aluminum was present in a higher concentration (78.0 µg/g), but an adult could consume, in a day, around 7 to 9 mg of Al without consequences. In the case of Cd, the European Union marks the maximum level of cadmium in cocoa foodstuffs being between 0.1 till 0.8 mg/kg depending on the type of cocoa taking into account the quantity of dry cocoa in the product. and 0.05 mg/kg the maximum level of lead (Commission Regulation Nº 488/2014). As it can be seen in the fig. 1, the average of the concentration found in these products was 0.068 µg/g for Cd and 0.043 µg/g for Pb, so it can be concluded that the concentration of Cd and Pb quantified in these samples did not exceed the maximum limit allowed.

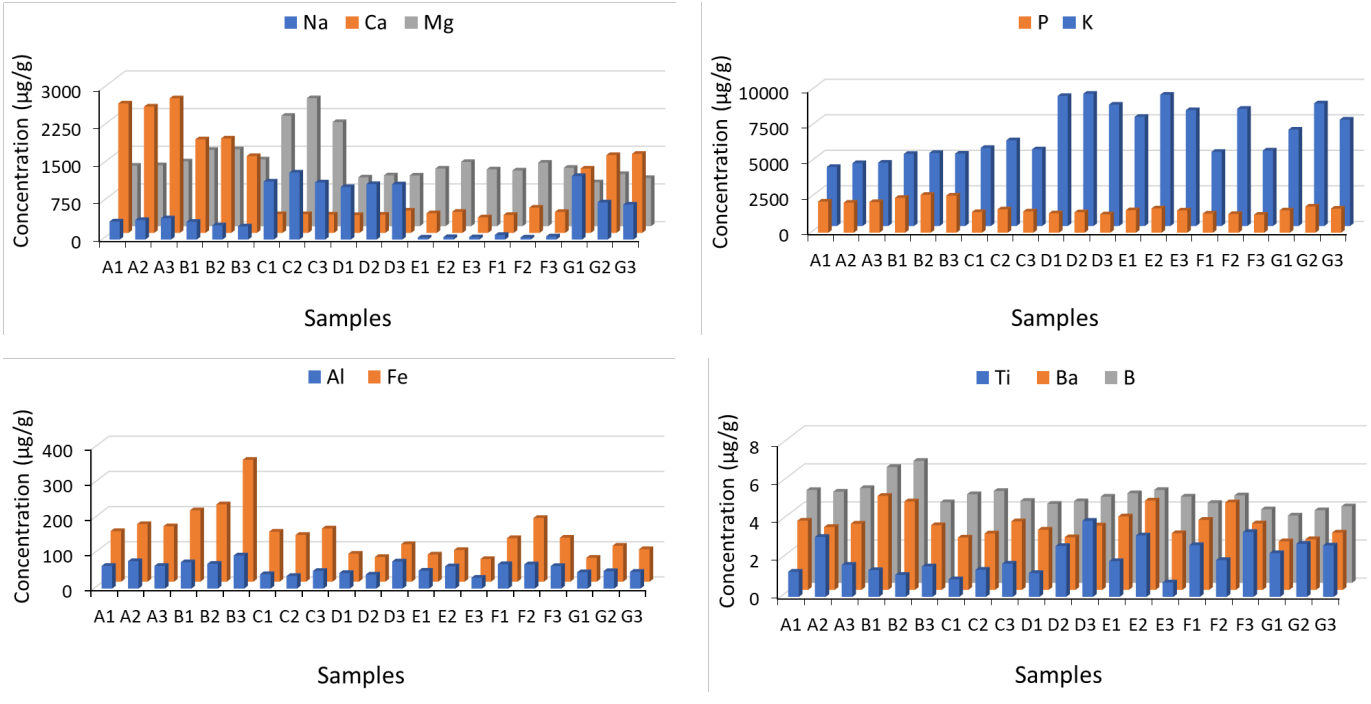

Fig. 1. Concentration of K, Ca, Fe, P, Mg, Na, Zn, Cu, Al, Mn, B, Ba, Ni, Sr, Ti, Cr, Cd, Co, Mo and Pb in cocoa powder samples analyzed by ICP-OES. Notes:

- A, B, C, D, E, F and G: different analyzed brands.
- 1, 2 and 3: lots of each brand analyzed.

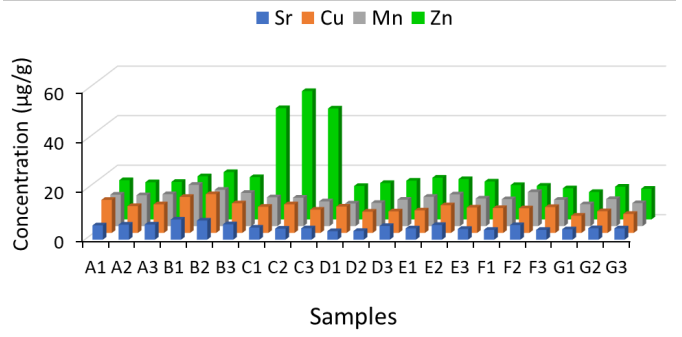

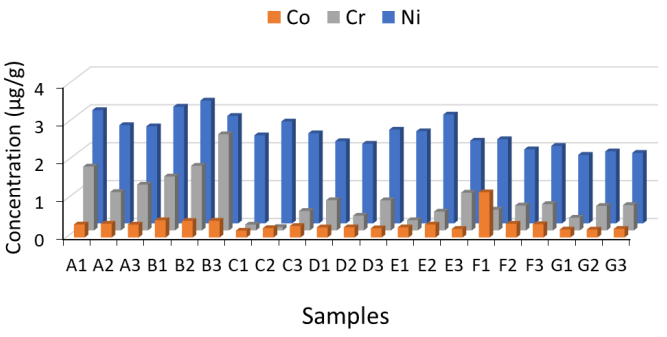

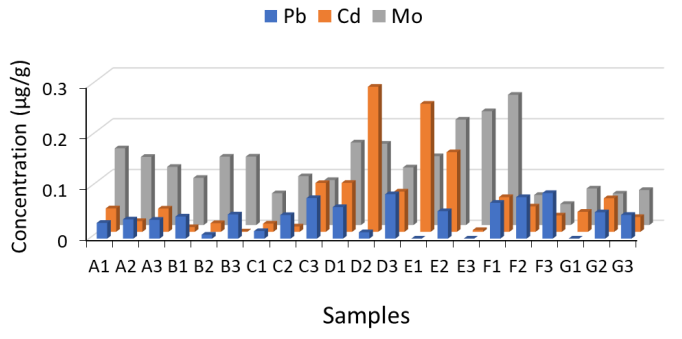

Fig. 1. Continuation.

3.2. Accuracy of ICP-OES measurements

NIES rice flour-unpolished certified sample was analyzed in order to assure ICP-OES analysis. **Table 2** shows the results obtained by the employed procedure and the certified values. These results were compared using the Application Note 1 of European Reference Materials (ERM) and the statistical analysis shows, in all the analytes, that expanded uncertainty was greater than the difference between mean measured and certified values, so means no significant differences were found between the measured results and the certified values.

Table 2. Concentration of mineral content in μg g^{-1} in Certified Reference Material Rice Flour from NIES.

Analytes	Obtained Values	Certified Values	Analytes	Obtained values	Certified Values
Ca	96.2 ± 1.1	95 ± 2	Mn	39.5 ± 0.8	40.1 ± 2.0
Cd	1.7 ± 0.3	1.82 ± 0.06	Mo	1.42 ± 0.17	1.6 ± 0.1
Co	0.0080 ± 0.0010	0.007*	Na	17 ± 4	14.0 ± 0.4
Cr	0.09 ± 0.02	0.08*	Ni	0.26 ± 0.08	0.30 ± 0.03
Cu	4.6 ± 0.3	4.1 ± 0.3	P	3400 ± 100	3350 ± 80
Fe	12.0 ± 0.6	11.4 ± 0.8	Sr	0.34 ± 0.16	0.2*
K	2771 ± 3	2750 ± 100	Zn	22.2 ± 0.7	23.1 ± 0.9
Mg	1220 ± 90	1250 ± 80			

Note: Data with * is for reference only

3.3. PLS models

3.3.1. Spectral range of X-ray fluorescence

For built PLS models, ED-XRF spectra of each sample analyzed was employed. Lines corresponding to mineral profile of the samples were located between 0 and 18 keV. Seven cocoa powder samples were used to perform the calibration set. A total of 761 variables were selected in all the models built and the best of them was chosen.

3.3.2. Latent variables

For the selection of the number of latent variables (LV), root mean square error of cross validation (RMSECV) in combination with X and Y explained variances were evaluated. **Table 3** shows the number of LV chosen in the model for each analyte. In each case, it was built the model with the minimum number of the LV. For Ca, Mg, Mn, Mo, P, Sr and Zn 2 LV were need and for Fe, K and Ni 1 LV was need for built the models with the minimum error. In all the cases, RMSEC and RMSECV decrease on increasing the number of LV.

Table 3 summarizes the different preprocessing employed for built the best models with the minimum error. Only the best models were selected for each analyte. This table shows the coefficient of determination of the PLS model calibration of each analyte and as can be see provide high coefficients of determination, with values from 0.89 till 0.998.

Table 3. Characteristics of the best PLS-ED-XRF models for the determination of mineral profile in cocoa powder samples.

Element	Range (μg g^{-1})	Mean (μg g^{-1})	SD (μg g^{-1})	Pre-process	LV	R^2	RMSEC (μg g^{-1})	RMSECV (μg g^{-1})
Ca	311-2681	1054	853	SD+MC	2	0.96	178	202
Fe	64-346	135	66	OSC+FD+MC	1	0.96	8	27
K	4158-9306	6621	1793	SMO+MSC	1	0.89	539	725
Mg	875-2550	1328	437	FD+MC	2	0.98	56	367
Mn	8.84-16.7	11.7	1.97	FD+MC	2	0.89	0.8	1.7
Mo	0.041-0.256	0.122	0.057	SD+OSC+MC	2	0.91	0.018	0.09
Ni	1.81-3.24	2.42	0.42	SD+OSC+MC	1	0.98	0.07	0.2
P	1267-2661	1750	439	SD+MC	2	0.86	149	279
Sr	3.43-8.12	5.15	1.26	FD+OSC+MC	2	0.998	0.06	1.1
Zn	11.1-51.8	19.5	11.8	FD+MC	2	0.97	1.9	12

Notes: SD: standard deviation; LV: latent variables; RMSEC: root mean square error of calibration; RMSECV: root mean square error of cross validation; MC: mean centering; FD: first derivate; SD: second derivate; OSC: orthogonal signal correction; SMO: smoothing; MSC: multiplicative signal correction; RMSEC: relative mean square error of calibration; RMSECV: relative mean square error of cross validation.

3.3.3. PLS-ED-XRF model characteristics

Table 3 summarizes the main characteristics of PLS-ED-XRF models selected for each analyte. For the 10 elements analyzed the best models built provided RMSEC values from 0.018 till 539 μg g^{-1} being the high concentration range of the model. If compare the RMSEC and RMSECV values with the average concentration of the samples, a high correlation between them was found. Regression lines $y = 0.081x + 4.572$ with $R^2 = 0.96$, and $y = 0.112x + 59.69$ with $R^2 = 0.82$ were found for RMSEC and RMSECV, respectively.

Fig. 2 shows the good agreement between concentrations predicted by PLS model and the ICP-OES reference data for cocoa samples. As it can be seen, the analytes with high concentrations in the samples, as Ca, K, Mg, Fe, P and Zn, had better correlation than the elements with low concentration, as Sr, Ni, Mn and Mo. In all the cases, with the exception of Mo, 0 value for the intercept was included and with the exception of Fe, P and Mo, 1 value for the slope was included in each equation line. Therefore, it can be concluded that no systematic error was made with the use of these expected concentrations. In the case of Mo, due to the low concentration of this element in the samples, can not predicted by ED-XRF-PLS model.

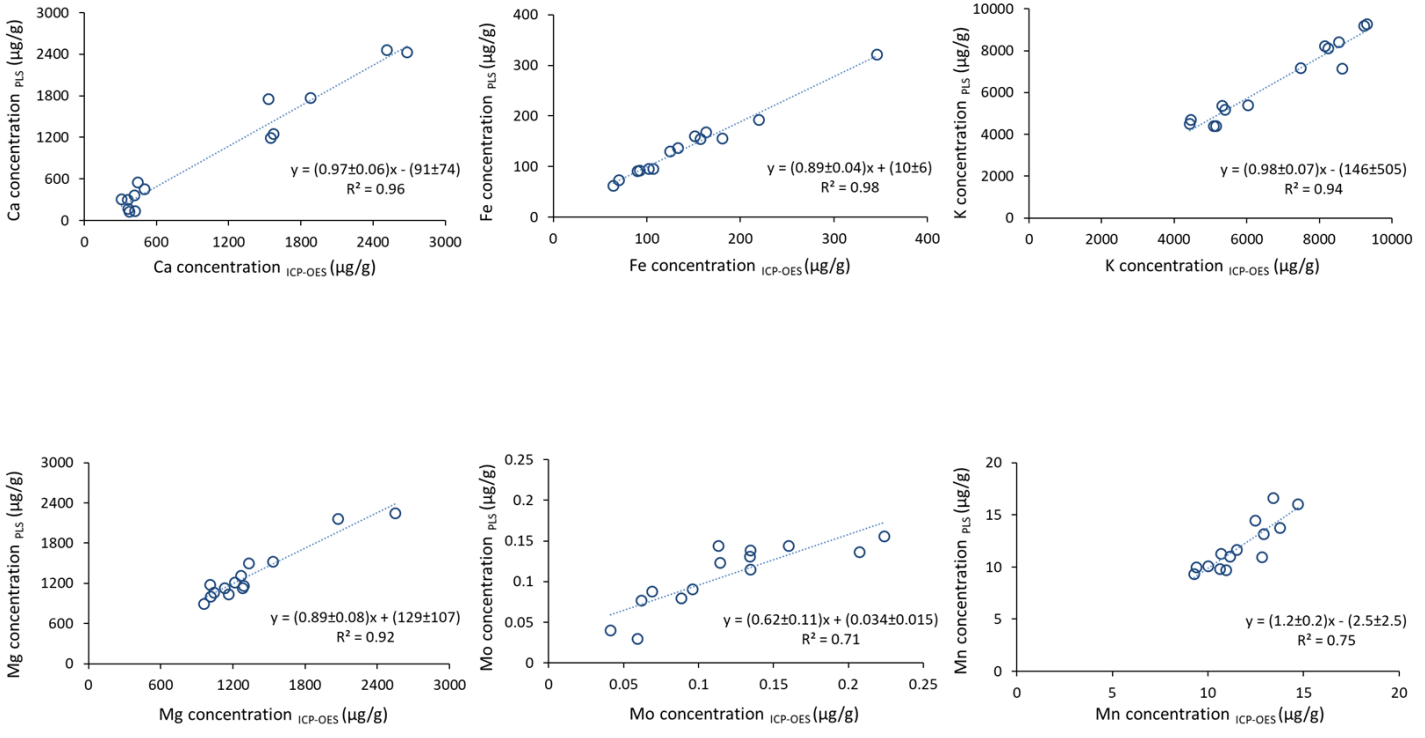

Fig. 2. Comparison between the concentration predicted by PLS and the concentration obtained by ICP-OES.

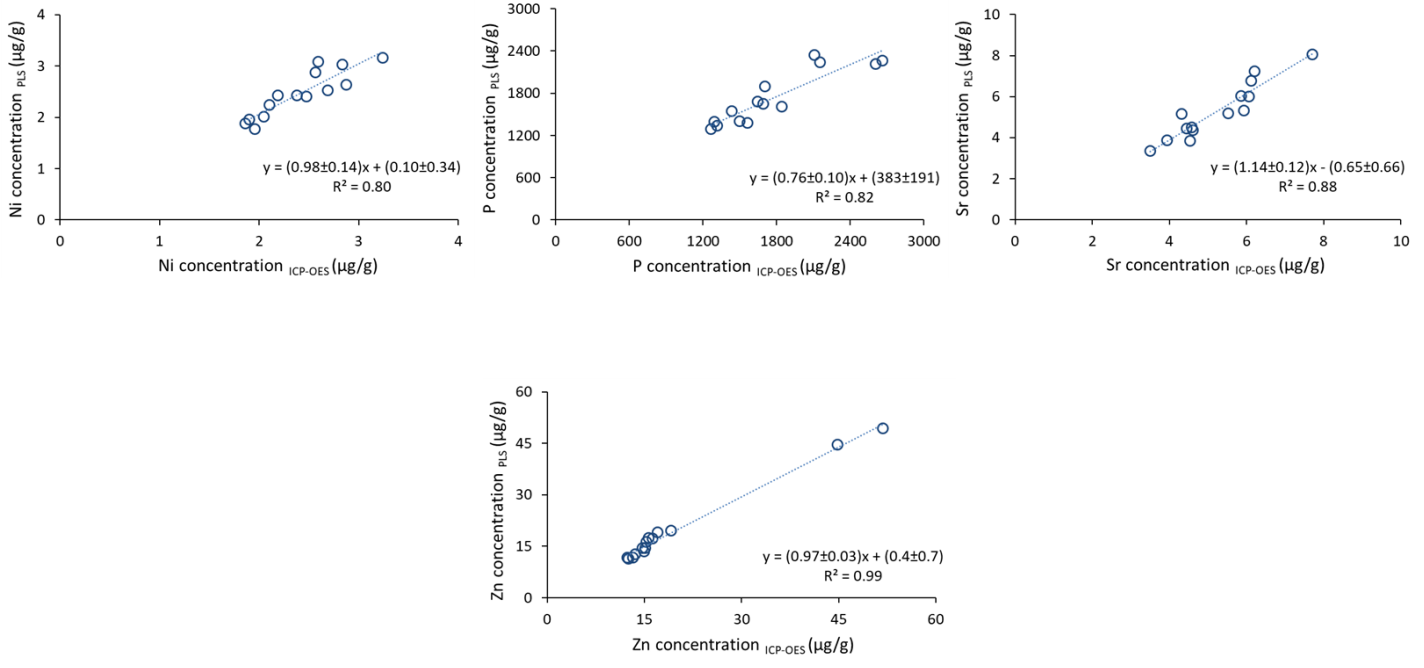

Fig. 2. Continuation.

3.4. Calculated intakes in the cocoas and DRI

In order to determinate the concentrations of essential elements that are introduced in the human body with the consumption of cocoa powder in each intake, itwas calculated from the daily reference intakes. **Fig. 3** shows the calculated daily intakes for each element (in %) taken into account the daily recommended portion of cocoa indicated at the package of each type of cocoa. For major elements (Ca, Mg, Na, K and P) the intakes calculated ranged were from 0.6 to 6 %, from 4 to 16 %, from 0.15 to 2 %, from 3 to 21 % and from 3 to 11 %, respectively. The daily intakes for each element depends of the type of cocoa powder, being the cocoa hot chocolates type those than had the highest concentration for most of the essential elements. However, the intakes calculated in all of the samples, considering the portion recommended for each brand shown in **Table 1**, were adequate for the daily reference intakes of these elements.

For the trace elements (Cu, Zn, Fe, Mn, Cr and Mo) the intakes calculated ranged in from 14 to 51 %, from 2 till 8 %, from 9 till 51 %, from 7 till 30 %, from 9 till 75 % and from 2 till 19 %, respectively. It happens the same that with the elements in high concentration; brands E, F and G had the highest concentration of these elements. In the case of Cu, the concentration was around the same in all the cocoa powder samples, but the intakes calculated were very different due to the recommended portion, being higher in cocoa type hot chocolate (brands E and F). In the case of Cr, as it can be seen in the **Fig. 3**, the intakes calculated (CDI) for the D, E and F samples were very high in comparison with the other elements. However, although the daily intake is high for only one intake, it should be note that chromium is very poorly absorbed, only around 0.5 % of the total of chromium ingested is absorbed by the human body. Therefore, could begin to produce toxic effects with intakes higher than 200 mg in a day. In the rest of the lots, and considering the daily reference intakes according the EU (Regulation Nº1169/2011 of the European Parliament and the Council) the calculated intakes were adequate.

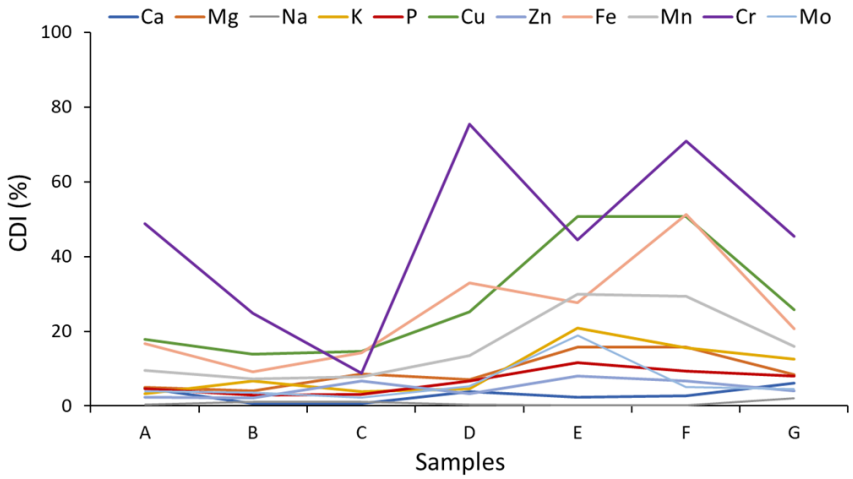

Fig. 3. Calculated daily intakes for essential elements in the samples analyzed.

3.5. Classification of the samples

To better understand the similarity and the variability between the lots of the brands analyzed, a dendrogram of the different samples was done. **Fig. 4** shows the dendrogram built for distinguish and classify the different types of cocoa according Ca, Fe, K, P, Mg, Na, Zn, Cu, Al, Mn, B, Ba, Ni, Sr, Ti, Cr, Cd, Co, Mo and Pb concentrations. It can clearly identify 3 groups; one with the brands A and B, other with the brand C alone and the last group with the brands D, E, F and G. The first group was very similar brands, both brands were cocoa type original, but it can be seen that sample B3 is more similar to brand A than their corresponding brand. The next group only has the brand C, which was a cocoa type instant solution; like brand D, but as it can be seen in this figure concentrations in brand D were more similar to the next group. The last group contains the rest of the brands and these were cocoa type instant solution (D) and cocoa type hot chocolates (brands E, F and G). In the top of the figure, brands G and F had the most obvious position in this group, but sample F3 was more similar that the brand D in concentration. Brand E was similar between their different lots and happens the same that in case of sample B3, sample E3 was more similar that brand B.

In view of the results, it can be concluded that it can be distinguish these samples in function to their concentration. Only in the case of brand D was confusing it classification.

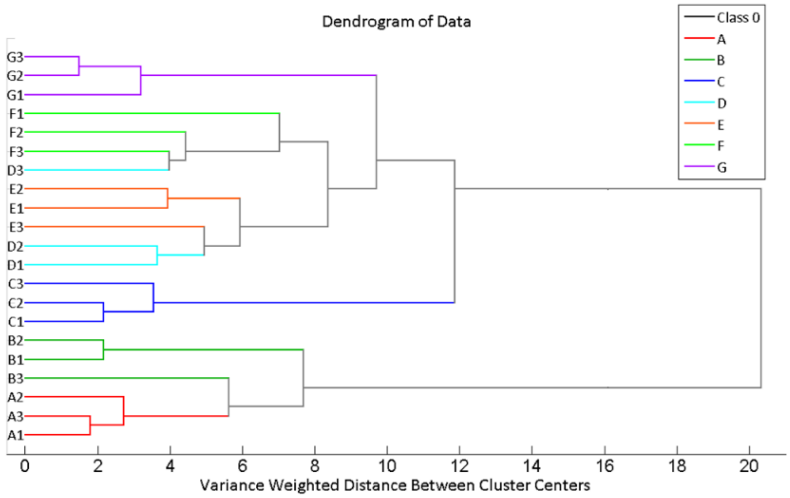

Fig. 4. Dendrogram of cocoa powder samples analyzed.

3.6. Elemental contents in cocoa samples

Table 4 shows the average concentration of elements in cocoa powder quantified in the present study and those obtained from the bibliography in which it was determine the mineral profile in cocoa samples and cocoa products. Bibliographic studies focus on the determination of the elemental profile in cocoa powder and it can be distinguishing 3 types of samples analysis: cocoa powder or drink powder, chocolate and 3 or 4 different cocoa products (with milk, dark or black, white and very dark). Five articles analyze 3 or 4 types of cocoa products, seven articles analyze cocoa powder and six articles analyze chocolate samples. The most of the bibliography use multielemental techniques, like IPC-OES and ICP-MS, for analyze the major number of analytes in these samples. In 5 articles analyze less than 3 elements, in 8 articles analyze between 6 and 10 analytes and finally only in 3 articles analyzed more than 14 elements, including the present study. The vast major of the articles analyze the composition of the elements in high concentration in the different samples, but only in some cases, as the studies

of Dahiya *et al.*, Güldas, Rehman *et al.*, Sepe *et al.*, Ieggli *et al.*, Yanus *et al.* and Mounicou *et al.*, analyze the trace heavy metals. In all data showed in table 4 there are no found high levels of heavy metals or other elements that, in high concentrations, can be toxic for human body. On another hand, the concentration obtained in the analyzed samples in our study are of the same order than in the before published works.

Table 4. Mineral profile of the samples analyzed in the bibliography. (Concentration average in mg/kg)

Villa, Catarine, Pereira & Cadore				Ieggli, Bohrer, do Nascimento & Carvalho				Alagić & Huremović						Shittu & Badmus	
	Chocolate bars (White)	Chocolate bars (Milk)	Chocolate bars (Dark)		Chocolate (White)	Chocolate (Milk)	Chocolate (Dark)		Chocolate (White)	Chocolate (Milk)	Chocolate (Black)	Cocoa powder	Chocolate for cooking		Powdered cocoa beverages
Ca	2739	1741	664	**Ca**	3845	1985	810							**Ca**	500.1
Na	1306	737	112	**Na**	1085	664	273								
K	3518	3600	6482	**K**	3216	3013	4276								
P	1996	1820	2570											**P**	1303.4
Mg	162	516	1810	**Mg**	385	696	1322								
Mn	0.2	3.3	12.2					**Mn**	0.50	2.99	13.1	31.4	8.17		
Cu	<0.17	2.7	11.5					**Cu**	0.77	2.96	10.6	33.8	5.81	**Cu**	11.0
Zn	8.3	9.6	43.8	**Zn**	12.3	8.92	15.7	**Zn**	3.78	8.14	20.5	64.7	9.84		
				Fe	1.88	20.6	62.7	**Fe**	8.75	19.5	41.5	96.1	32.9	**Fe**	224
								Cd	0.50	0.25	0.50	0.5	ND		
								Cr	2.77	3.30	0.30	3.39	4.90	**Cr**	1.79
								Pb	1.09	2.45	ND	3.95	1.23	**Pb**	2.27

Table 4. Continuation.

	Dahiya, *et al.*		**Ferreira, *et al.***		**Sepe, *et al.***		**Ieggli, *et al.***				**Mounicou, *et al.***		**Rehman & Husnain**
	Chocolates		Powdered chocolate		Chocolate		Chocolate (White)	Chocolate (Milk)	Chocolate (Dark)		Cocoa powder		Chocolate
				Al	9.2	**Al**	15.4	21.0	40.9				
Cd	0.105									**Cd**	0.528	**Cd**	0.0464
		Cu	3.3			**Cu**	1.72	4.48	10.8			**Cu**	2.5
												Fe	32
						Mn	0.15	1.90	7.31			**Mn**	3.6
Ni	1.626											**Ni**	2.0
Pb	0.927									**Pb**	0.221	**Pb**	0.306
		Zn	9.0									**Zn**	10.3

Table 4. Continuation.

Sager					Yanus *et al.*		Peixoto *et al.*		Anthemidis & Pliatsika		Güldas		Present study	
	Chocolate (Milk)	Chocolate (Dark)	Chocolate (Very Dark)	Cocoa		Chocolate		Chocolate drink powder		Cocoa powder		Chocolate with pistachio		Cocoa powder
Al	15.4	37.9	44.8	39.9			**Al**	27.6	**Al**	55			**Al**	10.5
As	<0.01	<0.01	<0.01	0.014	**As**	0.041					**As**	0.043		
B	2.22	6.62	9.93	26.8									**B**	4.59
Ba	1.59	4.29	5.01	12.7			**Ba**	3.1					**Ba**	3.50
Be	0.003	<0.003	0.003	0.012										
Bi	0.007	0.003	<0.001	<0.001	**Bi**	<0.006								
Ca	1945	601	652	1554			**Ca**	11100	**Ca**	1586			**Ca**	1050
Cd	0.017	0.037	0.194	0.122	**Cd**	0125	**Cd**	0.009			**Cd**	0.181	**Cd**	0.0677
Co	0.093	0.244	0.422	0.92	**Co**	0.757	**Co**	0.142	**Co**	2.91			**Co**	0.346
Cr	0.65	1.03	1.36	1.47	**Cr**	1.310	**Cr**	0.77	**Cr**	4.22			**Cr**	0.923
Cu	4.27	10.31	16.9	55.9			**Cu**	6.0	**Cu**	52	**Cu**	10	**Cu**	10.5
Fe	48.5	91.5	147	167			**Fe**	140	**Fe**	170	**Fe**	2.8	**Fe**	135
											Hg	0.061		
							K	5600					**K**	6620
I	0.740	0.193	0.102	0.107										
Mg	651	1263	1810	5443			**Mg**	884	**Mg**	5810			**Mg**	1330
Mn	4.60	11.6	16.6	49.0	**Mn**	36.081	**Mn**	7.9	**Mn**	42			**Mn**	11.7
Mo	0.166	0.152	0.201	0.420	**Mo**	0.297							**Mo**	0.122
Na	1135	54	36	131				656					**Na**	570
Ni	0.98	3.07	4.26	15.33					**Ni**	9.82	**Ni**	ND	**Ni**	2.42
P	2053	2055	2702	6632			**Na**	1420					**P**	1750
Pb	0.030	0.039	0.059	0.033	**Pb**	0.103					**Pb**	0.087	**Pb**	0.0429
S	773	801	896	2500										

Table 4. Continuation.

Si	25.6	59	65	60								
Sr	2.33	4.65	6.36	19.1							**Sr**	5.15
Ti	<0.002	0.002	0.003	0.003							**Ti**	2.10
V	0.07	0.10	0.13	0.19								
Zn	11.9	22.6	34.8	78.8	**Zn**	11.3	**Zn**	75	**Zn**	15	**Zn**	19.5

4. Conclusions

ICP-OES technique was successful for the determination of essential elements and non-essential elements in cocoa powder. The use of a previous microwave digestion step has been adequate and necessary for the measure of the samples by ICP-OES. Daily intakes calculated were adequate for the daily necessities of essential elements for the human body with the exception of Cr, but considering the bad absorption of this in the organism (~ 0.5 % only) there was no problem with this element in the cocoa consumption. No worrisome concentrations of the toxic elements for the organism have been found in any of the samples analyzed.

PLS-EDXRF model can be applied for the prediction of the mineral profile in cocoa samples. Results were agreeing as compared with the ICP-OES data reference methodology. Determination coefficients between the comparison of ED-XRF-PLS concentrations and ICP-OES concentrations were from 0.71 till 0.99 showing the agreement between them. This alternative to conventional methods offers a fast, cheap and green determination of major elements in food samples, without reactive consume nor waste generation.

5. Acknowledgements

Authors gratefully acknowledge the financial support of the Ministerio de Ciencia, Innovacion y Universidades-Agencia Estatal de Investigación-FEDER (EU) (Project CTQ2016-78053-R).

6. Conflict of interest

There are not conflict of interest involving any of the authors.

7. References

Afoakwa, E. O., Quao, J., Takrama, J., Budu, A. S., & Saalia, F. K. (2013). Chemical composition and physical quality characteristics of Ghanaian cocoa beans as affected by pulp pre-conditioning and fermentation. *Journal of Food Science and Technology*, 50, 1097-1105. 121, 199-204.

Alagić, N., & Huremović, J. (2015). Determination of metals contents in various chocolate samples. *Glasnik Hemičara i Technologa Bosne I Hercegovine*, 45, 39-42.

Anthemidis, A. N., & Pliatsika, V. G. (2005). On-line slurry formation and nebulization for inductively coupled plasma atomic spectrometry. Multi-element analysis of cocoa and coffee powder samples. *Journal of Analytical Atomic Spectrometry*, 20, 1280-1286.

Calatayud, M., López-de-Dicastillo, C., López-Carballo, G., Vélez, D., Hernández-Muñoz, P., & Gavara, R. (2013). Active films based on cocoa extract with antioxidant, antimicrobial and biological applications. *Food Chemistry*, 139, 51–58.

Commission Regulation (EU) Nº 488/2014 of 12 May 2014 amending Regulation (EC) Nº1881/2006 as regards maximum levels of cadmium in foodstuffs. https://eur-lex.europa.eu/legal-content/EN/TXT/PDF/?uri=CELEX:32014R0488&from=EN Accessed 22 May 2020.

Dahiya, S., Karpe, R., Hegde, A. G., & Sharma, R. M. (2005). Lead, cadmium and nickel in chocolates and candies from suburban areas of Mumbai, India. *Journal of Food Composition and Analysis*, 18, 517-522.

European Reference Materials, Application Note 1. https://ec.europa.eu/jrc/sites/jrcsh/files/erm_application_note_1_en.pdf Accessed 24 June 2020.

Faus, J., García-España, E., & Moratal, J. (2003). Introducción a la química bioinorganica. (1st ed.). Madrid: Síntesis.

Fernández-Murga, L., Tarín, J. J., García-Perez, M. A., & Cano, A. (2011). The impact of chocolate on cardiovascular health. *Maturitas*, 69, 312-321.

Ferreira, H.S., Santosa, A. C. N., Portugal, L. A., Costa, A. C. S., Miró, M., & Ferreira, S. L. C. (2008). Pre-concentration procedure for determination of copper and zinc in food samples by sequential multi-element flame atomic absorption spectrometry. *Talanta*, 77, 73-76.

Geleijnse, J. M., Launer, L. J., Hofman, A., Pols, H. A., & Witteman, J. C. (1999). Tea flavonoids may protect against atherosclerosis: the Rotterdam study. *Archives of Internal Medicine*, 159, 2170– 2174.

Güldas, M. (2008). Comparison of digestion methods and trace elements determination in chocolates with pistachio using atomic absorption spectrometry. *Journal of Food and Nutrition Research*, 47, 92-99.

Herreros-Chavez, L., Morales-Rubio, A., & Cervera, M. L. (2019). Green methodology for quality control of elemental content of infant milk powder. *LWT- Food Science and Technology*, 111, 484-489.

Hertog, M. G. L., Kromhout, D., Aravanis, C., Blackburn, H., Buzina, R., Fidanza, F., Giampaoli, S., Jansen, A., Menotti, A., & Nedeljkovic, S. (1995). Flavonoid intake and long-term risk of coronary heart disease and cancer in the Seven Countries study. *Archives of Internal Medicine*, 155, 381–386.

Ieggli, C. S. V., Bohrer, D., do Nascimento, P. C., de Carvalho, L. M., & Gobo, L. A. (2011). Determination of aluminum, copper and manganese content in chocolate samples by graphite furnace atomic absorption spectrometry using a microemulsion technique. *Journal of Food Composition and Analysis*, 24, 465-468.

Ieggli, C. V. S., Bohrer, D., do Nascimento, P. C., & de Carvalho, L. M. (2011). Determination of sodium, potassium, calcium, magnesium, zinc and iron in emulsified chocolate samples by flame atomic absorption spectrometry. *Food Chemistry*, 124, 1189-1893.

Jacquot, C., Petit, J., Michaux, F., Montes, E. C., Dupas, J., Girard, V., Gianfrancesco, A., Scher, J., & Gaiani, C. (2016). Cocoa powder surface composition during aging: A focus on fat. *Powder Technology*, 292, 195-202.

Jalbani, N., Kazi, T. G., Jamali, M. K., Arain, M. B., Afridi, H. I., Sheerazi, S. T., & Ansari, R. (2007). Application of fractional design and Doehlert matrix in the optimization of experimental variables associated with the ultrasonic-assisted digestion of chocolate samples for aluminum determination by atomic absorption spectrometry. *Journal of AOAC International*, 90(6), 1682–1688.

Mounicou, S., Szpunar, J., Andrey, D., Blake, C., & Lobinski, R. (2003). Concentrations and bioavailability of cadmium and lead in cocoa powder and related products. *Food Additives and Contaminants*, 20(4):4, 343-352.

Pedro, N. A. R., de Oliveira, E., & Cadore, S. (2006). Study of mineral content of chocolate flavoured beverages. *Food Chemistry*, 95, 94-100.

Peixoto, R. R. A., Devesa, V., Vélez, D., & Cervera, M. L. (2016). Study of the factors influencing the bioaccessibility of 10 elements from chocolate drink powder. *Journal of Food Composition and Analysis*, 48, 41-47.

Pouzar, M., Zvolská, M., Jarolím, O., & Vavrušová, L. A. (2017). The health risk of Cd released from low-cost jewelry. *International Journal of Environmental Research and Public Health*, 14(5), 520-527.

Regulation (EU) Nº 1169/2011 of the European Parliament and of the Council of 25 October 2011 on the provision of food information to consumers, amending Regulations (EC) Nº 1924/2006 and (EC) Nº 1925/2006 of the European Parliament and of the Council, and repealing Commission Directive 87/250/EEC, Council Directive 90/496/EEC, Commission Directive 1999/10/EC, Directive 2000/13/EC of the European Parliament and of the Council, Commission Directives 2002/67/EC and 2008/5/EC and Commission Regulation (EC) Nº 608/2004. https://eur-lex.europa.eu/legal-content/EN/TXT/PDF/?uri=CELEX:32011R1169&from=ES Accessed 22 May 2020.

Rehman, S., & Husnain, S. M. (2012). Assessment of trace metal contents in chocolate samples by Atomic Absorption Spectrometry. *Journal of Trace Elements Analysis*, 1, 1-11.

Sager, M. (2012). Chocolate and cocoa products as a source of essential elements in nutrition. *Journal of Nutrition and Food Sciences*, 2 (1), 1-10.

Sciuto, C., Allios, D., Bendoula, R., Cocoual, A., Gardel, M-E., Geladi, P., Gobrecht, A., Gorretta, N., Guermeur, N., Jay, S., Linderholm, J., & Thyrel, M. (2019). Characterization of building materials by means of spectral remote sensing: The example of Carcassonne's defensive wall (Aude, France*). Journal of Archaeological Science*: Reports, 23, 396-405.

Sepe, A., Constantini, S., Ciaralli, L., Ciprotti, M., & Giordano, R. (2001). Evaluation of aluminum concentrations in samples of chocolate and beverages by electrothermal atomic absorption spectrometry. *Food Additives and Contaminants*, 18, 788-796.

Shittu, T. A., & Badmus, B. A. (2009). Statistical correlations between mineral element composition, product information and retail price of powdered cocoa beverages in Nigeria. *Journal of Food Composition and Analysis*, 22, 212-217.

Villa, J. E. L., Pereira, C. D., & Cadore, S. (2015). A novel and simple acid extraction for multielemental determination in chocolate bars. *Microchemical Journal*, 121, 199-204.

Yanus, R. L., Sela, H., Borojovich, E. J. C., Zakon, Y., Saphier, M., Nikolski, A., Gutflais, E., Lorber, A., & Karpas, Z. (2014). Trace elements in cocoa solids and chocolate: An ICPMS study. *Talanta*, 119, 1-4.

BLOQUE II

ANÁLISIS MEDIANTE SMARTPHONE

CAPÍTULO 6

Determinación del contenido de clorofila en hojas mediante Smartphone

Determination of chlorophyll content in leaves by Smartphone

L. Herreros-Chavez[1], P. Martínez-López[1], M. J. Luque[2], A. Morales-Rubio[1], M. L. Cervera[1]

[1]Department of Analytical Chemistry, University of Valencia, 50 Dr. Moliner St., 46100 Burjassot, Valencia, Spain

[2]Department of Optics, University of Valencia, 50 Dr. Moliner St., 46100 Burjassot, Valencia, Spain

ABSTRACT

The aim of this work is the development of a direct and green methodology, avoiding the consumption of polluting reagents and reducing the generation of waste, for the determination of chlorophyll in leaves by employing a Smartphone. Mathematical models were created for the prediction of the concentration of chlorophyll in critic leaves from their color. Seventy-eight leaves were employed as calibration set and thirty-four samples were used as validation set. Each leaf was photographed and CIELAB color descriptors computed from their RGB values. Chlorophyll content was quantified by UV-Vis spectrophotometry and 2 direct techniques, Chlorophyll Content Meter (CCM) and Soil Plant Analysis Development (SPAD). Concentrations predicted by the models were correlated with the data obtained by CCM, SPAD and UV-Vis. Models generated provided for the calibration values of determination coefficients from 0.87 till 0.97 with a root mean square error from 258 till 263 μg g^{-1}, from 2.8 till 4.3 μg cm^{-2}, from 4.7 till 5.3 SPAD units and from 6.5 till 7.2 CCM units. There is a high correlation between concentrations predicted by the models employing RGB, Lab and LhC and the concentrations quantified by reference methods obtaining determination coefficients from 0.86 till 0.98.

Keywords: chlorophyll, UV-Vis, Smartphone, image treatment, SPAD, CCM.

1. Introduction

Chlorophyll (chl) is a natural pigment present in vegetation, responsible for the photosynthesis process, and its content is an indicator for a plant's health (Wang et al., 2013). Chl content gives information about nitrogen content because these analytes are correlated (Syvertsen, 1984; Evans, 1989), and reveals plant stress and nutrient deficiencies that result in changes in the green pigment composition (Carter, 1993; Bacci et al., 1998). Thus, quantification of chl provides important information about growth and survival of plants (Foyer et al., 1982; Peng and Gitelson, 2012) and, is also an indicator of mutations, stress, nutritional stage and the effects of the environments on the plant's growth (Evans, 1989).

There are five varieties of chl (a, b, c1, c2 and d) but the most abundant and important types are a and b; the other types are less frequent (Muñoz-Ortuño et al., 2017). Total chl content is commonly quantified by the sum of chl a and chl b content. Usually, quantification of chl a and b is performed by destructive methods such as fluorimetry (Peng et al., 2013), chromatographic (Hu et al., 2013; Peng et al., 2013) and UV-Vis spectrometry techniques (Peng et al., 2013; Jifon et al., 2005; Putra et al., 2017). These techniques, require extraction with toxic solvents such as methanol, ethanol or DMF (*N,N*-dimethyl formamide) (Putra et al., 2017; Hosikian., 2010; Jifon et al., 2005; Delegido et al., 2014) and separation step is required always. Moreover, chl is heterogeneously distributed in the plant, so for an accurate and precise analysis, a high number of measures is necessary (Delegido et al., 2014). Non-destructive methods have been developed in the last years to avoid the use of toxic reagents and sample manipulation.

Chl can be quantified by non-destructive techniques based on transmittance measures which have proved to be effective, cheap and rapid tools for chl quantification in a high number of plant types (Delegido et al., 2014; Jifon et al., 2005; Richardson et al., 2002). CCM-200 (Chlorophyll content meter) from Opti-Sciences (Tyngsboro, MA, USA) and SPAD-502 (Soil plant analysis development) from Minolta Camera Co. (Osaka, Japan) are two of these handheld chl-meters. These devices are cheaper and easier to use than chromatographic and spectrometric techniques but accessible to all users due to their cost.

Image analysis is a cheap, easy alternative to the methods listed above. Digital image processing is increasingly used to estimate different variables of interest for agronomic activities (Pandurng and Lomte, 2012). Color is directly correlated with the concentration of chl in leaves, with darker green correlated with higher chl content. Color spaces commonly used to describe color are RGB (Red, Green and Blue), CIE (Commission Internationale de l'Eclairage) L*a*b*, CIE-XYZ and CIE-xyY (Agarwal and Gupta, 2018). The most used color space in analytical chemistry is RGB (López-Molinero et al., 2010) and it is an independent device and has been employed for the determination of chlorophyll content (Agarwal and Gupta, 2018; Friedrichs et al., 2017) and nitrogen content (Saberioon et al., 2014; Wang et al., 2013).

The objective of this work is the determination of chl content by UV-Vis, SPAD-502 and CCM-200 employing two different solvents. Leaf samples were photographed by a Smartphone and custom developed Matlab software was used to obtain R, G, B, values of the images and to transform them to L*, a*, b*, hue (h) and Chroma (C*) values. Three different mathematical models (based on RGB, Lab and LhC, respectively) were used to predict the concentration of chl in leaves from a photography. The results of the model were compared with those obtained by SPAD-502 and CCM-200 and those derived from the models was fin.

2. Materials and methods

2.1. Samples

Samples analysed were lemon tree leaves (*Citrus limon*) and orange tree leaves (*Citrus sinensis*) collected in the zone of Llombai (Valencia) in spring 2019.

2.2. Reagents and materials

Acetone grade synthesis 99.5 % purity from Scharlau and ultrapure water from Adrona System (Riga, Latvia) were employed in the analysis.

2.3. Instrumentation

A Hewlett Packard – HP 8452A diode array spectrometer from Agilent Technologies Inc., (California, USA) with 1 cm quartz cuvettes was employed for the determination of chl content. For direct measurements, two

commercial chlorophyll content meters a CCM-200 from Opti-Sciences (Tyngsboro, MA, USA) and a SPAD-502 from Minolta Camera Co. (Osaka, Japan) were employed. Both devices measure by absorbance in two wavebands (at red, 650 nm, peak chlorophyll absorbance, and infrared, ~940 nm) and were calibrated before use following procedures recommended by their manufacturers. A Samsung Galaxy S7 Edge (Seul, South Korea) was used for the image acquisition of leaf samples. For image data treatment, Matlab from Mathworks (Natick, MA, USA) was employed.

2.4. Experimental procedure

2.4.1. Sample preparation

Leaf samples were cleaned with a brush and ultrapure water for dust particles elimination from surface. Later, the samples were rinsed again with ultrapure water and dried with paper. A laboratory punch was employed to cut circles in the leaves, 1.1 cm in diameter, avoid leaf nerves. Cut samples were weighted and stored in topaz vials of 10 mL until their analysis.

2.4.2. Smartphone calibration

A Samsung S7 Smartphone, with 12 megapixels camera with stabilization, was colorimetrically characterized, using as training samples a set of. 514 Munsell chips from sheets 1.25GY to 10YR, covering the range of chromaticities that appear in the leaves, plus the grey samples. Fluorescent lamps were used to photograph the samples. A 5-degree polynomial model was used to relate RGB camera response to the coloured samples and the grey sample of highest reflectance to the L*a*b values of the chips under standard illuminant D65. The coefficients of the polynomial were determined by least squares minimization, using a training set of 268 chips uniformly distributed in the Munsell color space and the grey samples. The performance of the model, assessed with the remaining chips, was reasonably good, with average prediction errors of 3±2 Lab units. This procedure is a modification of the method described by Hong and co-workers to derive XYZ tristimulus values from RGB responses and aims to reduce the dependence of the characterization polynomial with the spectrum of the illuminant (Hong et al., 2000). CIELAB values of the leaves were obtained with this model, using as inputs the average RGB values in a circular region of the leaf and the RGB values of a white sample.

2.4.3. Image acquisition

Fig. 1 shows the experimental set up for image acquisition and the computation of the color descriptors. Leaf circle was put in a blank support located inside an expanded polystyrene semi-sphere of 15 cm of diameter illuminated with a led strip of 5600 K. Semi-sphere was closed when photography was taken. Smartphone Samsung Galaxy S7 was placed in a methacrylate structure over the semi-sphere at a distance of 16 cm from the sample. For blank reference in CIELAB space a photography of the blank support (without sample) inside semi-sphere was taken.

2.4.4. Extraction procedure

Samples were crushed with cold acetone into a glass mortar cooled in an ice bath. Once the sample was completely crushed, it was transferred into a 10 mL volumetric flask diluted to volume with acetone. For UV-Vis measurements, a few mL of this extract was filtered and put inside a quartz cuvette of 1 cm optic pass. Employing the equations shown in **Table 1** (acetone 99.5 %), chl content was determined by UV-Vis.

Table 1. Equations for the chlorophyll determination by UV-Vis depending on the solvent employed and the percentage.

Solvent	Chlorophyll type	Chl Equation (μg mL^{-1})
Acetone 99.5 %	a	$11.24 \cdot A_{662} - 2.04 \cdot A_{645}$
	b	$20.13 \cdot A_{645} - 4.19 \cdot A_{662}$
	a + b	$7.05 \cdot A_{662} + 18.08 \cdot A_{645}$

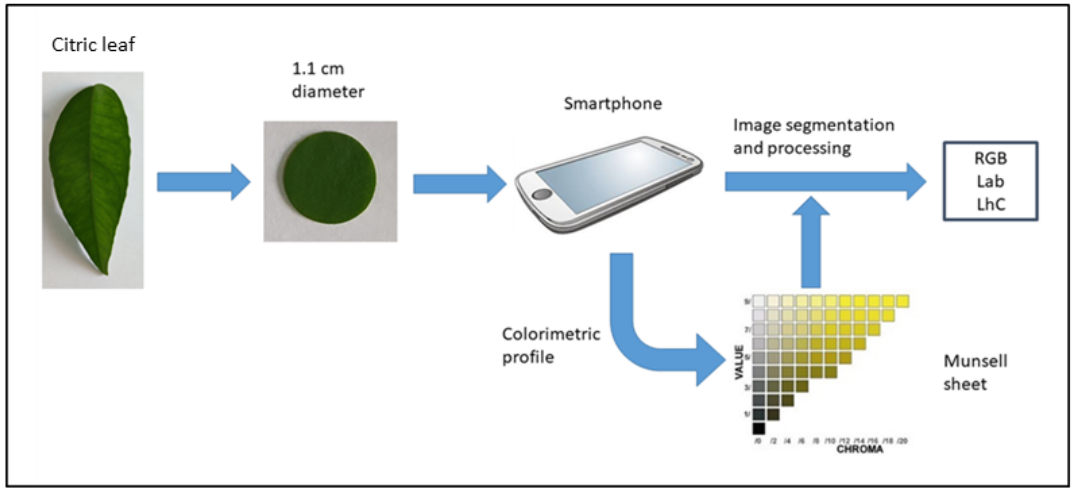

Fig. 1. Scheme of the acquisition image and obtaining of the color descriptors.

2.4.5. Data processing

Matlab 2017b from Mathworks was used for data treatment. Data were processed for building the best models for chl prediction in citric leaves. Data were set in X matrix R, G, B, L*, a*. b*, h and C* values alone and 2 or 3 combination of them of each sample and Y vector was loaded with the concentration of chl quantified by UV-Vis (μg g^{-1} and μg cm^{-2}), SPAD and CCM.

Models were evaluated by the terms of root mean square error (RMSE) of the calibration and the determination coefficient of the calibration (r^2). To validate the models, confidence interval, equation line and determination coefficient were employed.

3. Results and discussion

3.1. Correlation between CCM-200 and SPAD-502

Many authors employ these two hand-held chlorophyll meters commercially available, but there is not any study of the correlation between the measurements from both devices. Most of the papers in the literature use only one of these devices, SPAD being the more often used. In this study, one hundred and fifty-three samples were measured by CCM and SPAD and these values were compared. A high variety of sample colors, from yellow to deep green leaves, were analyzed, yielding values from 1.6 till 94.4 and from 1.4 till 82.0 CCM and SPAD, respectively. In both cases, the highest values correspond to green leaves which had more chl content and the lowest values correspond to yellow leaves which had less chl content. **Fig. 2** shows the comparison between CCM and SPAD values of 153 samples analysed. As it can be seen, there is an exponential correlation between both tools, that can be fitted by the equation $y = 1.626e^{0.055x}$ with a determination coefficient of 0.96. In view of these results, it can be concluded that these two tools had a high exponential correlation and with this equation the values of CCM can be converted in SPAD values.

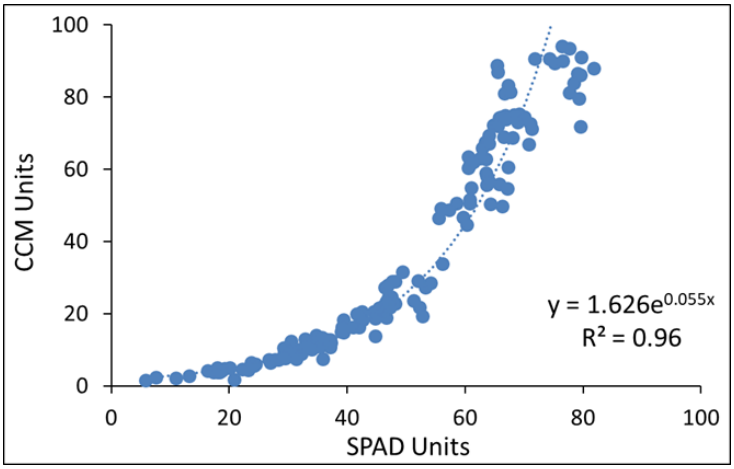

Fig. 2. Correlation between CCM units and SPAD units with the corresponding equation line.

3.2. Degradation of the chlorophyll with the time

Chlorophyll is an analyte which suffers a fast degradation with time once extracted. It was checked whether it was possible to analyse the leaf clippings several days after they had been cut or whether samples had to be cut and measured the same day. 9 samples were measured 2 days in a row by CCM and the values obtained in the second day were plotted as a functions of those obtained in the first day. Data was fitted by a linear regression, with the equation line y = (1.00 ± 0.06) x + (1.0 ± 1.9) with a determination coefficient of 0.98. Confidence interval of the regression parameters were [0.86;1.14] for the slope and [-4.37;4.57] for the intercept. Since these intervals include 1 and 0, respectively, no significant difference was between measurements made the same day of the cut or a day after, but another day variations were found.

3.3. Prediction models derived from Smartphone images

One hundred and twelve lemon and orange tree leaves were to obtain models to predict chl content from Smartphone images. Seventy-eight samples of the total set were employed for the calibration set and thirty-four samples for the validation set. Chl extraction was made following the procedure explained above. All the cut samples were photographed by the Smartphone and measured by CCM and SPAD before chl extraction.

R, G, B, L*, a*, b*, h and C values were obtained from images employing Matlab software. **Table 2** shows the root mean square error (RMSE) and the determination coefficient (r^2) of the RGB-based model calibration. As it can be seen, best model (lowest RMSE and the highest r^2) for chl content (µg g^{-1} and µg cm^{-2}) was based on the 3 digital values. Best models for SPAD and CCM were obtaining using R and B. The relative root mean square error (RRMSE) was 21 %, 10 %, 11 % and 20 %, respectively for the 3 methods, being the best models for chl in µg cm^{-2} and for SPAD which provided less RMSE.

Table 3 shows the RMSE and the r^2 of the Lab model calibration. As it can be seen, best model for chl content (µg g^{-1}) was employing 2 variables (a* and b*), for chl content (µg cm^{-2}) and SPAD was employing 3 variables (L*, a* and b*) and for CCM model was employing 2 variables (L* and b*) the lowest RMSE and the highest r^2 was obtained. In these models, RRMSE was 21 %, 15 %, 12 % and 23 %, respectively for each method.

Table 4 shows the RMSE and the r^2 of the LhC model calibration. As it can be seen, best model for chl content (µg g^{-1}) was employing 2 variables (L* and h), for chl content (µg cm^{-2}), SPAD and CCM best models were employing 3 variables (L*, h and C*) obtaining the lowest RMSE and the highest r^2. In these models, RRMSE was 21 %, 14 %, 12 % and 22 %, respectively for each method.

In view of these calibration models, RGB model provided the smallest error to predict chl content from a leaf image from the three color-space used and thus, it was selected as the best model to predicr the sample chl concentration from color parameters.

Table 2. Root mean square error (RMSE) and determination coefficient (r^2) of the calibration RGB model for the four units.

Variables	[Chlorophyll] (µg g^{-1})		[Chlorophyll] (µg cm^{-2})		SPAD		CCM	
	RMSE	**r^2**	**RMSE**	**r^2**	**RMSE**	**r^2**	**RMSE**	**r^2**
RGB	**258**	**0.87**	**2.84**	**0.97**	5.08	0.89	7.79	0.90
RG	273	0.86	5.42	0.89	6.53	0.83	9.84	0.84
GB	317	0.80	4.48	0.93	5.58	0.88	7.43	0.91
RB	282	0.84	3.23	0.96	**4.69**	**0.92**	**6.51**	**0.93**
R	259	0.87	5.82	0.87	6.57	0.83	10.4	0.82
G	328	0.79	6.42	0.84	7.15	0.80	10.4	0.82
B	429	0.63	9.15	0.69	10.1	0.59	11.4	0.79

Table 3. Root mean square error (RMSE) and determination coefficient (r^2) of the calibration Lab model for the four units.

Variables	[Chlorophyll] (µg g^{-1})		[Chlorophyll] (µg cm^{-2})		SPAD		CCM	
	RMSE	**r^2**	**RMSE**	**r^2**	**RMSE**	**r^2**	**RMSE**	**r^2**
Lab	265	0.86	**4.28**	**0.93**	**5.27**	**0.89**	7.50	0.91
La	322	0.79	6.67	0.84	6.77	0.81	8.45	0.88
ab	**258**	**0.87**	4.57	0.92	5.62	0.87	8.25	0.89
Lb	281	0.84	4.32	0.93	5.47	0.88	**7.22**	**0.91**
L	333	0.78	6.96	0.82	6.72	0.81	9.11	0.86
a	697	0.03	15.9	0.04	12.8	0.34	22.0	0.19
b	304	0.82	4.84	0.91	5.77	0.87	8.18	0.89

Table 4. Root mean square error (RMSE) and determination coefficient (r^2) of the calibration LhC model for the four units.

Variables	[Chlorophyll] (µg g^{-1})		[Chlorophyll] (µg cm^{-2})		SPAD		CCM	
	RMSE	**r^2**	**RMSE**	**r^2**	**RMSE**	**r^2**	**RMSE**	**r^2**
LhC	284	0.84	**3.93**	**0.94**	**5.34**	**0.88**	**6.93**	**0.92**
Lh	**263**	**0.86**	5.10	0.90	6.33	0.84	8.42	0.88
hC	267	0.86	4.56	0.92	5.43	0.88	8.12	0.89
LC	307	0.82	4.66	0.92	5.39	0.88	7.11	0.92
L	333	0.78	6.75	0.83	6.80	0.81	8.78	0.87
h	444	0.60	10.1	0.64	9.44	0.64	15.8	0.58
C	322	0.80	5.11	0.90	5.95	0.85	7.99	0.89

Fig. 3 shows the concentration predicted by RGB model versus the concentration obtained by the three reference methods UV-Vis, SPAD and CCM. Passing-Bablok plots show agreement between model and experimental data, because the theoretical ideal line is inside the confidence interval of the fit line, except for the low concentration range for the chlorophyll concentration in µg g^{-1}, where the model slightly over-estimates chl content. No outliers are present, with the exception of one sample in CCM model.

Equation lines for the models were y = (0.91 ± 0.03) x + (140 ± 40) with r^2 value of 0.95, y = (0.93 ± 0.04) x + (1.9 ± 1.2) with r^2 value of 0.94, y = (0.98 ± 0.04) x + (1.7 ± 1.8) with r^2 value of 0.94 and y = (1.00 ± 0.03) x + (1.23 ± 1.16) with r^2 value of 0.97, respectively for [chlorophyll] in µg g^{-1}, [chlorophyll] in µg cm^{-2}, SPAD and CCM. In view of these results it can be concluded that chlorophyll in µg cm^{-2}, SPAD and CCM models provided accurate and precise predicted results for the quantification of chlorophyll in citric leaves from Smartphone photograhpys.

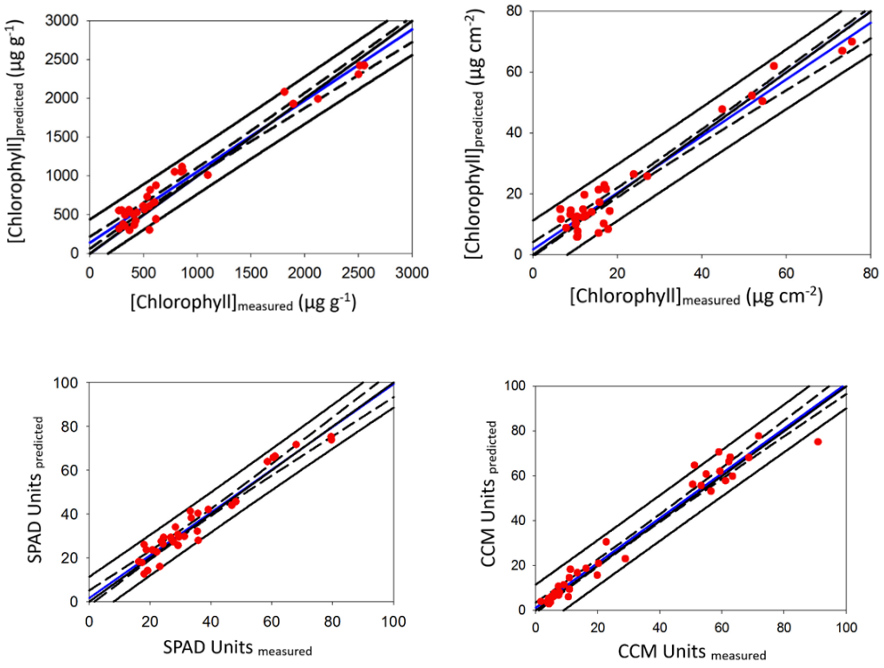

Fig. 3. Passing-bablok of the concentration predicted by RGB model in front of the concentration measured by the reference methods (UV-Vis, SPAD and CCM). Note: experimental regression line (in blue), the theoretical ideal line (in black) (y = x), in dotted line the 95 % confidence interval and in continuous black line the prediction interval.

4. Conclusions

In this manuscript, a new technique for direct chlorophyll determination in citric leaves has been developed. This technique provides a fast, non-invasive, cheap and accessible to everyone tool for chlorophyll quantification in leaves by employing a Smartphone. The procedure proposed improves on the traditional extraction technique as it reduces the volume of reagent and generated waste, in accordance with the Green Analytical Chemistry.

Employing a traditional method as UV-Vis and hand-held chlorophyll meters as SPAD-502 and CCM-200 in combination with Smartphone images, models for predicting chl concentration were developed. These models provide

accurate and precise predicted results with relative errors of 17 %, 9 %, 3 % and 12 %, respectively for chlorophyll content in µg g^{-1}, chlorophyll content in µg cm^{-2}, SPAD and CCM. Determination coefficients of the correlation between predicted concentrations versus the concentrations quantified by reference methods were 0.95, 0.94, 0.94 and 0.97, respectively for chl content in µg g^{-1}, chl content in µg cm^{-2}, SPAD and CCM. Additionally, new models must be implemented to account for differences between plant species.

Conflict of interest

The authors declare there is no conflict of interest regarding the contents of this paper.

Acknowledgements

The authors gratefully acknowledge the financial support of the Ministerio de Ciencia, Innovación y Universidades-Agencia Estatal de Investigación FEDER (EU) (Project CTQ2016-78053-R) and Generalitat Valenciana Project Prometeo-2019-056.

5. References

Agarwal, A., Gupta, S.D., 2018. Assessment of spinach seedling health status and chlorophyll content by multivariate data analysis and multiple linear regression of leaf image features. Comput. Electron. Agr. 152, 281-289.

Bacci, L., De Vincenzi, M., Rapi, B., Arca, B., Benincasa, F., 1998. Two methods for the analysis of colorimetric components applied to plant stress monitoring. Comput. Electron. Agric. 19, 167-186.

Carter, G.A., 1993. Responses of leaf spectral reflectance to plant stress. Am. J. Bot. 80, 239-243.

Delegido, J., Van Wittenberghe, S., Verrelst, J., Ortiz, V., Veroustraete, F., Valcke, R., Samson, R., Rivera, J.P., Tenjo, C., Moreno, J., 2014. Chlorophyll content mapping of urban vegetation in the city of Valencia based on the hypersepectral NAOC index. Ecol. Indic. 40, 34-42.

Evans, J.R., 1989. Photosynthesis and nitrogen relationships in leaves of C3 plants. Oecologia 78, 9-19.

Foyer, C., Leegood, R., Walker, D., 1982. What limits photosynthesis? Nature 298, 326.

Friedrichs, A., Busch, J.A., van der Woerd, H., Zielinski, O., 2017. SmartFluo: a method and affordable adapter to measure chlorophyll *a* fluorescence with Smartphones. Sensors 17, 678-692.

Hong, G., Luo, M.R., Rhodes, P.A., 2000. A study of digital camera colorimetric characterization based on polynomial modeling. COLOR Res. Appl. 26, 76-84.

Hosikian, A., Lim, S., Halim, R., Danquah, M.K., 2010. Chlorophyll Extraction from Microalgae: A Review on the Process Engineering Aspects. Int. J. Chem. Eng. 1-10.

Hu, X., Tanaka, A., Tanaka, R., 2013. Simple extraction methods that prevent the artifactual conversion of chlorophyll to chlorophyllide during pigment isolation from leaf samples. Plant Methods 9, 19-32.

Jifon, J.L., Syvertsen, J.P., Whaley, E., 2005. Growth environment and leaf anatomy affect nondestructive estimates of chlorophyll and nitrogen in *Citrus* sp. Leaves. J. Amer. Soc. Hort. Sci. 130, 152-158.

Lopez-Molinero, A., Liñan, D., Sipiera, D., Falcon, R. 2010. Chemometric interpretation of digital image colorimetry. Application for titanium determination in plastics. Microchem. J. 96, 380-385.

Muñoz-Ortuño, M., Serra-Mora, P., Herráez-Hernández, R., Verdú-Andrés, J., Campíns-Falcó, P., 2017. A new tool for direct non-invasive evaluation of chlorophyll *a* content from diffuse reflectance measurements. Sci. Total Env. 609, 370-376.

Pandurng, J.A., Lomte, S.S., 2012. Digital image processing applications in agriculture: a survey. IJARCSSE 5, 622-624.

Peng, F., Liu, S., Xu, H., Li, Z., 2013. A comparative study on the analysis methods for chlorophyll-a. Adv. Mater. Res. 726-731, 1411-1415.

Peng, Y., Gitelson, A.A., 2012. Remote estimation of gross primary productivity in soybean and maize based on total crop chlorophyll content. Remote Sens. Environ. 117, 440-448.

Putra, M.D., Darmawan, A., Wahdini, I., Abasaeed, A.E., 2017. Extraction of chlorophyll from pandan leaves using ethanol and mass transfer study. J. Serb. Chem. Soc. 82, 921-931.

Richardson, A.D., Duigan, S.P., Berlyn, G.P., 2002. An evaluation of non-invasive methods to estimate foliar chlorophyll content. New Phytol. 153, 185-194.

Saberioon, M.M., Amin, M.S.M., Anuar, A.R., Gholizadeh, A., Wayayok, A., Khairunniza-Bejo, S., 2014. Assessment of rice leaf chlorophyll content using visible bands at different growth stages at both the leaf and canopy scale. Int. J. Appl. Earth Obs. Geoinform. 32, 35-45.

Syvertsen, J.P., Smith, M.L., 1984. Light acclimation in citrus leaves. I. Changes in physical characteristics, chlorophyll, and nitrogen content. J. Amer. Soc. Hort. Sci. 109, 807-812.

Wang, Y., Wang, D., Zhang, G., Wang, J., 2013. Estimating nitrogen status of rice using the image segmentation of GR thresholding method. Field Crops Res. 149, 33-39.

CAPÍTULO 7

Predicción de compuestos polares totales en aceite de girasol usado mediante Smartphone

Prediction of total polar compounds in used sunflower oil by Smartphone

L. Herreros-Chavez[1], C. Galve[1], M. J. Luque[2], A. Morales-Rubio[1], M. L. Cervera[1]

[1]Department of Analytical Chemistry, University of Valencia, 50 Dr. Moliner St., 46100 Burjassot, Valencia, Spain

[2]Department of Optics, University of Valencia, 50 Dr. Moliner St., 46100 Burjassot, Valencia, Spain

ABSTRACT

This study presents a mathematical model to predict total polar compounds (TPC) in sunflower oil from the color of the sample, measured with a calibrated smartphone. The image treatment is a fast, cheap and green analytical procedure to determine whether fried oil is still fit for human consumption without harmful effects for health, taking into account the maximum TPC rate allowed by law in Spain. The colorimetric profile of the camera was obtained by measurements of RGB responses to a set of chips from the Munsell Atlas, covering the color region of the oil samples, and used to estimate the oil samples CIELAB color descriptors. Generalized linear models were derived to predict TPC values from lightness (L*), the red-green and blue-yellow responses (a* and b*) and chroma (C*). The models predict the concentration in samples with errors of the order of 10 % of TPC as estimated by a Testo-270 instrument, which permits the direct quantification of TPC without sample treatment.

Keywords: food analysis, smartphone image, color space, sunflower oil, total polar compounds (TPC), green analysis.

1. Introduction

Oil is an essential food in the daily diet for the majority of humans. Sunflower oil is one of the seed oils most frequently used for cooking in all the world

[1], due to its high content in polyunsaturated fatty acids (PUFA 85-95 %) [2], beneficial for human health [3]. Their high content in polyunsaturated fatty acids (PUFA) lend these oils susceptible to oxidative deterioration during cooking and can produce trans fatty acids which produce harmful effects in health [2]. Lipid oxidation when these oils are cooked is the principal cause of loss of quality, stability and safety [4] and depends on the temperature, time and quantity of oil used. The quality of the oil used for frying strongly determines the quality of the fried food.

Total polar compounds (TPC) are a group of substances including triglyceride oligomer, triglyceride dimer, oxidized triglyceride monomer, diglyceride and free fatty acid [5] produced from oil degradation through heat and are used as an indicator of the decomposition degree of oils. Maximum TPC rates and accepted analysis procedures are regulated in each European country and its maximum legally allowed value in Spain is 25 % [6]. TPC affects the consistency, taste, flavor and quality of oil. Food fried in degraded oil immediately develops a dark crust and absorbs more oil than food fried in non-degraded oil. The optimum TPC values for fried food are between 14 % and 20 % [7].

Commonly used methods for TPC quantification are column chromatography, which uses the polarity difference of the compounds for TPC quantification, and gas chromatography for volatile compounds [8-10]. These methodologies are time consuming and very expensive due to the high quality and often toxic reagents required. A greener alternative to these methodologies is the use of capacity measurement, based on dielectric constant reading [11-12]. This technique is an alternative to the conventional methods providing non-destructive, cheap and fast analyses. But even these advantages, in some cases cooking oil tester is not available for everyone.

Another accessible alternative to conventional methods is image processing of sample images captured by optic sensors [13]. During the last decades, different image-capture and processing techniques have been developed to perform in situ, or non-destructive analysis of samples, relating some analytical property to the sample color. Color offers qualitative and quantitative information about samples.

The RGB (Red, Green and Blue) color space representing the responses of the three sensors of image capture device is one of the more widely used color representations for these applications [14], but it is device dependent, and therefore other color spaces, such as CIELAB or CIECAM2000, would in principle be preferable [15-17].

The simplest procedure is the direct acquisition of the image for in situ analysis, without any recognition or chemical reactions. Although photographic cameras, scanners or smartphones have been used for this purpose, the use of smartphones as an analytic tool is on the increase [18-21].

The aim of this work is to study the relationship between the total polar compounds concentration in sunflower oil for human consumption with the number of heating or frying cycles, and the generation of models to predict the concentration of TPC as a function of oil color and to determine whether a particular oil sample is suitable for human consumption, taking account the maximum TPC value legislated in Spain.

2. Materials and methods

2.1. Samples

The sample analyzed was sunflower oil that was heated or used to fry with ultrafrozen potatoes; both, oil and potatoes, were purchased in a local supermarket (Burjassot, Spain).

2.2. Instrumentation

TPC was measured with a Testo-270 cooking oil tester from Instrumentos Testo S.A (Cambrils, Spain), which was previously calibrated with its own reference oil Nº 0554.2650. Two fryers of 1.5 L Orbegozo from Sonifer S.A (Murcia, Spain) were employed, one exclusively for heating and the other exclusively for frying experiments. For the photography of the oil samples, a small quantity of oil was taken with a dispenser from Thermo Fisher Scientific (Vantaa, Finland) and introduced in a white 4 cm of diameter circular container of high-density polyethylene (HDPE). Photographs were taken with a Samsung Galaxy S7 Edge (Seul, South Korea) and two iPhone 7 Plus (China).

A Hewlett Packard – HP 8452A diode array spectrometer from Agilent Technologies Inc., (California, USA) with 0.5 cm quartz cuvettes was employed for the transmittance measures. For image data treatment Matlab from Mathworks (Natick, MA, USA) with the COLORLAB library [22] was employed. Additionally, sheets 1,25GY to 10YR from the Munsell Book of Color (Glossy Finish Collection, 1976, Kollmorgen Corporation, Baltimere, Maryland), covering the region of color space of the oil samples, were used to derive de colorimetric profile of two of the smartphones used.

2.3. Experimental procedure

2.3.1. Sunflower oil TPC measurements

The two fryers were filled with 1.5 L of sunflower oil, controlling the higher heating temperature to 175ºC. One of the fryers was exclusively used for heating the oil and the other exclusively for frying. 140 g of potatoes were weighted in a balance and put inside the fryer basket. When the temperature was correct, the potatoes were submerged in the oil and both fryers were covered with the top lid. After 5 minutes of heating or frying, the fryers were disconnected and both baskets were extracted. For TPC measurement, the samples were left 15-20 min to cool down to about 140 ºC, to avoid damaging the Testo-270 sensor. Each measurement was repeated three times, and the sensor was cleaned with paper after each. Once the oil was measured, the same quantity of potatoes was weighted and the heating or frying cycle was repeated, three or four times every day.

2.3.2. Image acquisition and spectrophotometric measurements

For each smartphone, the empty high density polyethylene (HDPE) container was photographed in the first place, to provide the CIELAB reference white. After this, 5 mL of oil was taken from one of the fryers and introduced in the container, and three photographs were taken with each of the smartphones. The process was repeated with another sample from the second fryer. **Fig. 1** shows the experimental procedure scheme of image acquisition, showing the different color processing stages, from the capturing device's RGB values to the final CIELAB color descriptors.

Transmittance of the oil samples in the 180-780 nm range were carried out with 0.5 cm optic pass cuvettes filled with the corresponding oil, after air blank.

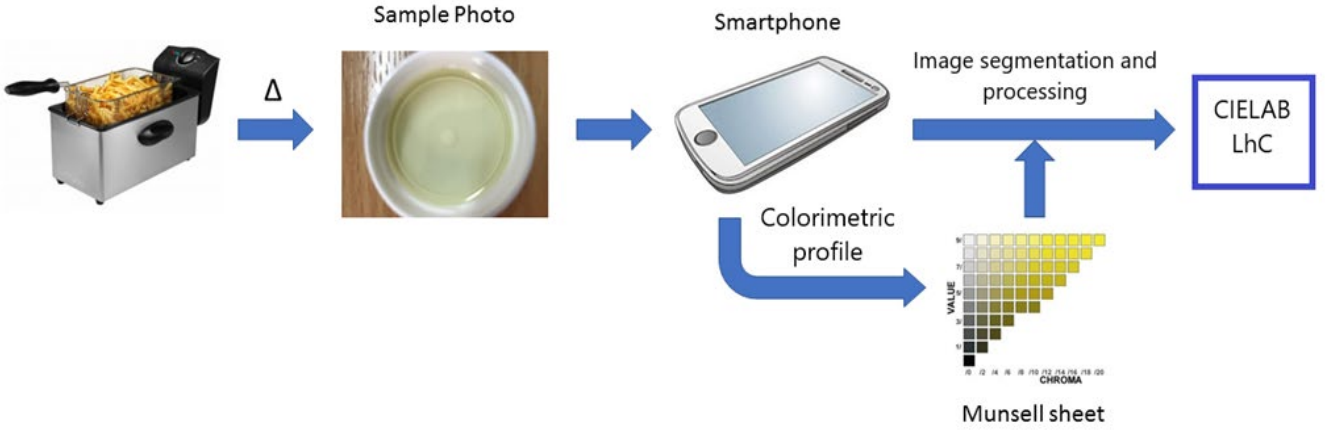

Fig. 1. Stages from image acquisition to estimation of CIELAB color descriptors.

2.3.3. Smartphone calibration

Two of the smartphones were colorimetrically, the Samsung S7 and one of the iPhone 7 plus (1), both with a 12 megapixels camera with stabilization. Photographs of 514 Munsell chips from sheets 1.25GY to 10YR, plus the gray samples, covering the range of chromaticities of raw and fried sunflower oil and the HDPE containers, were taken under the same illuminant used to photograph the oil samples. A 5-degree polynomial model was used to relate RGB camera responses to the L* a* b* values of the chips under standard illuminant D65, by least squares minimization, using a training set of 268 chips uniformly distributed in the Munsell color space. The performance of the model, assessed with the remaining chips, was reasonably good, with average prediction errors of 3±2 Lab units. This procedure is a modification of the method described by Hong and co-workers to derive XYZ tristimulus values from RGB responses [23].

3. Results and discussion

3.1. TPC determination in sunflower oil

Fig. 2 shows the change in TPC content in heated and fried sunflower oil with potatoes, as a function of the number of heating or frying cycles. As it can be seen, the TPC concentration values increases with the number of cycles, reaching higher values in fried oil, although the slopes of bot curves are similar, except during the first four cycles, where the increment rate for fried oil is the largest: four fried treatments is enough to increase the TPC from 9.5 % to 15 %. This value is reached in the heated oil when heated 24 times.

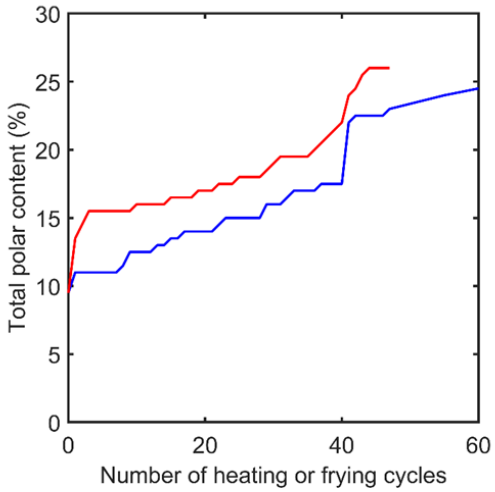

Fig. 2. Total polar compounds (%) quantified in the heated (blue) and fried (red) sunflower oil.

The blank oil, after 40 heating cycles, reached a TPC value of 18 %, well below the allowed limit of 25 contemplated in the Spanish legislation to be considered suitable for human consumption. The abrupt increase between cycles 40 and 41 appeared on the first heating cycle after a pause in the measurements comprising 14 days, during which the fryers were kept at environmental temperature and with their tops on. This can be produced by the effect of the waiting time and heating treatments. Subsequent heating cycles showed that the rate of change was again back to values before the pause. The experiment finished after the 60th cycle, when the sample had reached a value of 24 % TPC. As conclusion, sunflower oil is a resistant oil to the heat and could be employed many times without risk for human health.

In the case of fried sunflower oil, TPC values remained below 18% from the 2nd to the 25th frying cycle. From the 35th to the 40th frying cycles, values of TPC increase at a rate of 0.5 % per cycle and reaches values close to the allowed maximum suitable for human consumption. After the 14 days pause, the values of TPC was not as significantly increased as in the case of blank oil. After 40 frying cycles, the oil was still suitable for human consumption.

3.2. Transmittance measurements

It was done transmittance spectra for heated and fried sunflower oil. In the case of heated oil, transmittance was fall with increase the number of fried treatments, but there were some anomalies in these behaviors. This behavior was not so significance starting the 10 fried, because not decrease no much compared with the first fried done. The same happened to the fried sample due to both samples turn on dark and had more absorbance and less transmittance that the first measures.

3.3. Modelization of TPC values

Polynomial linear regression was used to model jointly TPC values from heated and fried sample as a function of the color descriptors of the sample. The best model was a five degrees polynomial in L*, a*, b* and C*. To compute the model's coefficient, our data was divided in two random halves, one of which was chosen as the training and the other as the checking set. Mean square error (MSE) obtained for the best models built for iPhone 7 (1), iPhone 7 (2) and Samsung S7 were 3.48 %, 4.80 % and 2.53 %. Root mean square error (RMSE) obtained for the best models created were 1.87 %, 2.15 % and 1.59 % of TPC for iPhone 1, iPhone 2 and Samsung S7, respectively. CIELAB descriptors for iPhone 1 and Samsung S7 were computed with their respective colorimetric characterization models, whereas for iPhone 2 we assumed the same characterization model than for iPhone 1, to check whether the error induced when using a generic colorimetric profile for our device was acceptable.

Fig. 3 shows the calibration obtained for built the models of TPC in heated and fried sunflower oil. A good correlation between TPC predicted and experimental TPC values employing the best models calculated for each smartphone were obtained in the three smartphone employed. **Fig. 3A** shows the correlation for iPhone 1 obtaining a mean square error of 3.48 %, a relative root mean square of 1.87 %, **Fig. 3B** shows the correlation for iPhone 2 obtaining a mean square error of 4.80 %, a root mean square error of 2.19 % and **Fig. 3C** shows the correlation for Samsung S7 with a mean square error of 2.53 % and a root mean square error of 1.59 %. as it can be seen it the three figures, the models obtained provides accurate results but the model than the y=x line was more similar to the calibration line was for Samsung S7 and the worst model was employing iPhone 2 as it can be seen in the figures.

In the case of iPhone 1 two values were outside of 95 % confidence interval (CI), in iPhone 2 three values were outside of the CI and in Samsung S7 three values were outside of the CI too. Nevertheless, a few values were outside of the confidence interval in the three calibration models of the total of the values obtained.

3.4. Agreement analysis

Agreement between model predictions and experimental TPC values has been analyzed by means of a modified Bland-Altman plot [24]. The difference between the model predictions and the experimental value has been plotted versus the experimental value for both heated (blue circles) and fried (red circles) samples. Although this procedure always shows a negative correlation between difference and magnitude [25], with this procedure it was easier to evaluate the risk of labelling an oil sample as unfit to use too soon or too late. Given that the data did not follow the normal distribution ($p<0.05$ in the Lilliefors composite goodness-of-fit test), we plotted the median and its 95 % CI, instead of the mean.

Except for iPhone 1, 0 belongs to the CI of the median and therefore model and experimental measurements agree. The three plots show that the model tends to overestimate low TPC values and underestimate high TPC values. Although this error will not cause the potential user to reject oil still fit to be used, it might lead the user to keep using oil with TPC values above the legal limit of 25 %, although in general still within the acceptability limits employed by health inspectors.

Fig 4A shows the BlandAltmanmod for calibrated iPhone 1. In this smartphone employing the best model build, samples fried were the samples with less predicted error (from 5 to -5 %) and it was produced this error in a low concentration of TPC. In this model, the 0 was outside from 95 % of confidence interval of the average, so it can be concluded that the difference between the compared values was significantly different from 0 at 95 %.

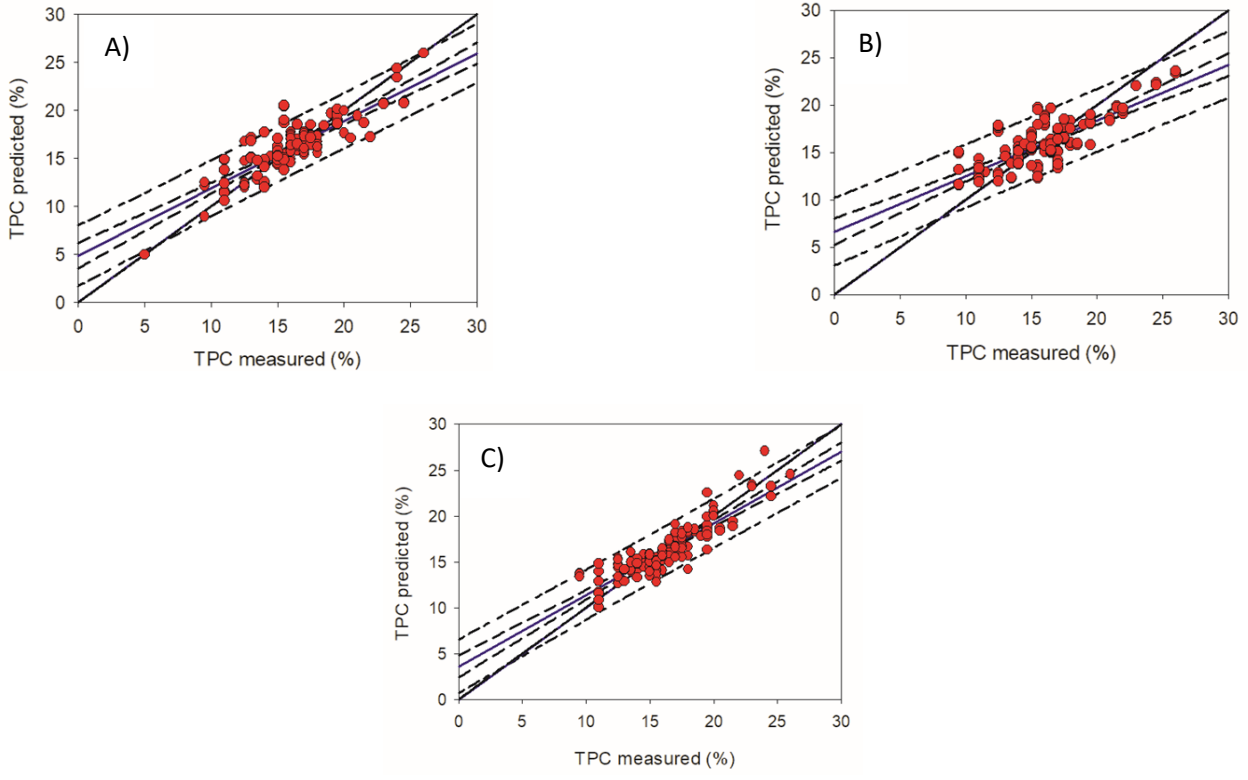

Fig. 3. Concentration predicted by corresponding models of TPC (in %) as function of the concentration determined by Testo-270. Notes: A: iPhone 7 (1); B: iPhone 7 (2); C: Samsung S7.

Fried samples were predicted from 10 till 17 % of TPC values and only 3 fried samples were outlier of the action line. These three values were anomalous. Only 2 fried samples were predicted with high values of TPC but these samples were in the action line (between 22 till 25 % of TPC) and it was can be dangerous for human consume due to the TPC maximum permitted in Spain. Samples heat had less error than fried samples, but this error it was produce when in the middle of the concentration of TPC. In these samples, only one sample was outside the action line.

Fig 4B shows BlandAltman for non-calibrated iPhone 2 and employing the best model built, the most of the samples were predicted from 11 till 20 % of TPC concentration and with less error (from 4 till -4 %). In this case, the 0 was inside from 95 % of confidence interval of the average, so it can be concluded that the difference between the compared values was no significantly different from 0 at 95 %, so the prediction was accurate.

Fried samples were predicted as iPhone 1 at low concentration of TPC and employing the best model, only 2 samples were outside of the action line. Only 2 fried samples were predicted to high concentrations (~ 23 % TPC). Heated samples had less error than fried samples, but the error was done at high values of TPC. 2 samples were predicted outside of the 95 % confidence interval.

Fig 4C shows BlandAltman for calibrated Samsung S7 and employing the best model built, the most of the samples were between 4 till -4 % of error. In this model, the 0 was inside from 95 % of confidence interval of the average, so it can be concluded that the difference between the compared values was no significantly different from 0 at 95 %.

Fried samples were predicted in low values of TPC with low errors and in this model, only 2 fried samples were predicted outside of the 95 % confidence interval. 3 fried samples were predicted at high values of TPC (~23-25 % TPC) but were inside of the action lines. Heated samples were predicted in high values of TPC than fried samples (~15 till 22 % TPC). In this model, 4 heated samples were outside the action lines.

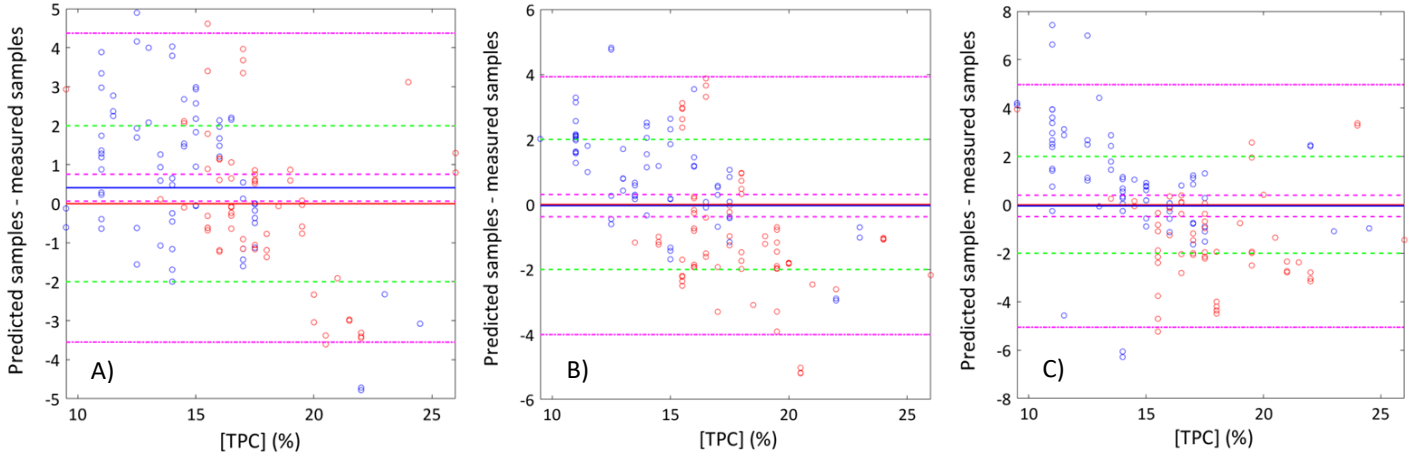

Fig. 4. Bland-Altman plots for the best models for each smartphone. The difference between model prediction and experimental TPC values has been plotted versus the experimental value. Magenta lines represent the median of the sample (continuous line), and 95% confidence interval of the median (dashed line) and the sample (dashed-dotted line). The green line represents the acceptability limits based in the intervals routinely used by health inspectors in Spain. Blue: oil fried with potatoes; Red: heated oil.

Notes: A: iPhone 7 (1); B: iPhone 7 (2); C: Samsung S7.

4. Conclusions

Models predicting TPC values based on the CIELAB L*, a*, b* and C* descriptors estimated from RGB values in a colorimetrically characterized smartphone camera agree with experimental values measured with Test, for both for heated oil and oil used to fry potatoes, taking into account the maximum TPC values permitted in Spain.

A green, fast and non-destructive method has been developed for the determination of TPC in sunflower oil employing a smartphone camera with prediction errors of the order of from 1.6 till 2.1 % of TPC content. This methodology can be used for the control of fried oil and estimate if an oil can be used again or not because the food fried helps oil degradation due to if it heats only oil there are not degradation before 40 fried.

5. Conflict of interest

The authors declare there is no conflict of interest regarding the contents of this paper.

6. Acknowledgements

The authors gratefully acknowledge the financial support of the Ministerio de Ciencia, Innovación y Universidades-Agencia Estatal de Investigación FEDER (EU) (Project CTQ2016-78053-R).

7. References

[1] Salas, J. J., Bootello, M. A., Garcés, R. 2015. Food uses of sunflower oil. Salas, J. J., Bootello, M. A., & Garcés, R. (2015). In E. Martínez-Force, N. T. Dunford, & J. J. Salas (Eds.). Sunflower: Chemistry, production, processing, and utilization (pp. 441–464). IL, AOCS press: Urbana.

[2] Wang, D., Fan, W., Guan, Y., Huang, H., Yi, T., J, J. 2018. Oxidative stability of sunflower oil flavored by essential oil from Coriandrum sativum L. during accelerated storage. Food Science and Technology, 98, 268-275.

[3] Tavakoli, A., Sahari, M. A., Barzegar, M., Gavlighi, H. A. 2019. Optimization of high voltage electric field as a novel non-thermal method of sunflower oil neutralization. Separation and Purification Technology, 211, 430-437.

[4] Jaswir, I., Man, Y. B. C., Kitts, D. D. 2000. Use of a natural antioxidants in refined palm olein during repeated deep-fat frying. Food Research International, 33, 501-508.

[5] Li, X., Wu, G., Yang, F., Meng, L., Huang, J., Zhang, H., Jin, Q., Wang, X. 2019. Influence of fried food and oil type on the distribution of polar compounds in discarded oil during restaurant deep frying. Food Chemistry, 272, 12-17.

[6] BOE-A-1989-2265. Orden de 26 de enero de 1989 por la que se aprueba la Norma de Calidad para los Aceites y Grasas Calentados.

[7] Abdel-Razek, Ragab, A. G., Gamal, H. A., Hatem, S. 1997. Quality of the deep-frying material as a function of the heating time according to Blumenthal. Aid Consumer Service. 57-59.

[8] Petersen, K. D., Jahreis, G., Busch-Stockfisch, M., Fritsche, J. 2013. Chemical and sensory assessment of deep-frying oil alternatives for the processing of French fries. Eur. J. Lipid Sci. Technol. 115, 935-945.

[9] Santos, C. S. P., Molina-Garcia, L., Cunha, S. C., Casal, S. 2018. Fried potatoes: Impact of prolonged frying in monounsaturated oils. Food Chemistry. 243, 192-201.

[10] Romero, A., Cuesta, C., Sánchez-Muniz, F. J. 1998. Effect of Oil Replenishment During Deep-Fat Frying of Frozen Foods in Sunflower Oil and High-Oleic Acid Sunflower Oil. JAOCS. 75, 161-167.

[11] Mlcek, J., Druzbikova, H., Valasek, P., Sochor, J., Jurikova, T., Borkovcova, M., Baron, M., Balla, S. 2015. Assessment of total polar materials in frying fats from czech restaurants. Ital. J. Food Sci., 27, 160-165.

[12] Bansal, G., Zhou, W., Barlow, P. J., Joshi, P. S., Ling, H., Chung, Y. K. 2010. Review of Rapid Tests Available for Measuring the Quality Changes in Frying Oils and Comparison with Standard Methods. Critical Reviews in Food Science and Nutrition. 50, 503-514.

[13] Capitán-Vallvey, L. F., Lopez-Ruiz, N., Martinez-Olmos, A., Erenas, M. M., Palma, A. J. 2015. Recent developments in computer vision-based analytical chemistry: A tutorial review. Analytical Chimica Acta, 899, 23-56.

[14] Lopez-Molinero, A., Liñan, D., Sipiera, D., Falcon, R. 2010. Chemometric interpretation of digital image colorimetry. Application for titanium determination in plastics. Microchemical Journal, 96, 380-385.

[15] Lin, C. J., Prasetyo, Y. T., Siswanto, N. D., Jiang, B. C. 2018. Optimization of color design for military camouflage in CIELAB color space. Color Research and Application, 44, 367-380.

[16] Athira, K., Sooraj, N. P., Jaishanker, R., Kumar, V. S., Sajeev, C. R., Pillai, M. S., Govind, A., Dadhwal, V. K. 2019. Quantitative representation of floral colors. Color Research and Application, 44, 426-432.

[17] Fondón, I., Valverde, J. F., Sarmiento, A., Abbas, Q., Jiménez, S., Alemany, P. 2015. Automatic optic cup segmentation algorithm for retinal fundus images base on random forest classifier. Proceedings- EUROCON 2015, 1-6.

[18] Cruz-Fernández, M., Luque-Cobija, M. J., Cervera, M.L., Morales-Rubio, A., de la Guardia, M. 2017. Smartphone determination of fat in cured meat products. Microchemical Journal, 132, 8-14.

[19] Salinas, Y., Ros-Lis, J. V., Vivancos, J. L., Martínez-Mánez, R., Aucejo, S., Herranz, N., Lorente, I., Garcia, E. 2014. A chromogenic sensor array for boiled marinated turkey freshness monitoring. Sensors and Actuators B: Chemical, 190, 326-333.

[20] Urazov, E. V., Gavrilenko, M. A., Belikov, M. K. 2018. Colorimetric Determination of Metal Ions Using Smartphone. Key Engineering Materials, 769, 235-241.

[21] Sanaeifar, A., Bakhshipour, A., de la Guardia, M. 2016. Prediction of banana quality indices from color features using support vector regression. Talanta. 148, 54-61.

[22] Malo, J., Luque, M. J. ColorLab: The Matlab toolbox for colorimetry and color vision. http://isp.uv.es/code/visioncolor/colorlab.html

[23] Hong, G., Luo, M. R., Rhodes, P. A. 2000. A study of digital camera colorimetric characterization based on polynomial modeling. COLOR research and application, 26, 76-84.

[24] Bland, J. M., Altman, D. G. 1986. Statistical methods for assessing agreement between two methods of clinical measurement. The Lancet, 327, 307-310.

[25] Bland, J. M., Altman, D. G. 1995. Comparing methods of measurement: why plotting difference against standard method is misleading. The Lancet, 346, 1085-1087.

CONCLUSIONES

BLOQUE I. ANÁLISIS MEDIANTE ED-XRF

Capítulo 1. Determinación directa del perfil mineral en muestras de cacao en polvo mediante ED-XRF portátil

En este capítulo se determinaron de forma exitosa cinco elementos mediante el equipo portátil ED-XRF. Los calibrados externos realizados en una muestra de cacao, de concentración conocida, diluida con glucosa permitieron la cuantificación del contenido mineral con desviaciones estándar menores al 8 % en el caso de K, Cu, Fe y Zn. Las desviaciones obtenidas en la determinación de Ca en las muestras de cacaos solubles y chocolates a la taza fueron entre 1.4 y 26 % debido a la diferencia de concentración en las muestras analizadas.

Los resultados obtenidos mediante ED-XRF se evaluaron comparándolos con los datos cuantificados por ICP-OES, obteniendo concentraciones coincidentes en los 5 analitos. Adicionalmente se comprobó la exactitud del método mediante el análisis de una muestra certificada y se consiguieron valores de exactitud entre 92 y 102 %.

A partir de los resultados obtenidos en este estudio se puede concluir que los calibrados externos realizados permiten la cuantificación del contenido mineral (Ca, Cu, Fe, K y Zn) en muestras de cacaos y chocolates a la taza siguiendo un procedimiento “verde”, sin la necesidad de emplear reactivos y sin generar residuos.

Capítulo 2. Metodología verde para el control de calidad del contenido elemental en leches infantiles en polvo

El objetivo fijado de este estudio fue desarrollar una metodología verde para cuantificar el contenido elemental en leches infantiles en polvo utilizando el equipo portátil ED-XRF. Se optó por emplear los calibrados externos realizados para la cuantificación del contenido elemental en cacaos y chocolates a la taza. Estos calibrados proporcionaron para las leches infantiles en polvo resultados coincidentes con los obtenidos en su cuantificación mediante ICP-OES y con los contenidos indicados en la

etiqueta de los productos. En las pruebas estadísticas ensayadas, no se hallaron diferencias significativas entre las concentraciones obtenidas mediante ED-XRF, ICP-OES y el etiquetado de cada producto analizado.

Las desviaciones estándar relativas obtenidas fueron en todos los analitos menores de 14 %. En esta ocasión, la exactitud del método obtenida mediante el análisis de una muestra certificada se encontró entre el 86 % y el 102 %. Finalmente se comprobó que no existe efecto matriz en la dilución de las muestras con lactosa para su interpolación en los calibrados externos realizados.

Capítulo 3. Modelización mediante mínimos cuadrados parciales de fluorescencia de rayos X con dispersión de energía

En este estudio se comprobó la capacidad de las técnicas multivariantes, en combinación con el análisis mediante ED-XRF, para cuantificar el contenido mineral en muestras de kaki. El empleo de la herramienta quimiométrica PLS para combinar los espectros obtenidos mediante ED-XRF con las concentraciones del perfil mineral determinadas por ICP-OES permitió la correcta predicción del perfil mineral en las muestras de kakis.

Se obtuvieron valores de RRMSECV menores al 20 % en Ca, Fe, K, Mg y P, y se puede considerar que los métodos de calibración multivariante ofrecen una alternativa sostenible para la determinación del contenido mineral en muestras de kaki. En concreto, el método PLS-ED-XRF desarrollado permite la cuantificación simultanea de 5 analitos sin emplear ningún tipo de reactivo ni disolvente, sin generar residuos y con un bajo tiempo de análisis y consumo de energía.

Capítulo 4. Perfil mineral de legumbres y frutos mediante fluorescencia de rayos X con dispersión de energía por mínimos cuadrados parciales

El objeto de este estudio fue el desarrollo de una metodología sostenible para la cuantificación del perfil mineral en frutos y legumbres mediante el uso de técnicas quimiométricas que combinaron los datos espectrales de las muestras, obtenidos con el ED-XRF, con las concentraciones de los elementos medidas por ICP-OES previa digestión de las muestras en horno de microondas.

Se crearon modelos binarios capaces de predecir el contenido mineral en muestras alimenticias en el que se utilizó el 40 % de las muestras para el set de calibración y el resto para el set de validación. De todos los modelos ensayados, el mejor modelo predictivo fue el que utilizó conjuntamente todas las muestras de cerezas y de legumbres. En los 7 analitos determinados se obtuvieron RRMSEP menores al 16 % y coeficientes de determinación mayores a 0.99. Se puede afirmar que la espectroscopia ED-XRF junto con el PLS permite cuantificar de un modo preciso, sin tratamiento de la muestra y de forma rápida Ca, Cu, Fe, K, Mg, P, Sr y Zn en frutos y legumbres.

Capítulo 5. Determinación de elementos esenciales y no esenciales en cacaos en polvo españoles mediante técnicas espectroscópicas

En este capítulo se determinó el contenido de 14 elementos esenciales (B, Ca, Co, Cr, Cu, Fe, K, Mg, Mn, Mo, Na, Ni, P y Zn) y 6 elementos no esenciales (Al, Ba, Cd, Pb, Sr and Ti) en cacaos y chocolates a la taza mediante detección por ICP-OES previa digestión ácida de las muestras.

Las concentraciones obtenidas mediante el método de referencia (ICP-OES) en las 21 muestras de cacao y chocolate analizadas son del mismo orden que las reportadas en la bibliografía para los 20 elementos estudiados, y no se encontraron concentraciones de elementos tóxicos superiores a los límites establecidos.

Así mismo se desarrolló una metodología verde para la cuantificación directa del perfil mineral mediante ED-XRF y PLS. Los modelos PLS-ED-XRF creados

permitieron cuantificar adecuadamente Ca, Fe, K, Mg, Mn, Mo, Ni, P, Sr y Zn. Los coeficientes de determinación obtenidos en la comparación de la concentración predicha por el modelo PLS-ED-XRF y los datos obtenidos mediante ICP-OES están entre 0.71 y 0.99 para todos los elementos.

Por otra parte, el cálculo de la ingesta diaria aportada por la ración recomendada de cada muestra alcanza valores entre 0.15 y 75 %.

La realización de un dendrograma reveló la clara existencia de 3 tipos de matriz analizadas teniendo en cuenta el perfil mineral de cada una de ellas.

En vista de los resultados se puede concluir que no hay concentraciones de elementos tóxicos superiores a las establecidas en la legislación. El método verde desarrollado PLS-ED-XRF permite la rápida cuantificación de 10 elementos esenciales en cacaos y chocolates a la taza sin el empleo de reactivos ni preparación de muestra.

Estos estudios muestran la capacidad de la ED-XRF para cuantificar el contenido mineral en muestras alimenticias y ofrece una alternativa verde a las técnicas tradicionales empleadas.

BLOQUE II. ANÁLISIS MEDIANTE SMARTPHONE

Capítulo 6. Determinación del contenido de clorofila en hojas mediante Smartphone

El objeto de este estudio fue la determinación directa del contenido de clorofila en hojas de la variedad *Citrus* mediante el empleo de las fotografías tomadas con un Smartphone.

Tras la extracción en frio con acetona de la clorofila, se llevó a cabo su determinación mediante el espectro UV-Vis. A partir de esta concentración y de los datos proporcionados por el CCM y SPAD, junto con los valores RGB extraídos de las fotografías de las muestras de las hojas se crearon diferentes modelos. Los coeficientes de determinación obtenidos en estos modelos de calibración fueron mayores de 0.94 y el error cuadrático medio de predicción obtenido en todos los casos fue menor al17 %.

Como conclusión de este estudio se puede decir que a partir de una simple fotografía con un Smartphone se puede predecir con fiabilidad la concentración de clorofila en hojas sin necesidad de realizar tratamiento de muestra ni el empleo de disolventes.

Capítulo 7. Predicción de compuestos polares totales en aceite de girasol usado mediante Smartphone

En este capítulo se desarrolló una metodología directa, evitando el uso de reactivos y disolventes, para la cuantificación de los compuestos polares totales en aceite de girasol por el color del aceite de fritura a partir de la imagen tomada con un Smartphone. Se crearon modelos con los valores L*, a* y b* obtenidos de las fotografías de las muestras en combinación con los valores de TPC obtenidos con el TESTO-270.

Se estudió el número de veces que es posible usar un mismo aceite para cocinar sin presentar riesgo para la salud. Se comprobó que el aceite de girasol puede ser reusado durante 40 ciclos de fritura sin llegar al límite máximo permitido en España del 25 % de TPC.

Se crearon 3 modelos, uno para cada Smartphone empleado (2 iPhone y un Samsung) y en los 3 se obtuvieron bajos errores cuadráticos medios de calibración siendo 1.9 % para el iPhone-1, 2.2 % para el iPhone-2 y 1.6 % para el Samsung.

En vista de los resultados se puede concluir que a partir de los modelos generados con los valores de TPC y los valores de L*a*b* de las fotografías de la muestra se puede predecir el contenido en compuestos polares sin el uso de reactivos ni de tratamiento de la muestra.

PUBLICACIONES DERIVADAS DE LA TESIS

La presente tesis doctoral presentada por Lidia Herreros Chavez presenta los siguientes 4 artículos científicos aceptados en revistas indexadas:

Artículo 1. L. Herreros-Chavez, M.L. Cervera, A. Morales-Rubio. Direct determination by portable ED-XRF of mineral profile in cocoa powder. *Food Chemistry*, 278 (2019) 373-379.

https://doi.org/10.1016/j.foodchem.2018.11.065

Factor de impacto en Journal Citation Reports (JRC), 2019: 5.399

Categoría y posición: Food, Science and Technology, 7/135 (Q1)

Número de citas: 7

Artículo 2. L. Herreros-Chavez, A. Morales-Rubio. M.L. Cervera. Green methodology for quality control of elemental content of infant milk powder. *LWT-Food Science and Technology*, 111 (2019) 484-489.

https://doi.org/10.1016/j.lwt.2019.05.055

Factor de impacto en Journal Citation Reports (JRC), 2019: 3.714

Categoría y posición: Food, Science and Technology, 23/135 (Q1)

Número de citas: 1

Artículo 3. L. Herreros-Chavez, A. Morales-Rubio, M.L. Cervera, M. de la Guardia. Partial least squares modelization of energy dispersive X-ray fluorescence. *Talanta*, 194 (2019) 158-163.

https://doi.org/10.1016/j.talanta.2018.10.023

Factor de impacto en Journal Citation Reports (JRC), 2019: 4.916

Categoría y posición: Analytical Chemistry, 11/84 (Q1)

Número de citas: 1

Artículo 4. L. Herreros-Chavez, F. Oueghlani, A. Morales-Rubio, M.L. Cervera, M. de la Guardia. Mineral profiles of legumes and fruits through partial least squares energy dispersive X-ray fluorescence*. Journal of Food Composition and Analysis*, 82 (2019) 103240.

https://doi.org/10.1016/j.jfca.2019.103240

Factor de impacto en Journal Citation Reports (JRC), 2019: 2.994

Categoría y posición: Food, Science and Technology, 37/135 (Q2)

Número de citas: 1

Así mismo, esta tesis ha dado lugar a 3 artículos científicos que aún no han sido publicados:

Artículo 5. L. Herreros-Chavez, A. Morales-Rubio, M.L. Cervera. Determination of essential and non-essential elements in Spanish cocoa powder by spectroscopic techniques.

Artículo 6. L. Herreros-Chavez, P. Martínez-López, M.J. Luque, A. Morales-Rubio, M.L. Cervera. Determination of chlorophyll content in leaves by Smartphone.

Artículo 7. L. Herreros-Chavez, C. Galve, M.J. Luque, A. Morales-Rubio, M.L. Cervera. Prediction of total polar compounds in used sunflower oil by Smartphone.